12-2021

Morphological Characterization and Functional Assessment of Trichomes in Solanaceae

Sakshi Watts
The University of Texas Rio Grande Valley

MORPHOLOGICAL CHARACTERIZATION AND FUNCTIONAL ASSESSMENT OF TRICHOMES IN SOLANACEAE

A Thesis

by

SAKSHI WATTS

Submitted in Partial Fulfillment of the

Requirements for the degree of

MASTER OF SCIENCE

Major Subject: Biology

The University of Texas Rio Grande Valley

December 2021

MORPHOLOGICAL CHARACTERIZATION AND FUNCTIONAL ASSESSMENT OF TRICHOMES IN SOLANACEAE

A Thesis
by
SAKSHI WATTS

COMMITTEE MEMBERS

Dr. Rupesh Kariyat
Chair of Committee

Dr. Mohammed Farooqui
Committee Member

Dr. Robin Choudhury
Committee Member

December 2021

ABSTRACT

Watts, Sakshi., Morphological Characterization and Functional Assessment of Trichomes in Solanaceae. Master of Science (MS), December 2021, 146 pp., 5 tables, 28 figures, references, 150 titles.

Chapter 1: This chapter provides an overview of various trichome types in plants, and also empirically examines detailed nomenclature, density, and dimension measurements of each trichome type in 14 *Solanum* species.

Chapter 2: Scanning electron microscopy was major component of methodology used in my thesis and in this chapter, a more efficient and cost-effective methodology for scanning electron microscopy has been explored.

Chapter 3: This chapter examines the relationship of trichome density and herbivore feeding behavior.

Chapter 4: This chapters provides the findings of two foliar surface defenses present in two Solanaceae species with significant variation in trichomes (epidermal hairs) and waxes (hydrophobic layer) and their interactions with a Solanaceae specialist herbivore.

Chapter 5: This chapter provides an overview of my major finding and also suggests future directions for research on plant surface defenses and their functional roles in deterring insect herbivory.

DEDICATION

I would like to dedicate my thesis to my late grandmother and grandfather, Mrs. Nirmala Rani and Mr. Ram Lal, and my mother and father, Mrs. Anita Rani and Mr. Surinder Kumar for their blessings, motivation and support.

ACKNOWLEDGMENTS

Firstly, I would like to immensely thank Dr. Rupesh Kariyat, my thesis advisor and mentor for providing me the opportunity to be a part of his lab and teaching me to do scientific research with all the ethics and grace. In these two years, I have learned and mastered numerous things and I would not have been able to do those without constant support of Dr. Kariyat. All in all, no matter how many good things I write about him, those words will not be enough to justify how great scientist, advisor, teacher and mentor he is.

I would also like to thank Dr. Mohammed Farooqui and Dr. Robin Choudhury for agreeing to be a part of my thesis committee. All the feedback provided by my committee members have been a great opportunity for me to learn and improve my thesis project.

I would also like to thank Dr. Parwinder Grewal and PGRA (Presidential Graduate Research Assistantship) for funding master's for whole two years. Being a PGRA awardee, I was able to gain experience of teaching undergraduate labs and grading certain undergraduate courses as well.

Additionally, I would like to acknowledge Dr. Jaspal Singh and Dr. Navprem Singh for writing recommendation letters for my admission to M.S. Biology in UTRGV.

I cannot thank my family and friends enough for being there for me whenever I needed support and motivation. Tripti Saini, Amit Sharma and Amandeep Singh, my friends, and roommates (at some point of time at least!) made this journey so easy and fun and provided me with innumerable precious memories for lifetime. You guys are the BEST! You added joy to my

everyday here.

Lastly, I would like to thank Sukhman Singh, Mandeep Tayal, Jasleen Kaur, Jesus Chavana, Zachary Johnson, Clarissa Deleon, MJ, Harpreet Kaur, Satinder Kaur, Adegboyega, Juan Raya, people who have helped me, taught me, inspired me, and made me laugh.

TABLE OF CONTENTS Page

LIST OF TABLES Page

LIST OF FIGURES

Page

CHAPTER I

MORPHOLOGICAL CHARACTERIZATION OF TRICHOMES SHOW ENORMOUS VARIATION IN SHAPE, DENSITY, AND DIMENSIONS ACROSS THE LEAVES OF 14 SOLANUM SPECIES

Abstract

Trichomes are the epidermal appendages commonly observed on plant surfaces including leaves, stem, and fruits. Plant trichomes have been well studied as a structural plant defense designed to protect plants against abiotic and biotic stressors such as UV rays, temperature extremities and herbivores. Trichomes are primarily classified into glandular and non-glandular trichomes, based on the presence or absence of a glandular head. The plant genus *Solanum* is the largest genus of family Solanaceae that houses ~3500 species of ecological and economic importance have a diverse set of trichomes that vary in density and morphology. However, due to the incomplete and contradictory classification system, trichomes have subjective names and have been largely limited to be grouped into glandular or non-glandular types. Through this study, we did a complete workup to classify and characterize trichomes on both adaxial and abaxial leaf surface of 14 wild and domesticated species of the genus *Solanum*. Using electron

microscopy, statistical analyses and artistic rendition, we examined finer details of trichomes and measured their density and dimensions to compile a detailed dataset which can be of use for estimating the variation in trichome types, and their density, with consequences for understanding their functional roles. Our study is the first of its kind that provides us with a better and well-defined classification, density, and dimension analysis to complete the morphological classification of trichomes on both leaf surfaces of a diverse range of members in *Solanum* genus.

Introduction

Plant surfaces show spectacular variation in the shape, size, location, function, and origin of epidermal projections (Werker, 2000). The most important and well-studied among these are trichomes: unicellular or multicellular appendages (hair like structures) originating from epidermal cells of various plant parts including leaves, stems and flowers (Oksanen, 2018), and developing outwards (Werker, 2000). Trichomes are distributed almost universally in the plant kingdom and exhibit dramatic variation in their morphology (Seithe and Sullivan, 1990; Dam et al., 1999; Adedeji et al., 2007; Kang et al., 2010; Nurit-Silva and Fatima Agra, 2011; Munien et al., 2015; Talebi et al., 2018) and density (Talebi et al., 2018), both intra (Kang et al., 2010; Munien et al., 2015; Dam et al., 1999) and inter-specifically (Seithe and Sullivan, 1990; Navarro and Oualidi, 1999; Mannethody and Purayidathkandy, 2018; Talebi et al., 2018; Yu et al., 2018), and also among and between related and distant plant families (Kariyat et al., 2018; Deore, 2020; Watts and Kariyat 2021). For example, Munien et al. (2015) found four types of trichomes (glandular, non-glandular dendritic, non-glandular bicellular and non-glandular multicellular) in *Withania somnifera* (intra-specific); Yu et al. (2018) found a great variation in trichome morphology, dimensions, distribution and density among seven *Mentha* species (inter-specific);

Deore (2020) identified variations in trichomes among 20 species belonging to 12 different plant families and most of the species were reported to have trichomes ranging from unicellular to multicellular, conical to elongated, smooth to grooved, thin to thick walled, and with or without a flat disc at the base. Further, Tsujii et al. (2016) found tremendous variation in trichome leaf dry mass per area in the plant tissue of *Metrosideros polymorpha* at different elevations (Tsujii et al., 2016). Clearly, within flowering plants, trichomes are both ubiquitous and morphologically diverse.

Trichomes, in general are considered as one of the first line of defenses possessed by plants to protect against abiotic stresses such as UV rays, water loss, temperature extremities (Ehleringer, 1982; Li et al., 2018; Oksanen, 2018) and herbivore damage (Kaur and Kariyat, 2020a; 2020b; Watts and Kariyat, 2021). Moreover, the leaf trichomes can also act as mechanoreceptors for detection of insects on leaf surface as observed in case of *Arabidopsis* (Zhou et al., 2017). In addition to defense-related functions, trichomes play a role in water usage strategies through maintenance of leaf water content and stomatal traits to name a few. For example, Pan et al. (2021) showed higher percentage increase of leaf water content in epiphytic plants with trichomes (Pan et al., 2021). Additionally, trichomes can play role in translocation and homeostasis of minerals in plants (Blamey et al., 1986; 2015; Li et al., 2021). But the relationships of such traits with trichome types and measurements such as density and dimensions are poorly understood.

Broadly, trichomes can be classified into glandular (presence of glandular head) and non-glandular (absence of glandular head) (Werker, 2000). Both glandular (Tang et al., 2020) and non-glandular (Karabourniotis et al., 2019) trichomes have been well documented to protect plants either by production of chemicals in their glandular heads or by their sturdy structure that

assist plants to adapt and/or protect from environmental conditions such as UV radiations and cold stresses. Glandular trichomes deter herbivory by physically entrapping herbivore into sticky exudates (Tingey and Laubengayer, 1981; Neal et al., 1990; Elle et al., 1999; Zalucki et al., 2002), secreting defensive chemical compounds such as proteinase inhibitors (Peiffer et al., 2009), production of volatile organic compounds (Avé et al., 1987; Murungi et al., 2016), or by altering herbivore body odour after providing a sugar rich first meal (Weinhold and Baldwin, 2011). On the other hand, non-glandular trichomes in the *Solanum* species are mostly spike like structures which deter herbivory primarily by deterring herbivore movement, feeding and oviposition (Corsi & Bottega, 1999; Kennedy, 2003; Løe et al., 2007; Dalin et al., 2008; Sletvold et al., 2010; Tian et al, 2012; Weigend et al., 2018; Kariyat et al, 2019). Additionally, non-glandular trichomes can cause post-feeding damage to caterpillars by rupturing of caterpillars' peritrophic membrane (gut lining; Kariyat et al., 2017; Andama et al., 2020). Moreover, some plant species also possess stinging hairs (trichomes with stinging cells which contain irritant fluids) which act as hypodermal syringes and can cause various allergic reactions such as pain, itching, oedema, and visible dermal reactions to mammalian herbivores (Ensikat et al., 2021). Glandular trichomes are more pliable, so may not cause physical damage (Kariyat 2017; 2019) but can be toxic and can release chemicals to intoxicate herbivores (Hare, 2005) and attract predators of herbivores in association with carcasses of herbivores (LoPresti et al., 2015). Contrary to this, non-glandular trichomes are usually devoid of toxins but their sharp and edgy structure can cause physical damage to herbivores. Thus, while the size and structure of the apical gland can inform about the amount of toxins and their content, knowledge about various types (e.g., unbranched vs stellate) and sizes of non-glandular trichomes can appraise us about their functional significance- either in deterring herbivory or protecting against abiotic stressors.

More specifically, in case of non-glandular trichomes, we now have multiple lines of evidence on how variation in trichome type and density differentially defend them against insect herbivores (Cho et al., 2017; Kariyat et al., 2017; 2019; Watts and Kariyat, 2021). For instance, Watts and Kariyat (2021) found significant variation in trichome density on abaxial and adaxial leaf surface of 11 Solanaceae species and demonstrated that this variation has functional consequences for caterpillar growth and feeding.

Clearly, a detailed examination and characterization of trichome morphology (even on abaxial and adaxial surfaces) can have multiple benefits, including a reliable and non-contradictory nomenclature of trichomes, understanding the prominent trichome types found in nature, and their diversity - which later can be explored for defensive functions against different herbivores, and abiotic stressors, with possible implications for our efforts to produce better defended plants for sustainable agriculture (Andama et al., 2020).

Solanaceae is one of the most important plant families consisting of 90 genera and ~3000-4000 ecologically and economically important species which are found in all habitats ranging from dry deserts to wet tropical rainforest and have growth habits ranging from small ephemeral herbs to large perennial trees (Knapp, 2002). Among all the genera in Solanaceae, the genus *Solanum* contributes ~75% of all species (Knapp, 2002; Symon, 1981). *Solanum* genus exhibits tremendous variation and diversity of trichomes; for instance, widely studied and domesticated crops such as tomato (*Solanum lycoperiscum*) and tobacco (*Nicotiana tabacum*) have different types of glandular trichomes, while wild weeds such as silverleaf nightshade (*Solanum elaeagnifolium*) and Carolina horsenettle (*Solanum carolinense*) possess only non-glandular trichomes (Peiffer et al., 2009; Weinhold and Baldwin, 2011; Burrows et al., 2013; Kariyat et al., 2018). A general convention in trichome literature is to reduce the diversity of

trichome types by constraining them to just types of glandular and non-glandular, while these types are quite diverse and are often complicated to resolve. Moreover, this basic classification also fails to explain the huge variation among sub-types of glandular and non-glandular trichomes, and consequently potential to explore their function.

Luckwill (1943) was the first to classify trichomes of *Lycopersicon* into seven distinct types (four glandular sub types and three non-glandular sub types) of trichomes based on their length, number of stalk and base cells, and the presence or absence of gland. Following Luckwill (1943), Uphof (1962) in a summary for different methods of classification of trichomes concluded that the final classification is still subjective. After that, Payne (1978) provided us with a glossary to name various trichomes or structures found in trichomes to improve trichome nomenclature. Later, Channarayappa et al. (1992) revised the trichome classification by Luckwill (1943) and the revised classification is used frequently in trichome related studies. While these studies have served as a model for trichome morphology assessment, we used scanning electron microscopy, and artistic rendering along with the previous classical classification systems (Roe, 1971) and the glossary provided by Payne (1978) to characterize and classify trichomes on both adaxial (upperside) and abaxial (lowerside) leaf surface of 14 representative species from *Solanum*.

Materials and Methods

Plant Materials:

A mixture of wild and domesticated species of genus *Solanum* (14 species in total) were included in the study. We bought seeds of forest bitterberry (*Solanum anguivi*; Product code: Y5SSSOIN), porcupine tomato (*S. pyracanthos*; Product code: Y5SSSOPY), African eggplant (*S. macrocarpon*; Product code: Y5SSSOMC), bittersweet nightshade (*S. dulcamara*; Product

code: Y5SSS0DU), lance-leaved nightshade (*S. lanceifolium*; Product code: Y5SSSOLA), potato tree (*S. grandiflorum*; Product code: Y5SSSOGR), tzimbalo (*S. caripense*; Product code: Y5SSSOCA), devil's fig (*S. asperolanatum*; Product code: Y5SSSOAS), *S. taeniotrichum* (Product code: Y5SSSOTA) from rarepalmseeds.com; tomato (*S. lycopersicum*; Variety: Valley Girl F1) seeds from Johnnyseeds.com; garden huckleberry (*S. melanocerasum*; Brand: Palm Beach Medicinal Herbs), easter eggplant (*S. ovigerum*; Brand: Helens Garden) and Turkish orange eggplant (*S. aethiopicum*; Seller: Seedville USA) from amazon.com, and Aubergine (*S. melongena*; Shikou hybrid Eggplant; Item: 52568-PK-P1) from parkseed.com.

Seeds of all the species were sown in potting mixture (Sunshine professional growing mix: Sun Gro Horticulture Canada Ltd., MA, USA; Tayal et al., 2020) filled trays (12.5" ×7.5" ×2") and kept in controlled environmental conditions (26℃ temperature, ~50% relative humidity and 16:8 light dark cycle). Germinated seedlings were transplanted in plastic pots (5" ×4" ×4") with similar soil media and environmental conditions and were watered regularly. For electron microscopy, plants of 4-6 weeks of age post transplanting with at least 10-12 fully developed leaves were used. Young and fully expanded leaves from randomly selected individuals (for each species, sample size varied by treatment, details below) were used for microscopy experiments.

Desktop Scanning Electron Microscope (DSEM):

To capture images from both abaxial and adaxial of leaves for trichome morphology (n= 3-11 plants/side/species), dimension measurements (n= 3-11 plants/side/species) and density analysis (n= 3-11 plants/side/species), a desktop Scanning Electron Microscope (SNE- 4500 Plus Tabletop; Nanoimages LLC, Pleasanton, California, USA; Watts et al., 2021 in press) was employed. Circular leaf discs (0.63 cm in diameter) of fresh leaf samples (collection method detailed above) were excised from the plants using a hole punch. No chemical treatments (e.g.,

glutaraldehyde; Kariyat et al., 2017), critical drying or sputter coating was done to the leaf samples, and fresh leaf discs mounted on the aluminum stubs using double-sided carbon tape were directly inserted in the DSEM for scanning and image processing. For more details on operational procedures and methodology of DSEM, see Watts and Kariyat (2021), and Watts et al., (2021) in press.

Trichome Morphology assessment:

Fresh leaf samples (n= 3-11 plants/side/species) as described above were used and magnified ranging from 45X to 1000X depending on trichome type and size, to achieve maximum resolution to extract finer details of trichomes. Images of different trichome types from both abaxial and adaxial surface of leaves were captured at different angles in 3-D and later used to classify them. Payne (1978; consisting of glossary for different shapes and structures of/in trichomes), Roe (1971; consisting of terminology for commonly found *Solanum* trichomes) and Werker (2000; glandular trichome characterization based on structure of secretory head) were the major literature used to characterize trichomes post image acquisition.

Trichome Density Assessment:

To determine the trichome density from both leaf surfaces of all the species (n= 3-11 plants/side/species), sample preparation was done as described above. The images for trichome count were consistently captured at 60X magnification which contains approximately 5.32 mm^2 leaf area measured using 'Nanoeye' software linked to DSEM. We calculated the trichome density 1 mm^2 as follows (Chavana et al., 2021; Watts and Kariyat, 2021):

Trichome density (1 mm^2) = Number of trichomes in the image taken at 60x magnification/5.32

Trichome Dimension Measurements:

While scanning the leaf samples (n= 3-11 plants/side/species), once the image achieved maximum resolution visually, scanning was paused using 'Nanoeye' software associated with DSEM, and dimensions of various trichome types were measured by tracing trichomes by straight line in 'M. tools' in 'Nanoeye' software. For non-glandular trichomes, length of spikes from base to tip was measured, and in case of glandular trichomes, length of trichome from base to tip and diameter of bulb containing glandular secretions were measured using the measurement tool embedded in the software (Figure 7). Magnification was altered among samples depending on trichome type at the best resolution.

Line art:

The SEM images were used to draw the trichomes manually on paper. The paper was scanned to make a digital copy and the trichomes were traced using a size 4 solid circle brush (Wacom Intuos Pro Digital Graphic Drawing Tablet; Adobe Photoshop). Further, custom brushes in Adobe Photoshop were used to create non-uniform surface of few trichome types. The images were saved into transparent PNG files and inserted into tables with the base of trichomes is on the bottom of the image.

Analysis

Our goal was to characterize and document the trichome types in these 14 species, and to define the finer details on individual trichome types, and their dimensions. Using previous publications as a composite reference, we classified the trichome types using images that reflected its most detailed morphological features. The nomenclature of trichomes was decided by following a checklist of features in the order described below: major shape of the trichome; glandular/non-glandular trichome type (italicized); additional minute morphological specifications. Further, additional features have also been added as a separate column to know

more details of each trichome type. For morphological representation of trichome types, line art was created for each individual trichome type, by a graphical artist.

Following this, mean trichome density for each trichome type or trichome types as broad groups (glandular; simple non-glandular; stellate non-glandular) was calculated manually from images at 60X magnification. 60X magnification includes 5.32 mm^2 of leaf area, and thus to get density of trichomes in 1 mm^2 of area, the trichomes density at 60x magnification was divide by a factor of *5.32*. The Mean±SE of trichome density has been incorporated in Tables 2 and 3. And, to test whether species and trichomes varied across the 14 species of interest, we also ran a Generalized regression analysis with Poisson distribution with species and types (total, glandular and non-glandular) and their interaction as factors, and trichome number as the response variables. Tukey's post hoc tests were conducted to examine pairwise comparisons. All analyses were carried out using JMP15 (SAS Inc, Cary, JJ, USA) software and the plots were built using GraphPad Prism (La Jolla, CA, USA). And finally Mean±SE total length and Mean±SE of the diameter of glands on glandular trichomes, and Mean ± SE spike length in case of non-glandular trichomes were measured.

Results

Trichome Morphology assessment:

Basic classification of trichomes includes classifying them into glandular and non-glandular types (italicized; Table 2 and 3). Here, detailed classification of trichomes was carried out using previously published works as a composite reference. The terminology used for nomenclature of trichomes is described below in Table 1.

Using above-mentioned terminology, we classified all the trichomes found in our samples. Although, three trichome types viz. stellate non-glandular, simple non-glandular, and

glandular type trichomes were the most found in the *Solanum* species in our study, these types have also been further characterized into a numerous sub-types based on minor morphological differences (Figure 1; Table 2 and 3).

Stellate non-glandular trichomes have further been divided into multitangulate, multiradiate, stellate non-glandular hair with subulate rays (2-6 in number) with the presence of pedestal (*Solanum aethiopicum*; adaxial) (Table 2; Serial number 2), porrect-stellate multiradiate non-glandular hair with subulate rays (varying in number) and with short central ray (*S. aethiopicum*; abaxial, *S. anguivi*; abaxial, *S. lanceifolium*; adaxial and abaxial, *S. ovigerum*; abaxial, *S. pyracanthos*; adaxial and abaxial) (Table 2; 9, 45; Table 3; 4, 7, 13, 45, 51), porrect-stellate multiradiate non-glandular hair with subulate rays (varying in number) with long central ray (*S. anguivi*; adaxial and abaxial, *S. lanceifolium*; adaxial, *S. ovigerum*; adaxial) (Table 2; 8, 10, 39; Table 3; 8), porrect-stellate multi-radiate cruciate non-glandular hair with subulate rays (4 in number) and with short central ray (*S. grandiflorum*; abaxial) (Table 3; 30), porrect-geminate stellate multi-radiate non-glandular hair with subulate rays (2-16 in number) and short central ray (*S. melongena*; adaxial and abaxial) (Table 2; 30; Table 3; 34). Moreover, some stellate trichomes also have a pedestal (*S. aethipicum*; adaxial, *S. anguivi*; adaxial and abaxial, *S. ovigerum*; abaxial, *S. pyracanthos*; abaxial) (Table 2; 2, 3, 8; Table 3; 7, 8, 45, 51). And some stellate trichomes with only two rays at an angle have been named separately as bifurcated non-glandular hair (*S. aethiopicum*; adaxial, *S. anguivi*; adaxial and abaxial, *S. lanceifolium*; abaxial, *S. pyracanthos*; abaxial) (Table 2; 3, 7; Table 3; 9, 14, 53). Within each stellate trichome, spike number also varied in almost all the species (Figure 1, Table 2 and 3).

Simple non-glandular trichomes have also been further sub-divided as osteolate (*S. dulcamara*; abaxial) (Table 3; 57), subulate (*S. aethiopicum*; adaxial and abaxial, *S. anguivi*;

adaxial and abaxial, *S. lycopersicum*; abaxial, *S. macrocarpon*; adaxial and abaxial, *S. melanocerasum*; adaxial, *S. grandiflorum*; adaxial and abaxial, *S. melongena*; adaxial and abaxial, *S. taeniotrichum*; abaxial, *S. caripense*; adaxial and abaxial, *S. ovigerum*; adaxial, *S. pyracathos*; adaxial, *S. dulcamara*; adaxial) (Table 2; 1, 6, 20, 22, 25, 31, 36, 37, 40; Table 3; 3, 6, 18, 23, 27, 33, 39, 40, 43), falcate (*S. grandiflorum*; abaxial, *S. ovigerum*; abaxial) (Table 3; 32, 44), setiform (*S. grandiflorum*; adaxial) (Table 2; 29), crescent (*S. melanocerasum*; abaxial) (Table 3; 24), attenuate (*S. lycopersicum*; adaxial and abaxial) (Table 2; 17, 18; Table 3; 19, 20), hooked (*S. aethiopicum*; abaxial; *S. lycopersicum*; adaxial and abaxial, *S. melongena*; abaxial, *S. caripense*; abaxial; *S. pyracanthos*; abaxial) (Table 2; 3, 16; Table 3; 18, 33, 40, 54). And most of these trichome types were smooth (all species) (Figure 1 and 2; Table 2 and 3) while few others were pustulated (*S. macrocarpon*; adaxial and abaxial, *S. dulcamara*; abaxial) (Table 2; 20; Table 3; 23, 57). Similar to stellate non-glandular trichomes, some simple non-glandular trichomes have pedestal (*S. macrocarpon*; adaxial and abaxial, *S. grandiflorum*; adaxial, *S. melongena*; adaxial, *S. asperolanatum*; adaxial, (Table 2; 20, 25, 29, 31, 41; Table 3; 23, 27) while others do not have pedestal.

The third most found trichome type was glandular type which has been further characterized based on the presence of a globular head (all species) (Figure 1 and 2; Table 2 and 3) or small glandular tip (*S. aethiopicum*; abaxial, *S. lanceifolium*; abaxial, *S. lycopersicum*; adaxial and abaxial, *S. macrocarpon*; adaxial, *S. melanocerasum*; adaxial and abaxial, *S. grandiflorum*; adaxial, *S. taeniotrichum*; adaxial and abaxial, *S. asperolanatum*; adaxial and abaxial, *S. dulcamara*; abaxial) (Figure 2 and 3; Table 2; 13, 19, 23, 28, 33; Table 3; 1, 10, 17, 20, 25, 36, 37, 56). Further globular head can be large (Table 2; 5, 11, 12, 14, 21, 24, 26, 32, 41; Table 3; 2, 5, 12, 15, 16, 22, 26, 28, 31, 35, 42, 48, 52) or small (Table 2; 4, 5, 34, 35, 38, 44, 48;

Table 3; 38, 46, 55, the characterization made based on comparative visual observations (Figure 2 and 3; Table 2 and 3). Globular headed trichomes can vary in shape as was observed in case of *S. lanceifolium* (doliform globular head; adaxial; Table 2; 9). Additionally, globular headed glandular trichomes having distinct four-celled head have also been observed (Table 2; 5; Table 3; 5, 15, 16, 42). Similar to simple non-glandular trichomes, glandular trichomes were also found in various major shapes such as attenuate (*S. aethiopicum*; abaxial, *S. lanciefolium*; abaxial, *S. lycopersicum*; adaxial and abaxial, *S. macrocarpon*; adaxial, *S. grandiflorum*; adaxial, *S. dulcamara*; abaxial) (Table 2; 13, 19, 28; Table 3; 1, 10, 20, 57), acuminate (*S. lycopersicum*; adaxial) (Table 2; 15), subulate (*S. lycopersicum*; abaxial, *S. melanocerasum*; adaxial and abaxial, *S. taeniotrichum*; adaxial and abaxial) (Table 2; 23, 33; Table 3; 17, 25, 36, 37), hooked (*S. lycopersicum*; abaxial) (Table 3; 17). In case of non-glandular hair with attenuate non-glandular branches and one gland-tipped branch in *S. asperolanatum*, trichome has one branch with a glandular tip making it both glandular and non-glandular type trichome but named as non-glandular because of a greater number of rays being non-glandular (Table 3; 50).

And based on previous literature (Werker, 2000) and since these trichome lack a clear distinction of glandular head, ovoid (*S. grandiflorum*; adaxial and adaxial, *S. asperolanatum*; adaxial and abaxial) (Figure 1, table 2; 27, 42; Table 3; 29), mammilla (*S. lycopersicum*; abaxial) (Table 3; 21) and verrucate (*S. lanceifolium*; abaxial) (Table 3; 11) trichomes were characterized as non-glandular.

Although DSEM microscope used in the study had numerous benefits including no sample preparation or the use of critical chemicals and machinery, and faster image processing (critical point dryers and sputter coaters; Kariyat et al., 2017), it also had some drawbacks. One of them was that we were unable to further classify the glandular trichomes based on the number

of their head cells as SEM images lacked those details. And, since fresh leaf samples were used for the study, few glandular trichomes with pliable heads burst on their encounter with vacuum of the machine while scanning, due to the lack of critical point drying and sputter coating. For detailed results of species, trichome type, their density, and dimensions with pictorial representation of each trichome type on adaxial leaf surface see table 2, and on abaxial leaf surface, see table 3.

Density Measurements:

Consistent with morphological diversity and variation among and within each species, density of trichomes also varied across species (Watts and Kariyat, 2021; Figure 2 and 3; Table 2 and 3). Oddly, in some of the species, while acquiring images for density count at 60X, we did not observe any trichomes, but while zooming in on different leaf samples at a higher magnification, we observed few trichome types although they were quite rare. These include attenuate basilatus glandular hair with small glandular tip on adaxial leaf surface of *S. macrocarpon* (Table 2; Serial number 19), attenuate basilatus glandular hair with small glandular tip; mamilla non-glandular hair on abaxial leaf surface of *S. lycopersicum* (Table 3; 20, 21), subulate *glandular* hair with multicellular jointed stalk and small glandular tip on abaxial leaf surface of *S. melanocerasum* (Table 3; 24), subulate *non-glandular* hair with multiseriate base and tall pedestal on abaxial leaf surface of *S. grandiflorum* (Table 3; 27), hooked subulate *non-glandular* hair on abaxial leaf surface of *S. caripense* (Table 3l; 40), and falcate *non-glandular* hair on abaxial leaf surface of *S. ovigerum* (Table 3; 44).

The trichome types with highest trichome density include glandular hair with large globular head, single stalk cell and no neck cell on adaxial leaf surface of *S. asperolanatum* (Figure 3, Table 2; 41), and porrect-stellate multiradiate *non-glandular* hair with subulate rays

(5-10 in number) and with short central ray on abaxial leaf surface of *S. aethiopicum* (Figure 2; Table 3; 4). Although the variation was huge, we found that some trichome types had higher trichome density than the other types in each species. For example, in *S. anguivi* (abaxial) porrect-stellate multi-radiate non-glandular hair with subulate rays (5-10 in number) with short/long central ray and pedestal (density: 13.00±1.56; Table 3; 7, 8 and 9) had considerably higher trichome density than the other two trichome types (Table 3; 5 and 6) (Figure 2). Almost all the species in which one/two trichome types dominated over the other. In addition to this, occasionally it was difficult at 60x to distinguish between some trichome types, so the density of some trichome types have been compiled. For example, manual counting of both glandular hair with large quadricellular globular head and single stalk cell in case of abaxial leaf surface of *S. lycopersicum* resulted into total density of 0.94±0.19 (Table 3; 15 and 16). Such cases were observed for all three major trichome types (stellate non-glandular, simple non-glandular and glandular trichomes) (Table 2 and 3). Additionally, we found significant variation in trichome numbers (total, glandular and non-glandular; at 60x magnification) among species (Generalized Regression; $p \leq 0.0001$) and interaction of species with trichome type (total, glandular and non-glandular) (Generalized Regression; $p \leq 0.0001$) (Figure 4, 5 and 6), but the variation was non-significant between trichome types (Generalized Regression; $p = 0.6971$).

Trichome Dimensions

Similar to density, dimensions of each trichome type also varied across species and location (Figure 7; Table 2 and 3). Subulate non-glandular hair with multiseriate base and tall pedestal on abaxial leaf surface of *S. grandiflorum* (Table 3; Serial number 27) was the longest in dimensions, and the shortest non-glandular trichome was subulate non-glandular hair with multicellular jointed stalk and multicellular base on abaxial leaf surface of *S. ovigerum* (Table 3;

43). Longest glandular trichome type was subulate glandular hair with multicellular jointed stalk, multicellular base, distinct subsidiary cells, and small glandular tip on adaxial leaf surface of *S. melanocerasum* (Table 2; 23), and the shortest glandular trichome type was glandular hair with large globular head on abaxial leaf surface of *S. melongena* (Table 3; 35). The glandular trichome with largest head was glandular hair with large quadricellular globular head and single stalk cell on abaxial leaf surface of *S. lycopersicum* (Table 3; 16). The glandular trichome with smallest glandular tip was hooked subulate glandular hair with multicellular jointed stalk and small glandular tip on abaxial leaf surface of *S. lycopersicum* (Table 3; 17). Dimensions of some trichome types seemed comparable and thus dimension data for few trichome types was collected as one type (Stellate and bifid trichomes; all globular glandular trichomes; glandular trichomes with small tip; simple trichomes).

Although the stellate trichomes had almost consistent spike length within a species or/and leaf surface, but central ray of stellate trichomes varied (long/short) resulting into sub-dividing them into stellate trichomes with short or long central ray. Simple trichomes had the most variation resulting them being both the shortest and the longest trichome found among species in the study. Further, in general, glandular trichomes with globular heads were shorter than glandular trichomes with small tip on the top. Additionally, glandular trichomes with globular heads had greater diameter of their glandular heads than glandular trichomes with small tip on the top. Due to the high species numbers, processing of multiple samples, and incredible trichome diversity, we could not acquire dimensions of some trichome types (for example, osteolate non-glandular hair with multicellular stalk on abaxial leaf surface of *S. dulcamara*; Table 3; 57).

Discussion

In this study, we examined the trichome characteristics including their nomenclature, density, and dimensions on both adaxial and abaxial leaf surface of 14 *Solanum* species using scanning electron microscopy on fresh leaf samples. We found that *Solanum* genus consists of numerous trichome types which vary not only among the species, but also within each species and between adaxial and abaxial leaf surfaces. We also found that three trichome types are most common in *Solanum*: stellate non-glandular, simple non-glandular and glandular trichomes. Broadly, all trichomes have been characterized into glandular and non-glandular trichomes, but it is not fair, because both glandular and non-glandular trichomes can further be classified into various types based on their shape, size, number of cells, basal cells, neck cells, etc. Besides, it was not certain whether ovoid, verrucate and mamilla trichomes are glandular or non-glandular because of their unusual and perplexing structure but we confirm that they can be characterized as non-glandular trichomes because of their lack of distinction of a clear glandular head.

Trichomes, in general, have been proven to be an excellent phenotypic trait for finding evolutionary and taxonomic relationships among species (Cantino, 1990; Khosroshahi and Salmaki, 2019). For example, *Phlomis* genus has characteristic multi-nodal branched trichomes and can be considered as synapomorphy for this group, but *Phlomoides* lacks this feature and thus, this feature most likely represents a plesiomorphy in the genus (Khosroshahi and Salmaki, 2019); and separation of African and Asian *Leucas spp* were made more explicit by the differences of capitate trichomes with definite morphology and absence of non-glandular trichomes with one cell and more than three cells (Mannethody and Purayidathkandy, 2018). Our study characterized the finer details of trichome morphology, and it can be of an aid in exploring phylogenetic and taxonomic relationships among the members of genus *Solanum*, and their

relationship with members of other genus of Solanaceae family and among other plant families. Additionally, trichomes act as excellent cell differentiation models (Hülskamp, 2004) and provided with the diversity from this study, it can be explored how differentiation in trichome cells result into production of glandular/non-glandular of various shapes and sizes.

Defense against herbivores is one of the major functions of trichomes, and both glandular and non-glandular trichomes have been well documented to deter herbivore movement and feeding (Kariyat et al., 2013; 2017; 2019). Morphology, density and dimensions relationships of sub-types of trichomes can be employed to find correlations between trichome characteristics with herbivore feeding intensity and behavior (Li et al., 2020). For instance, Watts and Kariyat (2021) found that significantly higher trichome density on abaxial leaf surface than adaxial leaf surface of Solanaceae species resulted into delayed feeding and lower mass gain of tobacco hornworm caterpillars (*Manduca sexta*; Lepidoptera: Sphingidae); Kariyat et al. (2017) found damage done to peritrophic membrane (gut-lining) of *M. sexta* caterpillars after feeding on stellate trichomes of horsenettle (*Solanum carolinense*; Solanaceae). Further, since the damage done by non-glandular trichomes is primarily because of their structure and many herbivores mow the trichomes off the plant surface before feeding (Kariyat et al., 2017; 2019; Kaur & Kariyat, 2020b), we speculate that trichomes with a greater number of spikes, and spikes with higher dimensions can result into higher negative impacts on herbivore feeding, but warrants closer examination (Medeiros & Moreira, 2005; Andama et al., 2020). The variation in trichome types, density, dimensions and their functional consequences (Watts and Kariyat, 2021) between abaxial and adaxial leaf surfaces also warrants detailed exploration, a reason why we examined these differences in detail (Tables 2 and 3). Contrary to non-glandular trichomes, glandular trichomes are the secretory structures and contain various types of chemicals in their head cells

and those chemicals have been found to trigger different defense related pathways against herbivores (Tissier, 2012), and some glandular trichome types have been found to play more prominent roles than the others. For example, type VI (as named by Luckwill, 1943; glandular trichomes with quadricellular head) trichomes of *Lycopersicon* genus were found to contain chemicals possessing insecticidal properties against lepidopteran larvae (Lin et al., 1987). Thus, knowledge of glandular trichome density and dimensions such as length and diameter can help us know the plant parts with higher trichome density, amount of chemicals possessed by trichomes and if the trichomes are tall enough to act against herbivores with its structural features along with chemical defense. Additionally, expanding on this study, histochemistry and volatile collection of various glandular secretions can be done, and anti-herbivore chemicals can be identified (Muravnik et al., 2019), and can lead to further functional assessment and classification, an area that we are currently exploring. Trichomes have been of great importance against herbivores as a defense trait, and thus, have been incorporated in integrated pest management of insect pests of various crops of economic importance including potato (*Solanum tuberosum*; Solanaceae), cotton (*Gossypium spp*.; Malvaceae), cowpea (*Vigna unguiculata*; Fabaceae), to name a few. For instance, *hooked* non-glandular trichomes of *Phaseolus vulgaris* (Fabaceae) entrap pests such as black bean aphid (*Aphis fabae*; Hemiptera: Aphididae) and green stink bug (*Nezara viridula*; Hemiptera: Pentatomidae) (Rebora et al., 2020). Trichomes also play multiple roles in plants including leaf water uptake and protection from UV light, in addition to defense against herbivores (Sack and Buckley, 2020). For example, Li et al., 2021, showed that among three trichome types viz. non-glandular trichomes, linear glandular trichomes and glandular trichomes, only non-glandular trichomes of Sunflower (*Helianthus annuus*) were found to accumulate and translocate Zinc, an important micronutrient for plants, an potential area

of research to be explored for mineral and nutrient uptake to enhance crop yield through trichomes. Clearly, trichome characteristics has the potential to be explored in relation plant ecophysiological functions such as water use efficiency (Thitz et al., 2017), UV protection and mineral uptake.

Taken together, this study documented the variation in trichome types, their density and dimensions in representative *Solanum* species. So far, the major reasons which withheld the detailed classification and nomenclature of trichomes were (i) the conventional approach to classify trichomes as just glandular or non-glandular trichomes failed to document their morphotypes and function, (ii) the requirement of expensive machinery and skilled professionals, required to process samples across species and families, and (iii) the need of intensive and detailed workflow for the closer examination of images to extract all the data on morphology, density and dimensions. By overcoming these challenges, we show the variation in trichome traits within a subset of the genus *Solanum* and encourage more detailed examination across various plant families.

Conclusions

Overall, the study provides unusually fine details and morphological characterization of trichomes of a mixture of wild and domesticated, annual, and perennial, food crops and weed species of genus *Solanum* which can act as referral source for further studies of most of trichome related parameters and their relationships with biotic and abiotic stresses (Tian, 2012). Since *Solanum* is the largest genus of one of the major angiosperm family viz. Solanaceae, exploring trichome diversity by considering fourteen species from various groups (eg. *S. macrocarpon* and *S. lycopersicum* are cultivated species, while *S. anguivi* and *S. pyracanthos* are wild species) of the family provided us with an updated data source of trichome characteristics with such details

that never has been done before. Further, future directions in trichome studies can be focused on understanding variability and organ development while studying gene expression simultaneously using trichomes as a model. Moreover, trichomes are also known to play role in multi-trophic interactions in ecosystem (Weinhold and Baldwin, 2011) and thus, each trichome type can be explored for its potential in strengthening plants' defenses.

Table 1. List of terminology used to define trichomes in the study.

Terminology	*Definition (compiled from previously published literature)*
Attenuate	Long and gradually tapering
Base	Lowermost part of the trichome
Basilatus	Emerging from a broad base
Bifurcated	Divided into two branches
Brevicolate	Short-necked
Compound	Having multiple rays
Cruciate	Shaped as a cross with four equal arms
Doliform	Barrel-shaped

Falcate	Sickle-shaped
Glandular	Has secretory/excretory function
Hooked	Bent/incurved apex shaped
Head	Has an enlarged terminal portion
Jointed	Presence of apparent articulation
Mamilla	Nipple-shaped projection
Multiradiate	Multi-rayed
Multitangulate	Rays at many angles
Muticous	No pointed tip
Neck	Middle cell of a uniseriate glandular hair
Non-glandular	Without secretory/excretory function
Osteolate	Thighbone shaped with many cells having swollen ends

Ovoid	Egg-shaped with attachment at larger end
Pedestal	Raised base to which hairs are attached
Porrect-geminate	Similar to porrect stellate but consisting of two whorls of rays one over the other
Porrect-stellate	Resemblance with porrect rays of cacti with multiple horizontal rays and a central ray
Pulvinate	Swollen base
Pustulated	Blistered surface
Quadricellular	Four cells
Sessile	Without stalks (for glands)
Setiform	Bristle-shaped
Simple	Unbranched
Smooth	Without any surface irregularities
Stalk	Supporting part of a hair

Stellate	Star-shaped
Subsidiary cells	Neighboring base cells
Subulate	Awl-shaped
Tufted/penicillate	Branched from a base
Uniseriate	Single rows/columns of cells
Verrucate	Warty shaped

Table 2. Detailed morphological characterization (Major shape and additional features) of trichomes on adaxial leaf surface along with pictorial representation, density, and dimensions of trichomes in fourteen *Solanum* species in the study ('very rare' in density table indicate the absence of certain trichome types while counting trichomes at 60X, however the trichome was present very rarely in very few images which were not at 60X magnification; Blank values in density and dimensions table indicate that the density of that particular trichome types has already been included in the density of a broader trichome type, such as density of all glandular trichomes, or density of simple non-glandular trichome types or density of all stellate trichome types as one number rather than individual density of all sub-types of these trichomes; 'no data' in dimension table indicate the lack of dimensions of that trichome;

Asterisks in dimensions table indicate the multiplication sign showing the length of trichome multiplied by width of gland of trichome, in case of glandular trichomes).

Species	*Serial number*	*Trichome types (Major shape)*	*Additional features (Simple smooth uniseriate-S; Compound smooth uniseriate- C; Simple pustulated uniseriate- P)*	*Line art of morphology*	*Density (Average±Standard error; trichome number/mm^2 leaf area)*	*Dimensions (in µm; Length in case of non-glandular trichome; Length*width of gland in case of glandular trichome; Average±Standard error)*

Ethiopian eggplant (*Solanum aethiopicum*)	1.	subulate basilatus *non-glandular* trichome with distinct subsidiary cells	S	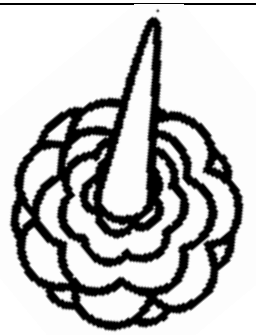	4.73±1.02	153.71±15.67
	2.	multitangulate multiradiate stellate *non-glandular* hair with subulate rays (2-6 in number) with the presence of pedestal	C	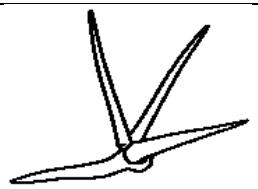	1.06±0.73 (#2 + #3)	185.08±7.29 (#2 and #3)
	3.	bifurcated *non-glandular* hair with subulate rays with the presence of pedestal	C	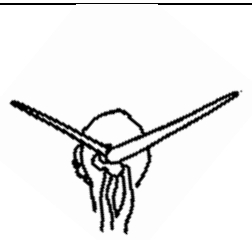	see #2	see #2

	4.	*glandular* hair with small globular head on the top	S	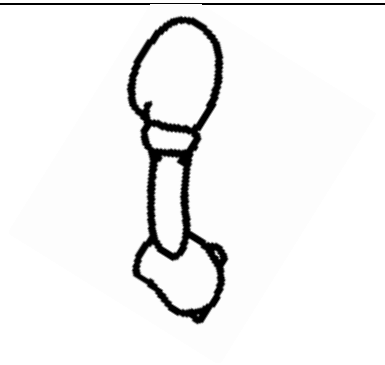	4.88±1.40	65.25±5.58* 25.08±1.88
Forest bitterberry (*Solanum anguivi*)	5.	*glandular* hair with single stalk and neck cell and large quadricellular globular head	S		3.50±0.60	59.58±3.13* 27.11±1.69
	6.	subulate basilatus *non-glandular* hair	S		2.40±0.90	93.14±9

	7.	bifurcated basilatus *non-glandular* hair with subulate rays (one shorter than the other)	C		see #8	see #8
	8.	porrect-stellate multi-radiate *non-glandular* hair with subulate rays (3-10 in number) with long central ray and pedestal	C	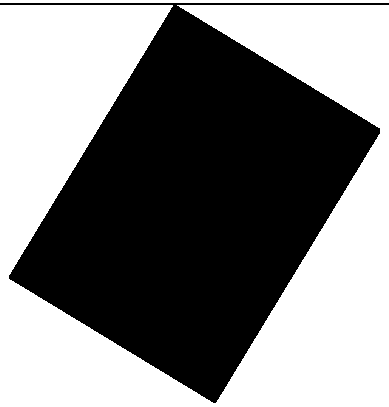	5.92±0.96 (#7 + #8)	133.01±5.39 (#7 and #8)
((Lance-leaved nightshade (*Solanum lanceifolium*)	9.	porrect-stellate multi-radiate *non-glandular* hair with subulate rays (2-7 in number) and short central ray	C	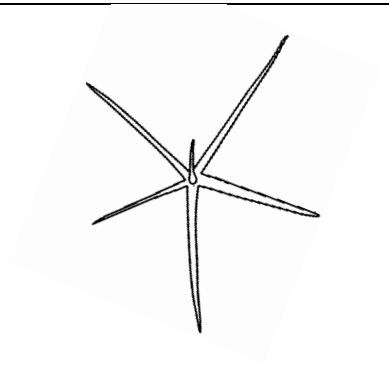	0.72±0.14 (#9 + #10)	193.75±10.22 (#9 and #10)

	10.	porrect-stellate multi-radiate *non-glandular* hair with subulate rays (2-7 in number) and long central ray	C	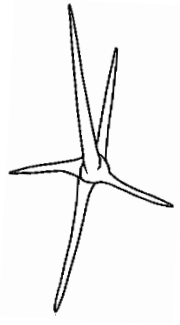	see #9	see #9
	11.	*glandular hair* with single stalk and neck cell and large doliform globular head	S	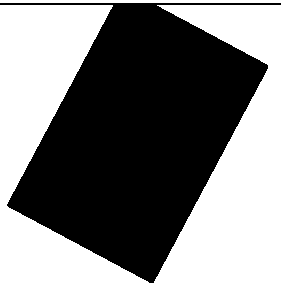	see #12	see #12
	12.	*glandular* hair with large globular head	S		1.45±0.21 (#11 + #12)	66.46±7.19* 28.64±2.67 (#11 and #12)

Garden tomato (*Solanum lycopersicum*)	13.	attenuate *glandular* hair with small glandular tip	S	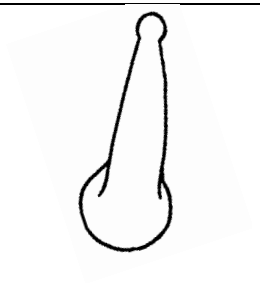	0.55±0.15	63.55±6.35* 9.85±1.25
	14.	*glandular* hair with large globular head	S		0.44±0.11	58.74±3.18* 25.38±2.23
	15.	acuminate *glandular* hair with bicellular stalk and small glandular tip	S		0.05±0.05	327±93.30

	16.	hooked *non-glandular* hair	S		0.97±0.22	218.21±18.24
	17.	attenuate *non-glandular* hair with multicellular jointed stalk and multicellular base	S	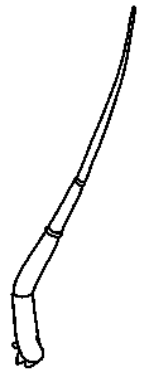	0.17±0.05	327.33±93.30

	18.	attenuate *non-glandular* hair with jointed multicellular stalk	S		0.12±0.06	436.33±44.63
African eggplant (*Solanum macrocarpon*)	19.	attenuate basilatus *glandular* hair with small glandular tip	S	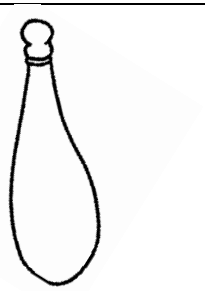	very rare	no data
	20.	subulate *non-glandular* hair with pulvinate base and a pedestal	P		0.22±0.09	288

	21.	*glandular* hair with multicellular large globular head and single stalk cell	S	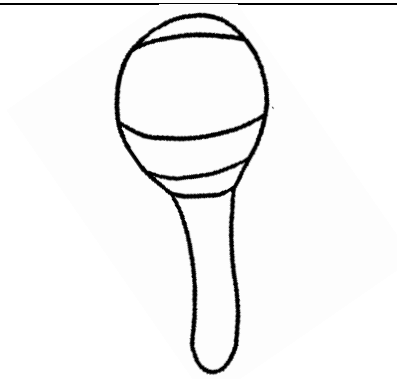	1.88±0.36	72.05±6.99* 24.23±1.55
Huckleberry (*Solanum melanocerasum*)	22.	subulate *non-glandular* hair with multicellular jointed stalk, multicellular base, and distinct subsidiary cells	S	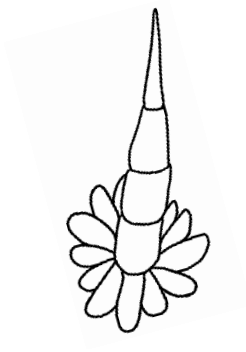	0.23±0.07	421.42±43.01

	23.	subulate *glandular* hair with multicellular jointed stalk, multicellular base, distinct subsidiary cells and small glandular tip	S	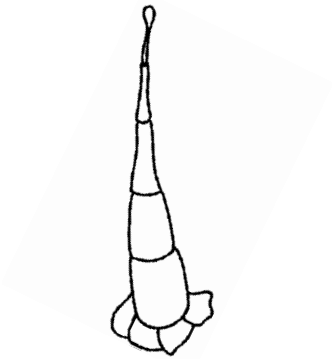	0.02±0.02	461.8±26.03 *20.68±3.67
	24.	*glandular* hair with large globular head, single stalk cell and no neck cell	S		0.77±0.18	78.81±3.11* 32.37±1.49
Potato tree (*Solanum grandiflorum*)	25.	subulate *non-glandular* hair with multiseriate base and tall pedestal	S		0.47±0.47	583.83±121.39

	26.	*glandular* hair with large globular head and single stalk cell	S	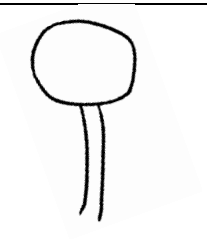	14.57±6.48	80.55±12.72 *32.21±4.34
	27.	ovoid sessile *non-glandular* hair	S		0.19±0.19	no data
	28.	attenuate basilatus *glandular* hair with small glandular tip	S	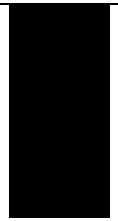	0.19±0.19	256*25.2
	29.	setiform *non-glandular* hair with multicellular base and a pedestal	S	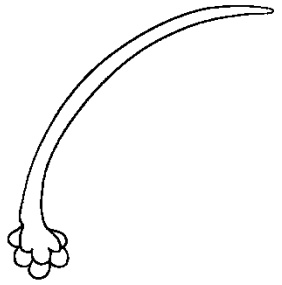	0.94±0.75	549.25±96.85

Eggplant (*Solanum melongena*)	30.	porrect-geminate stellate multi-radiate *non-glandular* hair with subulate rays (2-16 in number) and short central ray	C	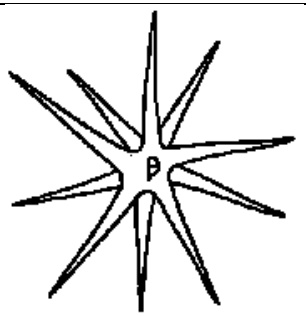	8.34±1.26	168±7.46
	31.	subulate *non-glandular* hair with pulvinate base and pedestal	S		0.19±0.19	64.4±14
	32.	*glandular* hair with large globular head	S		0.41±0.20	47.3±0.9*13.1±0.85

Solanum taeniotrichum	33.	subulate *glandular* hair with multicellular jointed stalk and small glandular tip	S	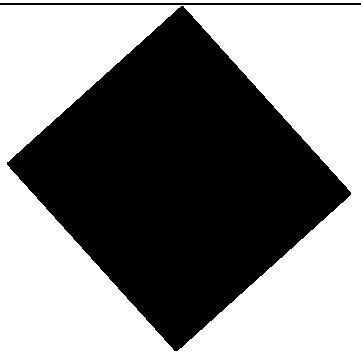	7.20±0.76	385±75*48.1±23.8
	34.	*glandular* hair with small globular head	S	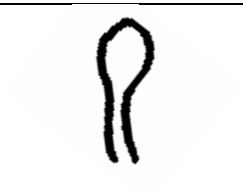	0.44±0.35	no data
Pepino lloron (*Solanum caripense*)	35.	*glandular* hair with small globular head	S	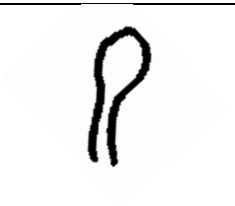	0.75±0.11	52.3±14.2*32.2±12.5

	36.	subulate basilatus *non-glandular* hair with multicellular jointed stalk and multicellular base	S	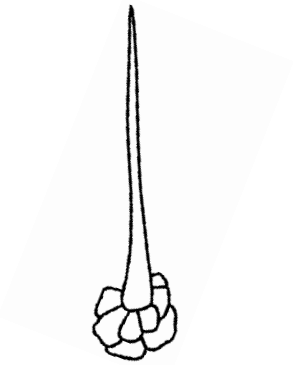	0.88±0.19	431.44±73.48
	37.	subulate *non-glandular* hair with multicellular jointed stalk	S	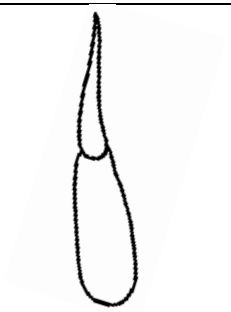	0.12±0.06	287±107
Easter white eggplant (*Solanum*	38.	*glandular* hair with small globular head	S		0.44±0.22	54.3±7.17*2 2.4±4.14

ovigerum)	39.	porrect-stellate multi-radiate *non-glandular* hair with subulate rays (3-7 in number) and with long central ray	C	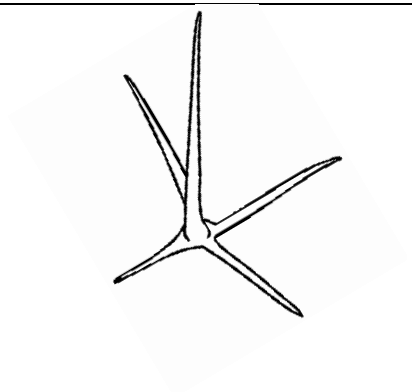	1.38±0.56	198±10.8
	40.	subulate *non-glandular* hair with pulvinate base	S	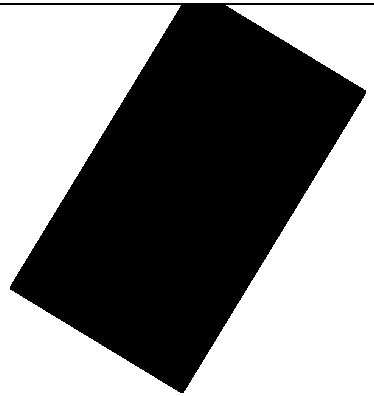	2.13±0.49	153.84±42.38
Solanum asperolanatum	41.	*glandular* hair with large globular head, single stalk cell and no neck cell	S	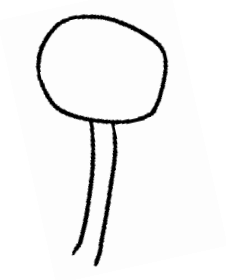	17.30	68.9±5.4*20.6±10.9

	42.	ovoid sessile *non-glandular* hair	S		2.25	105±55
	43.	tufted/penicillate *non-glandular* hair with multiseriate long pedestal	C	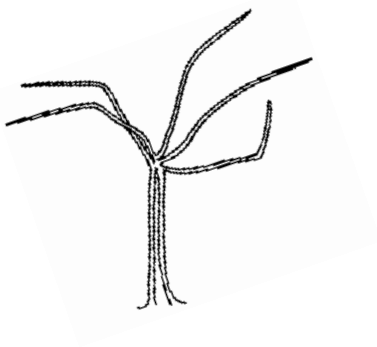	1.31	918±30.7
Porcupine tomato (*Solanum*	44.	*glandular* hair with small globular head	S		0.62±0.24	48.6±2.87*28±2.12

pyracanthos)	45.	porrect-stellate multi-radiate *non-glandular* hair with subulate rays (2-12 in number) and short central ray	C	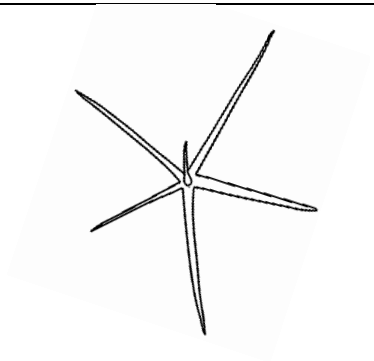	4.13±1.02	199±6.61
	46.	subulate *non-glandular* hair with multicellular stalk and base cells	S	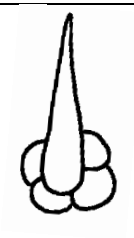	0.60±0.20	107±15.6
Bittersweet nightshade (*Solanum*	47.	subulate basilatus *non-glandular* hair with multicellular stalk	S		0.52±0.10	158±14

dulcamara)	48.	*glandular* hair with small globular head	S		0.19±0.11	no data

Table 3. Detailed morphological characterization (Major shape and additional features) of trichomes on adaxial leaf surface along with pictorial representation, density, and dimensions of trichomes in fourteen *Solanum* species in the study ('very rare' in density table indicate the absence of certain trichome types while counting trichomes at 60X, however the trichome was present very rarely in very few images which were not at 60X magnification; Blank values in density and dimensions table indicate that the density of that particular trichome types has already been included in the density of a broader trichome type, such as density of all glandular trichomes, or density of simple non-glandular trichome types or density of all stellate trichome types as one number rather than individual density of all sub-types of these trichomes; 'no data' in dimension table indicate the lack of dimensions of that trichome; Asterisks in dimensions table indicate the multiplication sign showing the length of trichome multiplied by width of gland of trichome, in case of glandular trichomes).

Species	*Serial number*	*Trichome types*	*Additional features (Simple smooth uniseriate- S; Compound smooth uniseriate- C; Simple pustulated uniseriate- P)*	*Line art of morphology*	*Density (Average±Standard error; trichome number/mm^2 leaf area)*	*Dimensions (in µm; Length in case of non-glandular trichome; Length*width of gland in case of glandular trichome; Average±Standard error)*

Ethiopian eggplant (*Solanum aethiopicum*)	1.	attenuate *glandular* hair with small glandular tip	S	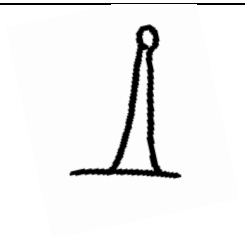	0.86±0.86	101.24±20.42*13.66±1.74
	2.	*glandular* hair with large globular head on the top	S		0.52±0.20	52.06±3.83*17.11±0.82
	3.	subulate hooked *non-glandular* hair with pulvinate base	S		0.82±0.79	88.55±10.79

	4.	porrect-stellate multiradiate *non-glandular* hair with subulate rays (5-10 in number) and short central ray	C	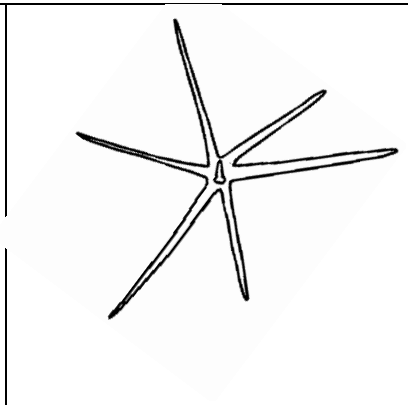	15.26±4.60	241.82±6.36
(Forest bitterberry (*Solanum anguivi*)	5.	*glandular* hair with single stalk and neck cell and quadricellular globular head	S		0.72±0.21	46.6±5.1*23 .35±0.25
	6.	subulate *non-glandular* hair with pulvinate base	S		0.19±0.14	113±28.63

	7.	porrect-stellate multi-radiate *non-glandular* hair with subulate rays (5-10 in number) and short central ray and pedestal	C	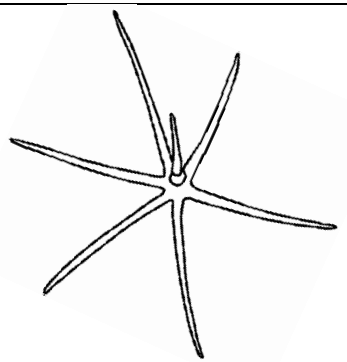	13.00±1.56 (#7 + #8 + #9)	290.85±9.83 (#7, #8 and #9)
	8.	porrect-stellate multi-radiate *non-glandular* hair with subulate rays (5-10 in number) with long central ray and pedestal	C	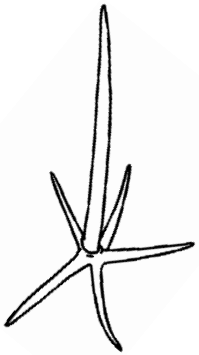	see #7	see #7
	9.	bifurcated basilatus *non-glandular* hair with subulate rays (one shorter than the	C		see #7	see #7

		other)				
Lance-leaved nightshade (*Solanum lanceifolium*)	10.	attenuate *glandular* hair with small globular tip	S		see #12	no data
	11.	verrucate *non-glandular* hair	S		see #12	no data
	12.	*glandular* hair with large globular head	S		6.04±0.35 (#10, #11 and #12)	40.88±1.22* 23.79±1.23

	13.	porrect-stellate multi-radiate *non-glandular* hair with subulate rays (2-6 in number) and with short central ray	C	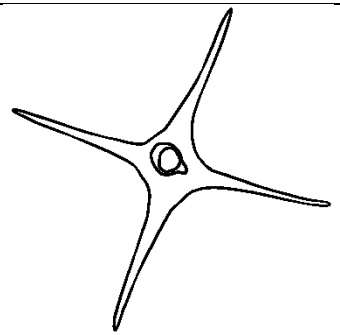	3.38±0.63 (#13+ #14)	156.28±11.76 (#13 and #14)
	14.	bifurcated basilatus *non-glandular* hair with subulate rays (one arm reduced)	S		see #13	see #13
Garden tomato (*Solanum lycopersicum*)	15.	*glandular* hair with large quadricellular globular head and single stalk cell	S		0.94±0.19 (#15 + #16)	42.25±4.69* 23.32*3.07

	16.	*glandular* hair with large quadricellular globular head and single stalk cell	S	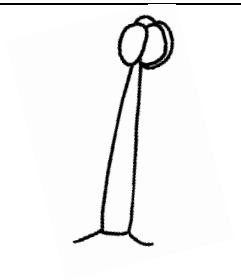	see #15	158±21.38* 66.57±3.45
	17.	hooked subulate *glandular* hair with multicellular jointed stalk and small glandular tip	S	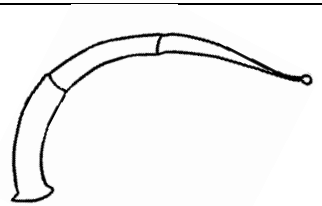	0.30±0.22	378.5±29.23 *3.50
	18.	hooked subulate *non-glandular* hair	S		5.4±1.03	204.34±16.40

	19.	attenuate *non-glandular* hair with jointed multicellular stalk	S		0.35±0.10	884.38±84.30
	20.	attenuate basilatus *glandular* hair with small glandular tip	S		very rare	57.45±8.14* 7.55±0.91
	21.	mamilla *non-glandular* hair	S		very rare	no data
Gboma (*Solanum macrocarpon*)	22.	*glandular* hair with large globular head and single stalk cell	S	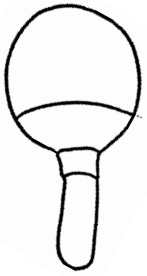	3.03±0.58	72.83±6.79* 31.69±1.38

	23.	subulate *non-glandular* hair with pulvinate base and a pedestal	P		0.02±0.02	301.66±21.6
Huckleberry (*Solanum melanocerasum)*	24.	crescent *non-glandular* hair with multicellular jointed stalk	S		0.18±0.05	312±38.83
	25.	subulate *glandular* hair with multicellular jointed stalk and small glandular tip	S		very rare	337.5±39.63 *24.85±2.7

	26.	*glandular* hair with large globular head, single stalk cell and no neck cell	S	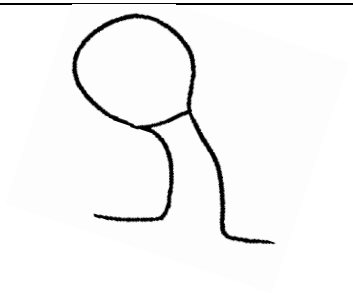	0.81±0.12	73.46±4.52* 35.09±2.16
Potato tree (*Solanum grandiflorum*)	27.	subulate *non-glandular* hair with multiseriate base and tall pedestal	S		very rare	1194±395.5
	28.	*glandular* hair with large globular head and single stalk cell	S		10.15±2.25 (#28 + #29 + #31)	283.2±180.46*37.9±7.26 (#28, #29 and #31)
	29.	ovoid sessile *non-glandular* hair	S		see #28	see #28

	30.	porrect-stellate multi-radiate cruciate *non-glandular* hair with subulate rays (4 in number) and short central ray	C	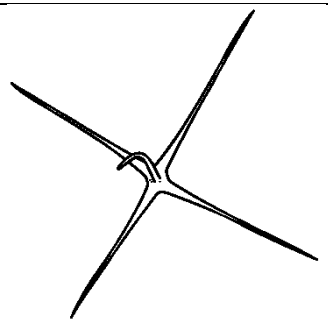	0.47±0.09	887.25±103.31
	31.	*glandular* hair with large globular head, single stalk cell and no neck cell	S	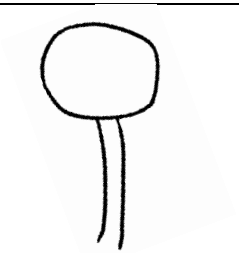	see #28	see #28
	32.	falcate *non-glandular* hair with pulvinate base	S		0.56±0.19	no data

Eggplant (*Solanum melongena*)	33.	hooked subulate *non-glandular* hair with a pulvinate base	S		0.08±0.04	103
	34.	porrect-geminate stellate multi-radiate *non-glandular* hair with subulate rays (2-16 in number) and short central ray	C	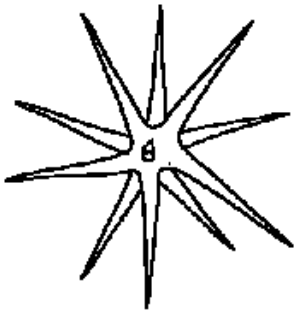	10.12±1.96	211±8.9
	35.	*glandular* hair with large globular head	S		1.48±0.33	44.3±3.86*1 6.9±0.94

Solanum taeniotrichum	36.	subulate basilatus *glandular* hair with multicellular jointed stalk and small glandular tip	S	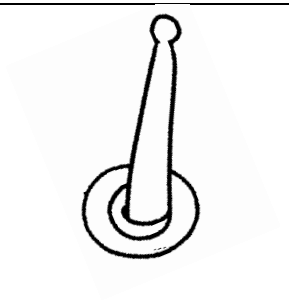	8.21±0.76 (#36+ #37)	344±62*21.8±2.33 (#36 and #37)
	37.	subulate basilatus *glandular* hair with multicellular jointed stalk, multicellular base and small glandular tip	S	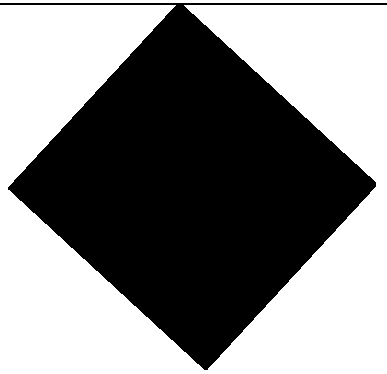	see #36	see #36
	38.	*glandular* hair with small globular head	S		0.44±0.27	51.9±2.55*24.4±8.83

	39.	subulate *non-glandular* hair	S		0.06±0.06	1010
Pepino lloron (*Solanum caripense*)	40.	hooked subulate *non-glandular* hair	S		very rare	no data
	41.	subulate *non-glandular* hair	S		0.66±0.11	318±58.5
	42.	*glandular* hair with large quadricellular globular head	S		0.66±0.22	53±8*22.9± 4.65

Easter white eggplant (*Solanum ovigerum*)	43.	subulate *non-glandular* hair with multicellular jointed stalk and multicellular base	S	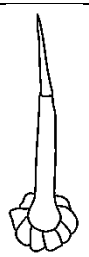	0.23±0.12	63.7±6.35
	44.	falcate *non-glandular* hair	S		very rare	no data
	45.	porrect-stellate multi-radiate *non-glandular* hair with subulate rays (2-12 in number) and with short central ray and pedestal	C	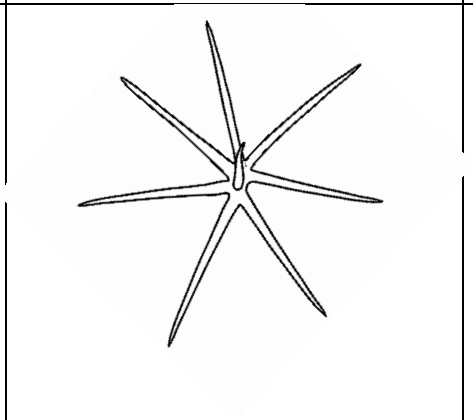	2.4±0.76	229±11.7

	46.	*glandular* hair with small globular head	S	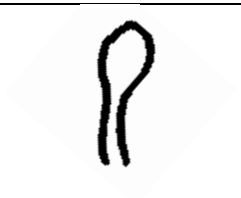	0.90±0.32	49.6±5.32*3 2.7±28
Solanum asperolantum	47.	ovoid sessile *non-glandular* hair	S		0.38±0.38	no data
	48.	*glandular* hair with large globular head, single stalk cell and no neck cell	S	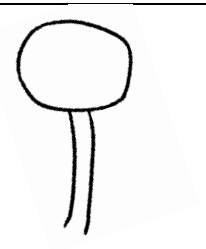	3.95±1.03	118±19.4*2 6.55±1.82
	49.	porrect-stellate multi-radiate *non-glandular* hair with subulate rays (4-5 in number) and with short central ray	C	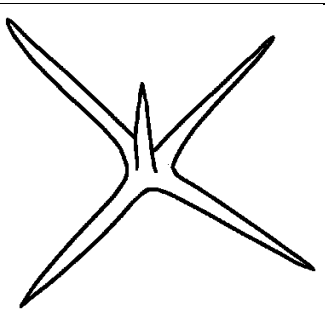	0.12±0.12	127±20.4

	50.	*non-glandular* hair with attenuate non-glandular branches and one gland-tipped branch	C	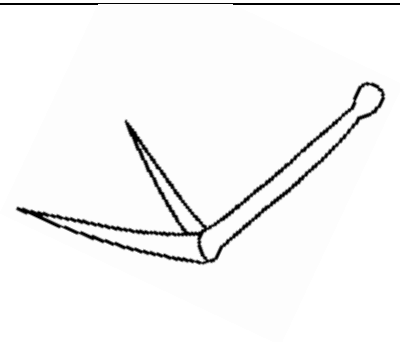	0.06±0.06	201*39.4
Porcupine tomato (*Solanum pyracanthos*)	51.	porrect-stellate multi-radiate *non-glandular* hair with subulate rays (2-12 in number) and with short central ray and pedestal	C	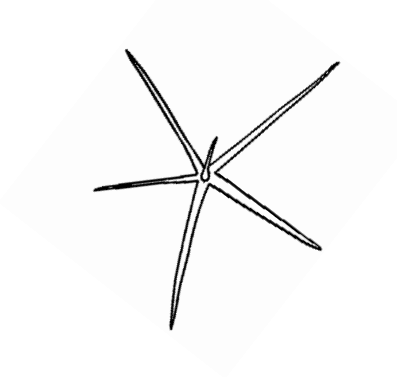	7.08±1.50 (#51+ #53)	265±8.5 (#51 and #53)

	52.	*glandular* hair with large globular head	S		0.53±0.24	55±5.2*30.1 ±3.29
	53.	bifurcated *non-glandular* hair with subulate rays with pulvinate multicellular base	C		see #51	see #51
	54.	hooked *non-glandular* hair	S		0.25±0.14	126±6.5

Bittersweet nightshade (*Solanum dulcamara*)	55.	*glandular* hair with small globular head	S		3.2±0.33	86.7±5.25*28±1.65
	56.	attenuate basilatus *glandular* hair with small glandular tip	S		0.04±0.04	no data
	57.	osteolate *non-glandular* hair with multicellular stalk	P		0.07±0.05	no data

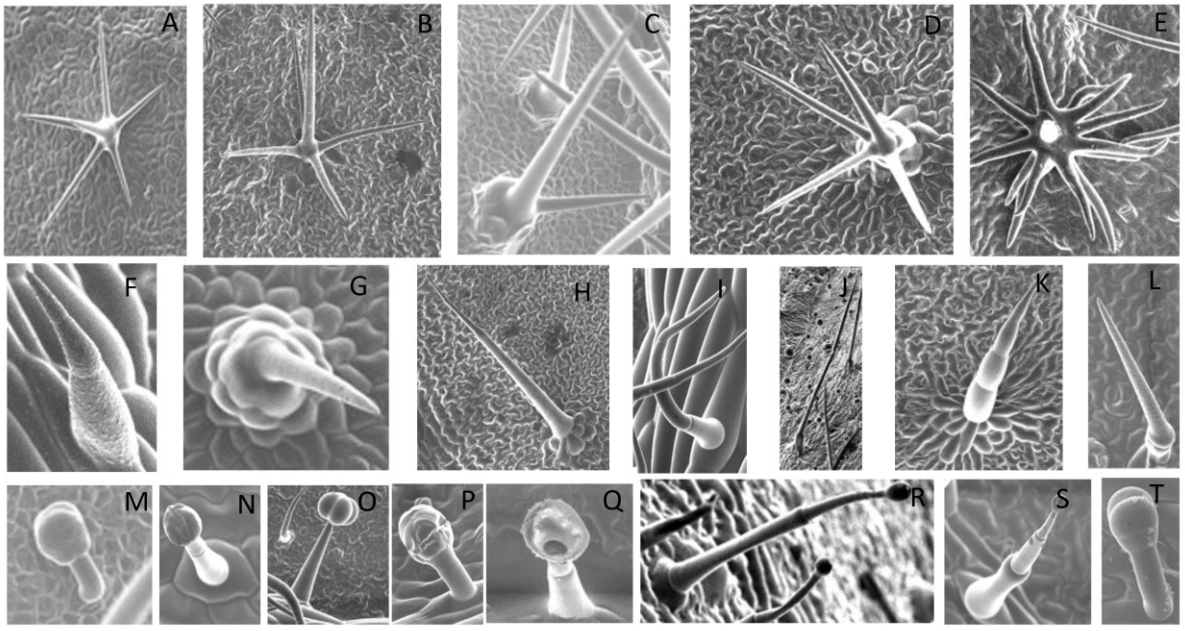

Figure 1: The three major trichome types found in the study includes (A-E) Stellate non-glandular trichomes, (F-L) Simple non-glandular trichomes, and (M-T) glandular trichomes. Figure shows scanning electron microscopic images of (A) porrect-stellate multi-radiate non-glandular hair with subulate rays (2-7 in number) and with short central ray on adaxial leaf surface of *Solanum lanceifolium* (B) porrect-stellate multi-radiate non-glandular hair with subulate rays (3-7 in number) and with long central ray on adaxial leaf surface of *S. ovigerum* (C) bifurcated basilatus non-glandular hair with subulate rays (one shorter than the other) on adaxial leaf surface of *S. anguivi* (D) multitangulate multiradiate stellate non-glandular hair with subulate rays (2-6 in number) with the presence of pedestal on adaxial leaf surface of *S. aethiopicum* (E) porrect-geminate stellate multi-radiate non-glandular hair with subulate rays (2-16 in number) and short central ray on abaxial leaf surface of *S. melongena* (F) osteolate non-

glandular hair with multicellular stalk on abaxial leaf surface of *S. dulcamara* (G) subulate basilatus non-glandular trichome with distinct subsidiary cells on adaxial leaf surface of *S. aethiopicum* (H) subulate basilatus non-glandular hair with multicellular jointed stalk and multicellular base on adaxial leaf surface of *S. caripense* (I) hooked subulate non-glandular hair on abaxial leaf surface of *S. lycopersicum* (J) subulate non-glandular hair with multiseriate base and tall pedestal on *S. grandiflorum* (K) subulate non-glandular hair with multicellular jointed stalk, multicellular base and distinct subsidiary cells on adaxial leaf surface of *S. melanocerasum* (L) subulate non-glandular hair with pulvinate base and a pedestal on adaxial leaf surface of *S. macrocarpon* (M) glandular hair with single stalk and neck cell and large quadricellular globular head on adaxial leaf surface of *S. anguivi* (N) glandular hair with single stalk and neck cell and large doliform globular head on adaxial leaf surface of *S. lanceifolium* (O) glandular hair with large quadricellular globular head and single stalk cell on abaxial leaf surface of *S. lycopersicum* (P) glandular hair with large globular head and single stalk cell on abaxial leaf surface of *S. macrocarpon* (Q) glandular hair with large globular head and single stalk cell on abaxial leaf surface of *S. grandiflorum* (R) subulate basilatus glandular hair with multicellular jointed stalk and small glandular tip on abaxial leaf surface of *S. taeniotrichum* (S) subulate glandular hair with multicellular jointed stalk and small glandular tip on adaxial leaf surface of *S. taeniotrichum* (T) glandular hair with small globular head on adaxial leaf surface of *S. ovigerum.*

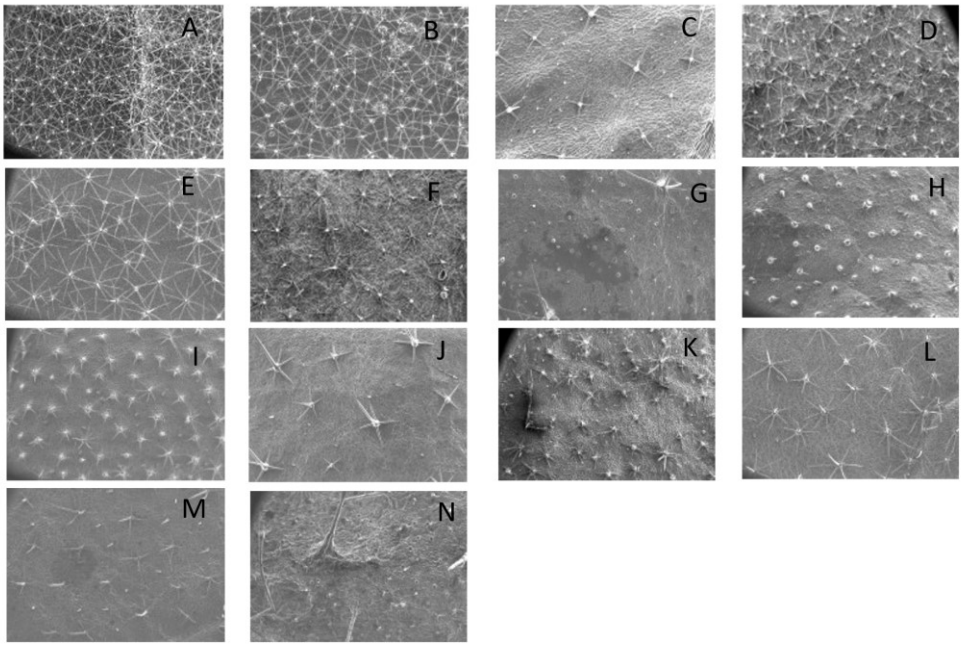

Figure 2: Scanning Electron Microscopic (SEM) images captured at 60X magnification of abaxial (A-G) and adaxial (H-N) leaf surface of (A, H) *Solanum aethiopicum* (B, I) *Solanum anguivi* (C, J) *Solanum lanceifolium* (D, K) *Solanum melongena* (E, L) *Solanum pyracanthos* (F, M) *Solanum ovigerum* (G, N) *Solanum grandiflorum* with the presence of stellate non-glandular trichomes as one of the major trichome types.

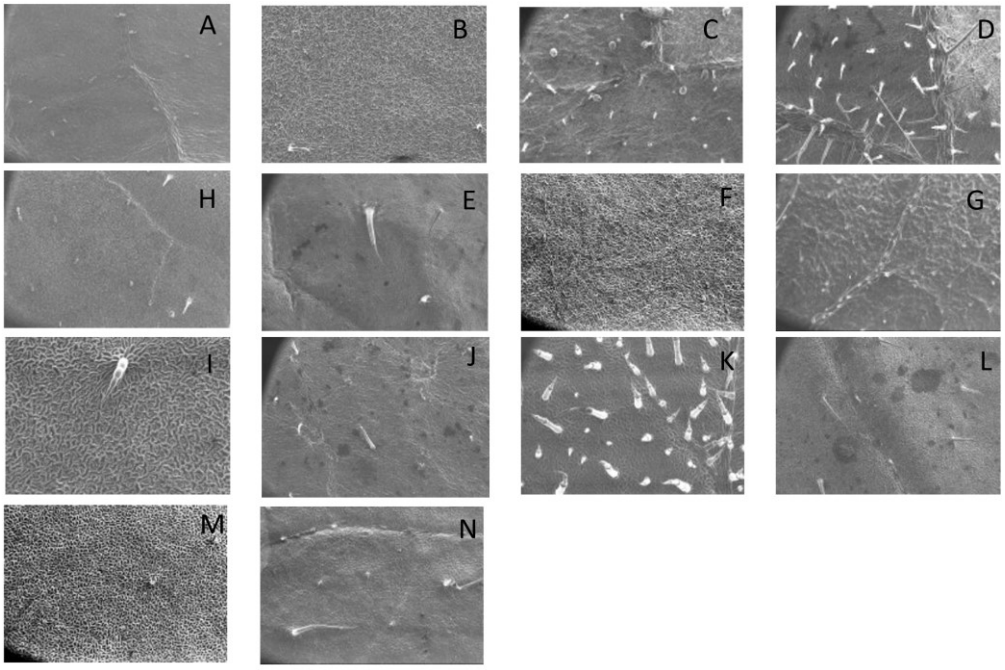

Figure 3: Scanning Electron Microscopic (SEM) images captured at 60X magnification of abaxial (A-G) and adaxial (H-N) leaf surface of (A, H) *Solanum macrocarpon* (B, I) *Solanum melanocerasum* (C, J) *Solanum asperalanatum* (D, K) *Solanum taeniotrichum* (E, L) *Solanum caripense* (F, M) *Solanum dulcamara* and (G, N) *Solanum lycopersicum*, with stellate non-glandular trichome absent as a major trichome type.

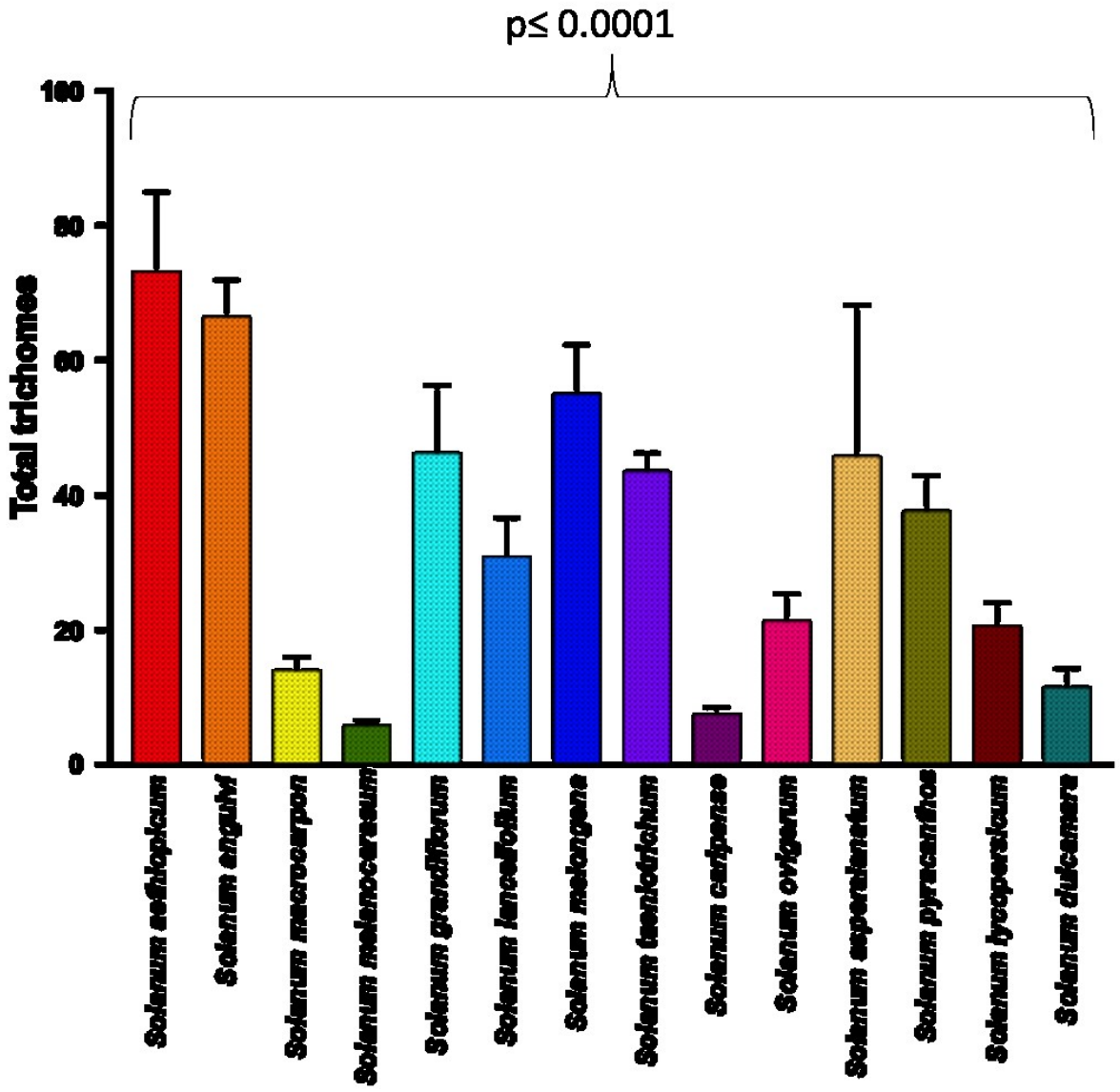

Figure 4. Significant variation in total trichome density (Generalized regression; p= <0.0001) among 14 *Solanum* species.

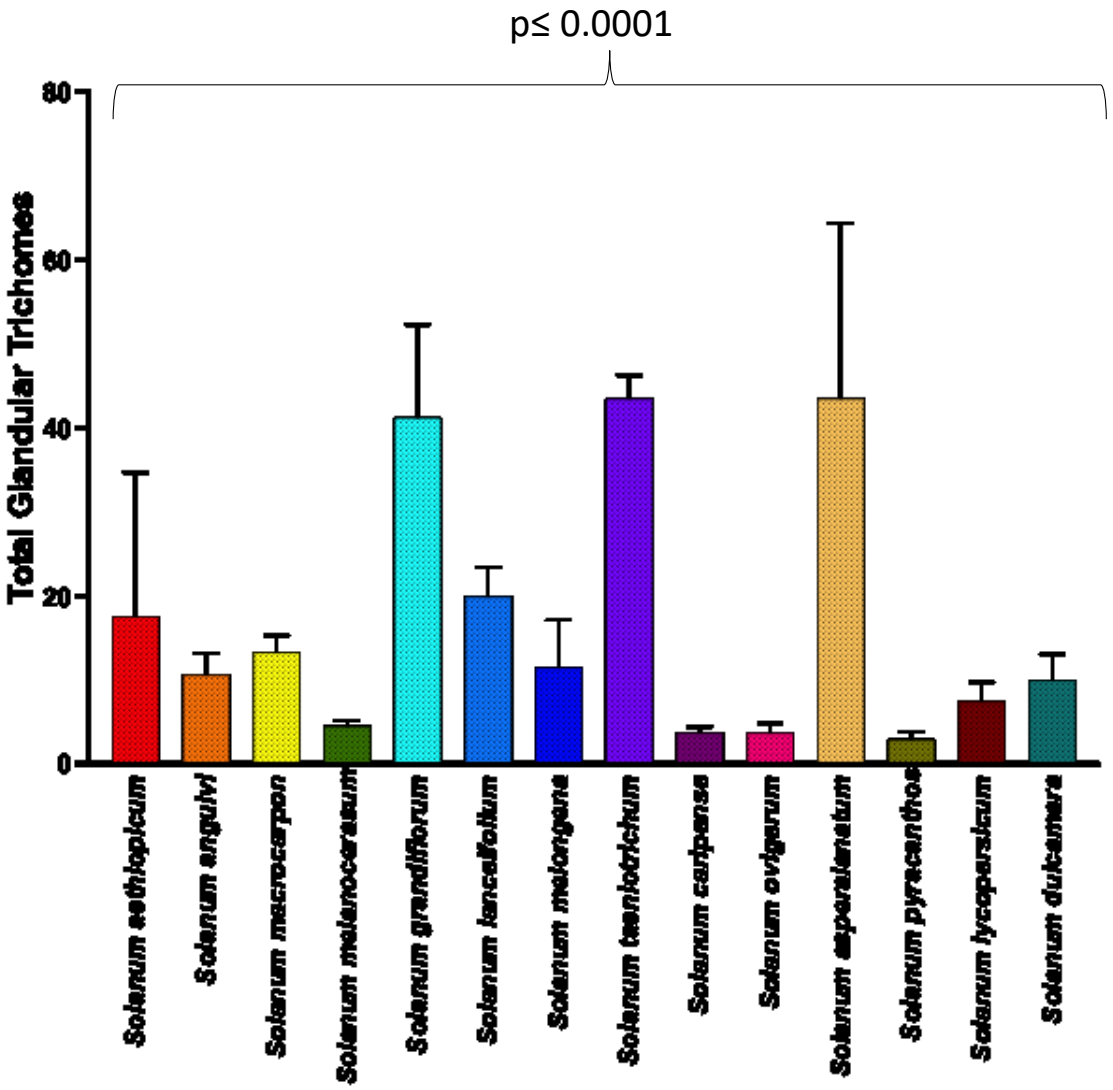

Figure 5. Significant variation in total glandular trichome density (Generalized regression; p= <0.0001) among 14 *Solanum* species.

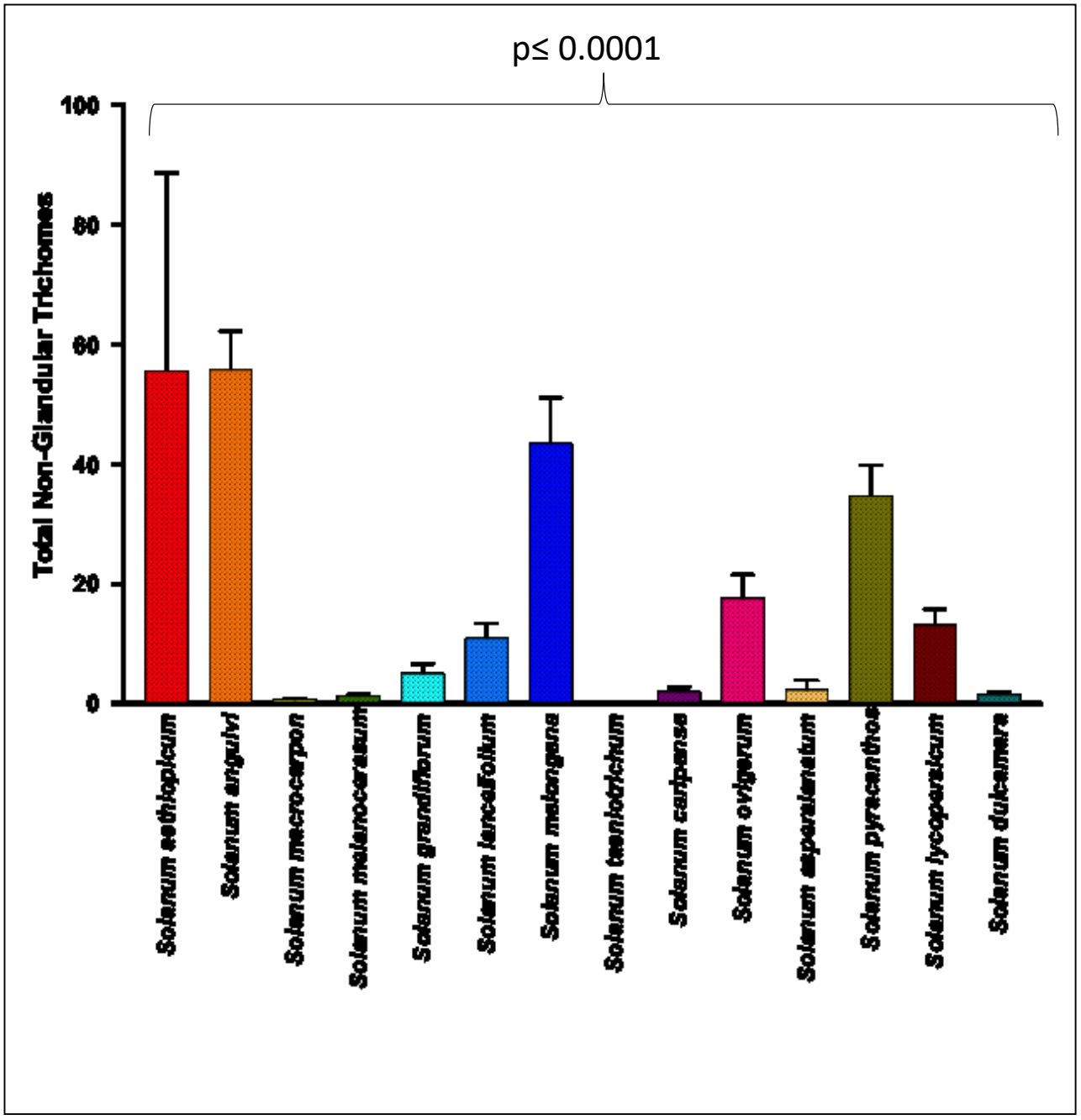

Figure 6. Significant variation in total non-glandular trichome density (Generalized regression; p= <0.0001), among 14 *Solanum* species.

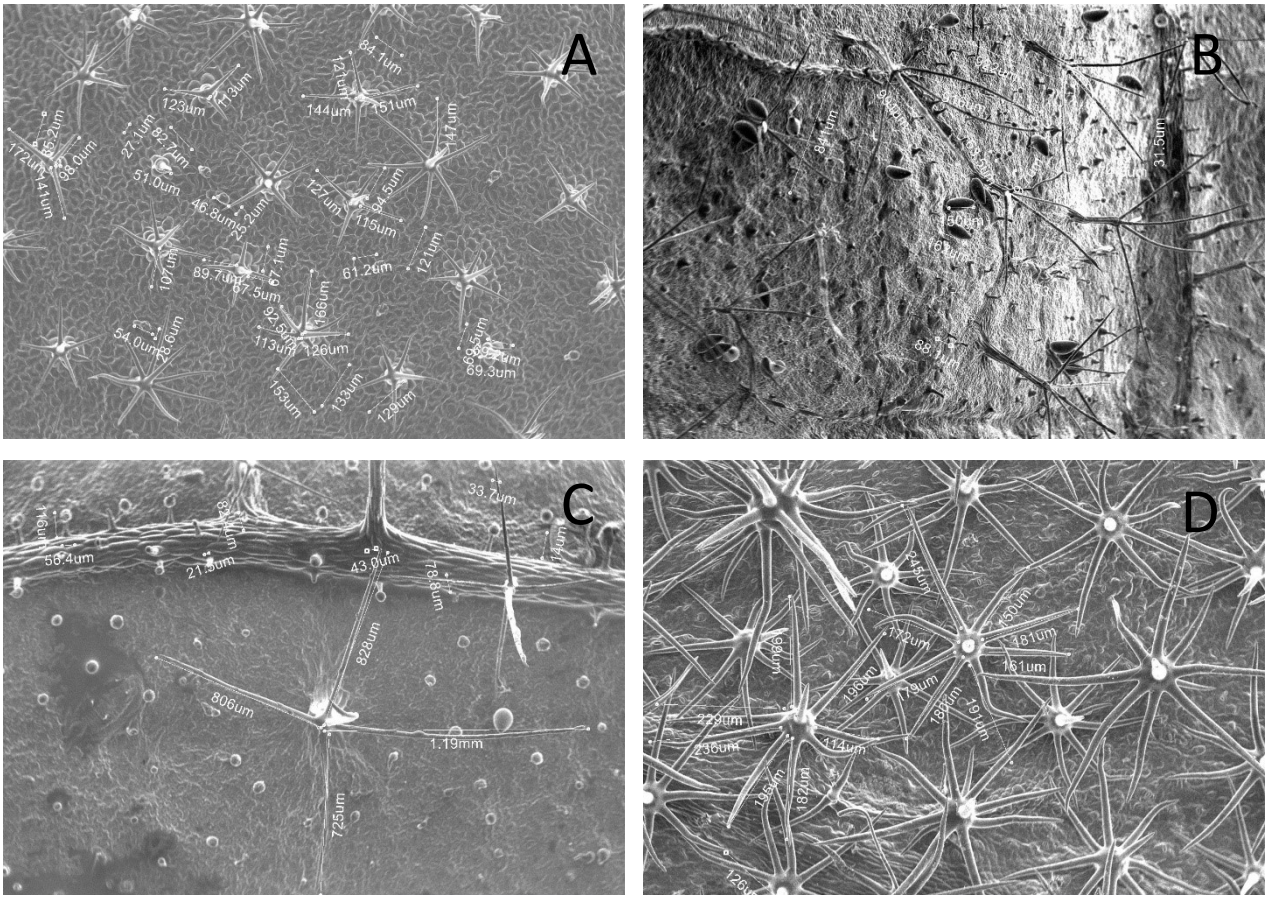

Figure 7: Dimension measurement of different trichome types on (A) adaxial leaf surface of *Solanum anguivi at* 100X (B) adaxial leaf surface of *S. aperolanatum* at 45X (C) abaxial leaf surface of *S. melongena* at 150 X (D) abaxial leaf surface of *S. grandiflorum* at 60X, by tracing the trichome projections (length of hair and diameter of bulb in case of glandular trichomes, and length of hair/spike in case of non-glandular trichomes) using the 'Nanoeye' software.

CHAPTER II

DESKTOP SCANNING ELECTRON MICROSCOPY IN PLANT-INSECT INTERACTIONS RESEARCH: A FAST AND EFFECTIVE WAY TO CAPTURE ELECTRON MICROGRAPHS WITH MINIMAL SAMPLE PREPARATION

Abstract

The ability to visualize cell and tissue morphology at a high magnification using scanning electron microscopy (SEM) has revolutionized plant sciences research. In plant-insect interactions studies, SEM based imaging has been of immense assistance to understand plant surface morphology including trichomes (plant hairs; physical defense structures against herbivores (Kaur and Kariyat, 2020a, 2020b; Watts and Kariyat, 2021), spines, waxes, and insect morphological characteristics such as mouth parts, antennae and legs, that they interact with. While SEM provides finer details of samples, and the imaging process is simpler now with advanced image acquisition and processing, sample preparation methodology has lagged. The need to undergo elaborate sample preparation with cryogenic freezing, multiple alcohol washes and sputter coating makes SEM imaging expensive, time consuming, and warrants skilled

professionals, making it inaccessible to majority of scientists. Here, using a desktop version of Scanning Electron Microscope (SNE- 4500 Plus Tabletop), we show that the "plug and play" method can efficiently produce SEM images with sufficient details for most morphological studies in plant-insect interactions. We used leaf trichomes of *Solanum* genus as our primary model, and oviposition by tobacco hornworm (*Manduca sexta*; Lepidoptera: Sphingidae) and fall armyworm (*Spodoptera frugiperda*; Lepidoptera: Noctuidae), and leaf surface wax imaging as additional examples to show the effectiveness of this instrument and present a detailed methodology to produce the best results with this instrument. While traditional sample preparation can still produce better resolved images with less distortion, we show that even at a higher magnification, the desktop SEM can deliver quality images. Overall, this study provides detailed methodology with a simpler "no sample preparation" technique for scanning fresh biological samples without the use of any additional chemicals and machinery.

Introduction

While we can clearly see leaves, roots, and flowers with our naked eye- plants and animals have functionally complex and morphologically diverse structures which necessitates the need of advanced microscopy techniques to comprehend microscopic structures such as tissues and cells (Caldwell and Iyer-Pascuzzi, 2019). These structures tend to have complex morphological variations, which can only be visualized by advanced and powerful microscopy (Palaiologou et al., 2020). For example, while pollen is visible, individual pollen grains typically range in size between 25 and 50 μm (Kelly et al., 2002) and can be studied more effectively with microscopy. Similarly, insect antennae and trichomes also range in micrometers and are difficult to observe in detail with the naked eye. Therefore, to understand the ultra-structure and to penetrate beyond the visible surface morphology, various microscopy tools are routinely

employed (Mustafa et al., 2018). Light microscope is popular and commonly used for this purpose but is limited by extremely low resolution and limited specimen compatibility (Wollman et al., 2015).

Alternatively, a Scanning Electron Microscope (SEM) can acquire images ranging from magnifications of 10X to 500,000X, using secondary electrons (Zhu et al., 2009), X-rays (Kotula et al., 2003) and electron beams (Nakamura et al., 2021) that interact with the specimen while collecting the scattered radiation to produce an image (Inkson, 2016). For the past few decades, SEM has revolutionized imaging by helping to understand the microstructure of biological samples, cell lines, superconductors, micro-crystallization of nano particles, and many more (Zhang et al., 2020a). Plant-insect interactions studies utilize SEM quite often because the filed routinely examines morphological traits of insects and plants and their interactions between them, and among other components of the environment (Pathan et al., 2008; McCully et al., 2009; Kaur et al., 2020). For example, plants morphological traits including trichomes, stomata, waxes, and pollen show tremendous variation like their insect counterparts including their antennae, eggs, mouth parts, legs, and wings vary immensely among them (Krenn, 2009; Singh and Kumari, 2020), commonly imaged using SEM.

As the use of SEM has exponentially increased in last few decades, the technological advances in microscopy have also improved (Sujata and Jennings, 1991; Stokes, 2004; Newbury and Ritchie, 2015; Weigend et al., 2017). However, due to the lack of innovation in sample preparation methodology, SEM imaging remains a time consuming and expensive process (Inkson, 2016; Kariyat et al., 2017). As a result of the time consuming and expensive sample preparation associated with SEM prior to the actual scanning of sample, SEM is still limited to core facilities across various research and educational institutions. Due to the lack of a simpler

protocol, microscopists follow lengthy and complex procedures of sample preparation and image processing involving fixation of sample using critical buffers (e.g., glutaraldehyde) overnight, tissue drying through sequential alcohol washes, critical point drying and sputter coating of sample, which not only adds up cost and efforts, but can also take minimum of 6-10 hours to get samples ready to be processed for imaging (Kariyat et al., 2017; Table 1). Moreover, SEM demands skilled personnel and technical expertise to acquire quality images, thus limiting its use to core facilities or big-budget laboratories with the technicians available. It is quite evident that SEM imaging warrants methodology that can retain its quality in imaging, but it can also shorten the timeline.

To overcome intensive and expensive methodology associated with traditional SEM, we have been using the SNE- 4500 Plus, a tabletop SEM (Nanoimages LLC, Pleasanton, CA, USA) that requires almost no sample preparation before imaging. The Desktop SEM (DSEM) can capture images up to x200,000 magnification, while providing precise 3-D imaging of morphology and dimensions of structures seen in the samples. The DSEM is equally capable of capturing miniature plant features and ultra-structures of objects, thus providing detailed morphological characterization. For instance, one of the biggest advantages of DSEM is its ability to use fresh specimens (having high water content such as leaves an almost impossible task with a traditional SEM), cutting back on elaborative and tedious sample preparation time. Since DSEM requires no sample preparation before imaging and only takes 15 minutes for image acquisition (Table 2), it allows for more throughput processing unlike traditional SEM (Table 1). Moreover, it is user-friendly as it requires little or no technical expertise, and its cost effectiveness makes it possible for individual laboratories to possibly acquire and can also serve

as a learning opportunity for students who can use it on a routine basis by themselves without supervision.

DSEM is even more beneficial in plant-insect interactions studies, where plant and insect images are routinely studied at microscopic levels (Silva et al., 2017; Watts and Kariyat, 2021). Previously, we have documented that trichomes not only act as a mechanical barrier to the movement and feeding of caterpillars but can also damage the peritrophic membrane of caterpillars and are even present in the frass pellets of these caterpillars (Kariyat et al., 2017; 2019). Furthermore, to test for subtle differences in treatments (e.g., damaged versus undamaged; inbred versus outbred plants; Kariyat et al., 2017), we require fast and throughput imaging, an almost impossible feat with traditional high-performance SEM. Resorting to simple light microscopy on the other hand can lead to missing key details. For example, trichomes can be classified into glandular and non-glandular types, based on the presence or absence of glandular top, and silverleaf nightshade (*Solanum elaeagnifolium* Cav.; Solanaceae), a worldwide invasive weed, has been found to have a dense mat of non-glandular stellate trichomes (Kariyat et al., 2018; Chavana et al., 2021). However, using the DSEM, we recently found that in addition to non-glandular stellate trichomes, also possess a low density of glandular trichomes, almost impossible to detect through light microscopy. And, in a recent study (Watts and Kariyat, 2021), we imaged 11 Solanaceae species, and leaves for each leaf surface (adaxial and abaxial) to determine the statistical significance between treatment groups (species; leaf surface)- clearly showing the need for extensive and thorough imaging which could have only been possible with SEM needing no prior sample preparation. DSEM can also distinguish the sub-parts of these microscopic hairs. In addition, DSEM also aided us to observe epicuticular wax along with trichomes present on the leaf surface in species like *Solanum glaucescens* Zucc.

We show how DSEM can acquire images of various biological samples and their morphological features with precision, without the costs or time associated with traditional SEM.

Materials and Methods

Instrument specific methodology for image acquisition:

There are four major steps in imaging using DSEM. The first step 'Pre-Sample Preparation DSEM Operation' involves preparing the DSEM before placing the sample in the vacuum chamber. The second step 'Sample Preparation' includes setting up the sample stage without the use of chemicals and other machinery. The third step 'post-sample preparation DSEM Operation' involves the steps to be followed post sample set up in the machine. The final step 'Image capturing and processing using 'Nanoeye'' involves steps to be followed to acquire SEM image post sample insertion and vacuum build up in machine.

Below is the description of these major steps:

A. Pre-Sample Preparation DSEM Operation

Before turning on the DSEM and computer, the vacuum pressure should range from 90 to 120psi on the air compressor (rotary vane pump). Confirm that the vacuum pumps are functional for the entire duration of imaging and that the fastened stage with/without sample is under vacuum despite the fact it is turned off to avoid any debris entering the machine. Allow the vacuum to build in DSEM by pressing the 'Exchange' button. A stable green light indicates that full vacuum has been established into the column containing stage inside the DSEM. After the establishment of full vacuum, press the 'Exchange' switch again to initiate release of vacuum from DSEM. Then, launch 'Nanoeye' software associated with DSEM on the computer linked to DSEM. Then, pull out the motorized stage smoothly, fully open the door, loosen the stage using

hex key (Figure 12A1) and take out sample along with aluminum stub using the SEM mount forceps (Figure 12A2). Select the ‘Calibration’ icon on the Motor Control Panel of ‘Nanoeye’ software and allow the stage to come to its originally assigned 3-D position.

B. Sample Preparation

Any fresh biological/non-biological sample can be used for image acquisition in SNE-4500 Plus. A general principle for sample preparation is to get an excised sample of diameter up to 80 mm and thickness up to 50 mm (based on size of the stage). Then, fix the sample onto a double-sided conductive carbon tape (Figure 12C) glued to an aluminum stub of suitable diameter (15mm, 25mm and 40mm) depending on the size of the sample (Figure 12B).

C. Post-sample preparation in DSEM Operation

The diameter and height of stub along with sample should be recorded using the machine jig (Figure 12D) by aligning the specimen stage with the groove in the middle. The recorded parameters should be entered into the ‘Nanoeye’ software. It is imperative that the height entered is 2-3 mm more than the recorded height to avoid contact of sample to electron gun. In the case of single aluminum stub (15 mm, 25 mm, or 40 mm in diameter), it can be directly placed on the motorized stage and stage should be fastened using a hex key. Use the ‘Camera’ button on the Motor Control Panel of software screen to capture the image of the stage as it will later act as a map to capture magnified images of different regions of the specimen. It is important to note that the center of x-y coordinates on the camera navigation should align with the center of the fastened stage. Press “Exchange” switch while keeping the door slightly pushed for few seconds using one hand. After loading a fresh unprepared sample, the user has approximately five minutes to acquire images.

D. Image capturing and processing using ‘Nanoeye’

On the Start Page of Nanoeye software screen, select 5KV voltage, SE detector and High/low vacuum (we used high vacuum for most samples). Then, press “START” to start scanning of specimen inside vacuum chamber. After pressing start button, check to see that the emission current rises to 110μA. The initial page of Image Window shows the fast-scanning mode with minimum resolution. Use X, Y, Z, R and T on Motor Control Panel to select the region/coordinates of sample to be scanned at certain rotation and angle. By default, the Z is an equal height of fastened stage, and X, Y, T and R is 0. When selecting X-Y coordinates, double click on camera navigation and later minor changes in the coordinates can be made using X-Y motor operation. Initially, increase the magnification up to 500-1000X to focus rather than focusing at a magnification lower than 500X. Then, decrease the magnification as per requirement and the image to be captured. Select 10-30% spot size on Image Control as per requirement before changing the scan mode. Select the slow photo 2 scan mode (on the extreme bottom right; Image Control) for highest resolution publication quality image. Then select “Auto” on the brightness/contrast focus area on Image Control. On the bottom bar of Image Window, company label, researcher’s name and specimen label can be modified. Monitor the complete scanning on the screen and just before the scanning is completed, click the “Camera” icon on bottom right corner of Image Control, and save the image at a designated storage location. To measure the dimensions of the various components in the image, pause the scanning by clicking on pause icon on bottom bar and click M. Tools. Select length to measure two-point/multi-point length and markings (arrow, square, and rectangle) to mark the components of image. Click on the operation button on top right bar of Image control and a dropdown menu will appear. Select “Stop” to stop scanning. Once Stop” is selected on the Nanoeye page, the power switch can be pressed to stop operation of DSEM and Nanoeye window will be closed. A

detailed flowchart comparing traditional SEM and DSEM is presented respectively in tables 3 and 4.

Results and Discussion

Here we document a detailed procedure of a possible alternative to traditional electron microscopy that removes the major bottlenecks while sustaining image quality. Using SNE-4500 Plus Tabletop Desktop SEM, we captured images of fresh leaf samples of different species of Solanaceae (Figure 8B, 8C, 8D, 9A and Figure 3), Cucurbitaceae (Figure 8A and 9B), Asteraceae (Figure 9C) and Poaceae (Figure 9D) plant families to study their surface features (eg. trichomes, stomata, and waxes) (Figure 9B). We varied magnifications to estimate the density of trichomes depending on the characteristics of plant families (Figure 9). Additionally, we captured images of insect eggs (Figure 8E; Figure 10A), pollen grains (Figure 8D), and caterpillars using DSEM. Images of fall armyworm (*Spodoptera frugiperda*; Lepidoptera; Noctuidae) and tobacco hornworm (*Manduca sexta*; Lepidoptera; Sphingidae) (Figure 10A) eggs laid by adult moths on tomato (*Solanum lycopersicum*: Solanaceae) leaf surface were collected to assess any damage caused by trichomes present on the leaf surface to eggs.

In DSEM imaging of insect eggs, we did observe some structural distortion (shrinkage) after placing them under vacuum in DSEM (Figure 10A). However, aldehyde fixing, and sputter coating would resolve this issue. Previously, Kariyat et al. (2017), had captured images of *M. sexta* caterpillars' peritrophic matrix and frass pellets to study the effects of trichomes of horsenettle (*Solanum carolinense*: Solanaceae) post-feeding (Kariyat et al., 2017; Figure 11A and 11C). This was done with a traditional Cambridge S360 SEM (Huck institutes of life sciences, Microscopy Core Facility, Pennsylvania State University, USA) and used typical SEM preparation protocol which includes overnight fixation of the sample at 4ºC in 25%

glutaraldehyde solution, dehydration rinses through series of ethanol solutions, critical point drying, and sputter coating of critically dried sample (Figure 11A and 11C; Table 4). However, without using the abovementioned method, we captured images of frass pellets of cabbage loopers (*Trichoplusia ni*; Lepidoptera: Noctuidae) to detect the presence of undigested trichomes when the caterpillars were fed on cucumber (*Cucumis sativus*; Cucurbitaceae) and bottle gourd (*Lagenaria sicerraria*; Cucurbitaceae) leaves. Interestingly, we obtained similar results of the trichomes being embedded in these frass pellets (Figure 8F; Figure 11B, 11D) to the images earlier captured by Kariyat et al. (2017). Additionally, plant waxes, one of first line of defenses encountered by herbivores, were also observed very clearly in our SEM images from *S. glaucescens* (Figure 8B). Additionally, the resolution of DSEM is 5nm which is comparable to traditional SEMs with nanoscopic resolution. This strengthens our point that DSEM is equally capable of capturing minute details from the specimens with no sample prep which was earlier thought to be only captured by expensive high-tech SEMs which use extensive sample preparation methodology.

While sample preparation and image acquisition are much easier and can be accomplished quickly, there are some concerns. We found that it is difficult to estimate the gland cell number and the exact shape of the gland of glandular trichomes, and eggs of insects due to the damage sustained after placing the sample under vacuum in DSEM (Figure 10). Alternatively, we found that shape of non-glandular trichomes of tomato was not distorted under vacuum. Sputter coating and would have possibly produced better images of glandular trichomes. Using a more efficient method for capturing SEM images by placing the sample on the stage can produce similar results as produced by using more complicated and traditional SEM. This is especially true for plant-insect interactions studies where routine imaging of plant

and insect parts could be fast tracked using DSEM. Overall, we demonstrate that using DSEM, which is fast, easy to operate, and inexpensive, can produce quality images similar to other SEM, with significantly lower costs of purchase, maintenance and methodology.

Table 4. A flowchart representing the basic steps involved in image acquisition on traditional SEM

TRADITIONAL SCANNING ELECTRON MICROSCOPY

Fixation of sample: 2.5% glutaraldehyde in phosphate buffer	AT LEAST SIX HOURS
Post fixation: three changes in phosphate buffer which takes 5 min Placing sample in 1% osmium tetroxide	
Dehydration – serial dehydration each of 25%, 50%, 70 %, 80%. 90% and 100%, each at 30 min (varies with sample type)	
Critical point drying: slide is transferred to critical point apparatus liquid carbon dioxide is passed through the sample and temperature is raised to 34^0C, raised to 1280 Psi	
Sputter coating: heavy metal coating with gold and palladium/ Vacuum evaporation coating	
Transferring the specimen to the specimen stub with the help of liquid adhesives such as cyanoacrylate or conductive tapes such as carbon and sticky tabs	
The machine is under vacuum; Clicking vent switch in software to de-vacuum Scanning electron microscope (SEM)	
Placing the sample stub in the specimen holder (9 samples can be processed at a time)	
Adjust working distance	
Close the SEM door and turn on the vacuum	
Turn on the electron beam	
Image is focused and magnified	
Saturation of electron beam must be self-adjusted	
To obtain high resolution image, SEM involve technical expertise and playing with other different parameters such as wobble and stagnation.	

Table 5. A flowchart representing the basic steps involved in image acquisition on SNE- 4500 Plus Tabletop SEM with representative images of SNE- 4500 parts

DESKTOP SCANNING ELECTRON MICROSCOPY

1. Pump should be operating with a pressure of 90-120 psi

2. Before de-vacuuming the DSEM, build a complete vacuum which is indicated by vacuum LED filled with green light

3. After de-vacuuming, slide the chamber door to take out the stage until you hear a 'click' sound

4. Open 'Nanoeye' software and the window displayed can be divided into three separate sections: Motor Control Panel- controls the motor and navigates samples; Image Window- displays image of the specimen; Start Page- customize basic settings for imaging before imaging before starting scanning of sample

5. Measure the height and width of sample stage and enter them in Motor Control of 'Nanoeye' software before putting the sample on the stage and inserting it into vacuum chamber

6. Prepare the sample stage by fixing fresh biological/non-biological sample on double-sided carbon tape

7. After placing the sample stage in the vacuum chamber and building the vacuum completely, press 'Start' on Start Page and when emission current reaches 110 µA, the entire window can be divided into three separate sections: Motor Control; Image Window; Image Control- adjusts the focus, spot size, brightness and contrast of the specimen image, and images at different scanning modes can be captured,

8. For measuring specific structures in the sample, scanning is paused, and measurements can be recorded by selecting different shapes from 'M. tools' menu. After measurement, images can be captured by clicking camera icon on Image Control and saved at desired location.

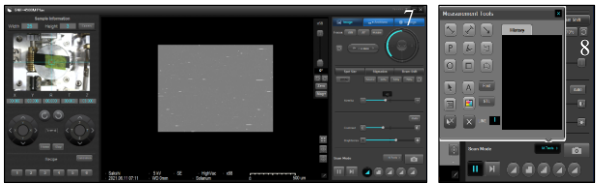

TAKES FIFTEEN MINUTES

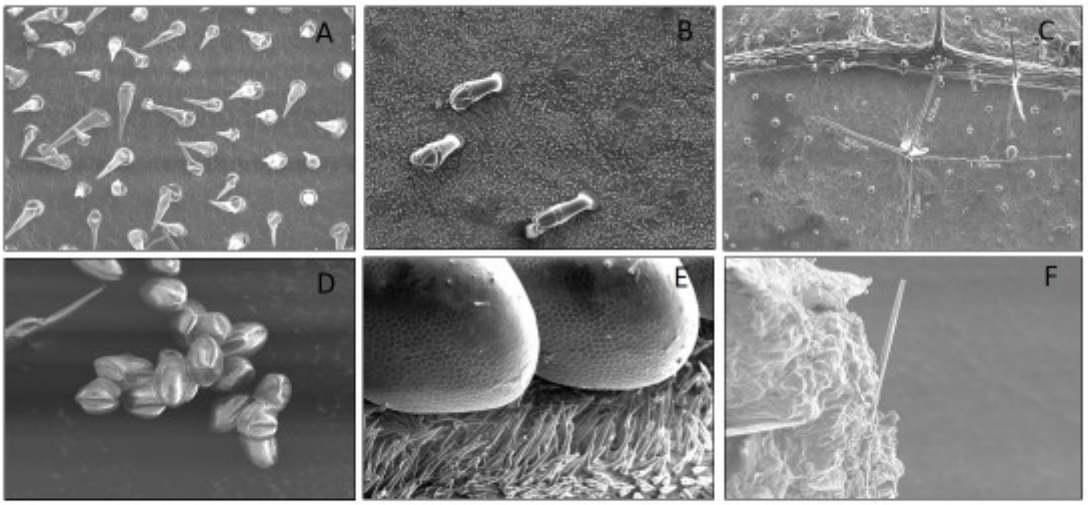

Figure 8. Schematic representation of the wide diversity of functions performed by high- tech, no sample prep Desktop Scanning Electron Microscopy (DSEM) in plant-insect interactions studies including (A) density of trichomes present on cucumber (*Cucumis sativa*: Cucurbitaceae) leaf at estimated at 180 X magnification, (B) waxes and glandular trichomes (gland on the top of hair) of *Solanum glaucescens* (Solanaceae) magnified at 150X, (C) potato tree (*Solanum grandiflorum*; Solanaceae) magnified at 60X for measurement of dimensions of different trichome types, (D) pollen grains of silverleaf nightshade (*Solanum elaeagnifolium*: Solanaceae) flowers magnified at 250X, (E) surface interphase of squash bugs (*Anasa tritis;* Hemiptera: Coreidae) eggs and plant surface of cucumber magnified at 90 X, and (F) microstructural details of presence of undigested trichomes of bottle gourd (*Lagenaria siceraria*: Cucurbitaceae) embedded in frass pellets of cabbage loopers *Trichoplusia ni* (Lepidoptera: Noctuidae) magnified at 700 X.

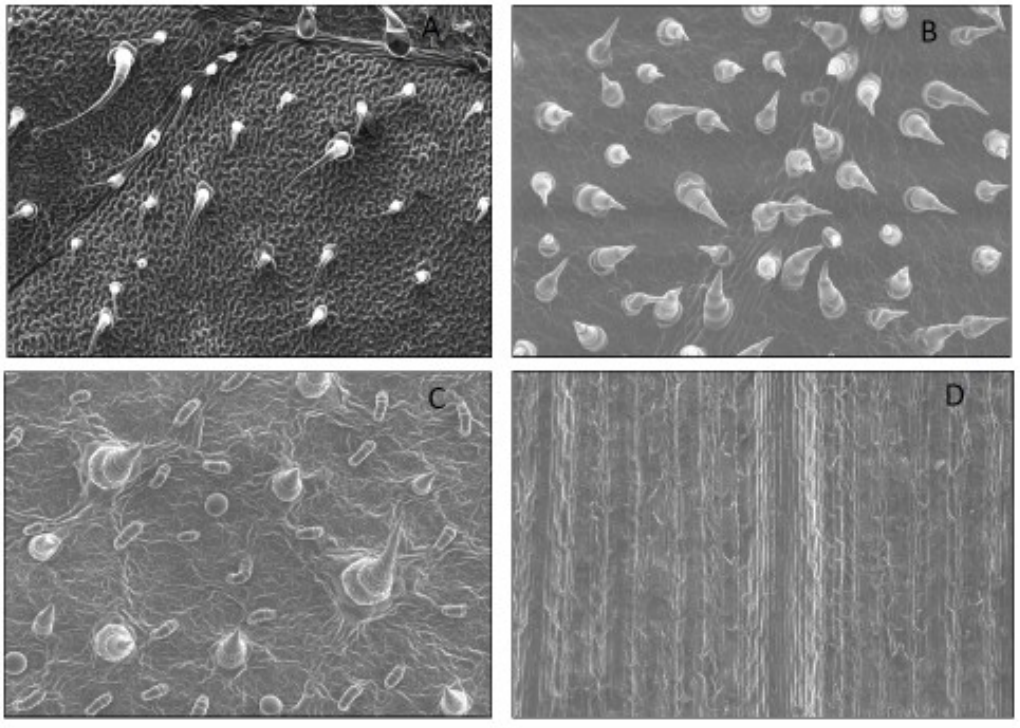

Figure 9. Desktop Scanning electron microscopic images of various kinds of trichomes present in different plant families including (A) Solanaceae (tomato; *Solanum lycopersicum)* at 140X, (B) Cucurbitaceae (bottle gourd; *Lagenaria siceraria*) at 200X, (C) Asteraceae (sunflower; *Helianthus annus*), and (D) Poaceae (sorghum; *Sorghum bicolor*).

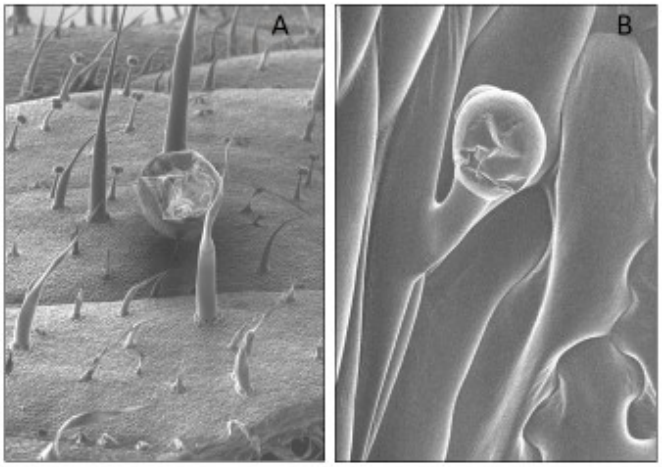

Figure 10. Desktop scanning electron microscopy showing shrunken (A) egg of fall armyworm (*Spodoptera frugiperda*) on tomato (*Solanum lycopersicum*; Solanaceae) leaf surface at 75X, and (B) glandular trichome of African eggplant (*Solanum macrocarpon*; Solanaceae) at 1000X, indicating that the although the surface features of a biological sample are visible, but not fixing sample and leaving out sputter coating can lead to deviation of image from its original structure.

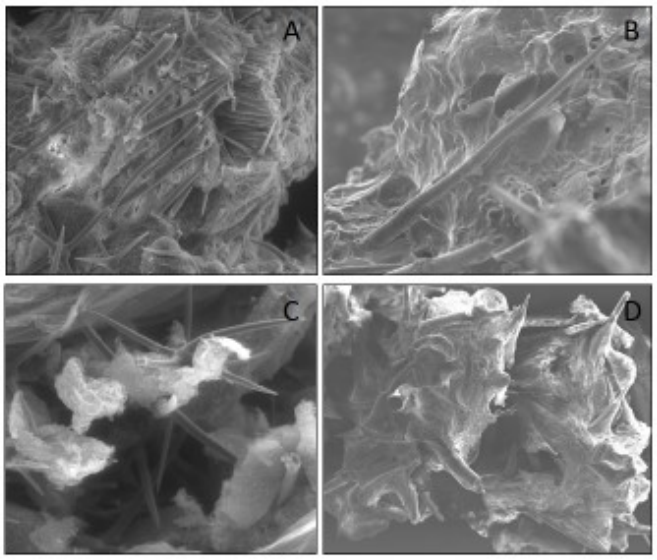

Figure 11. Scanning electron microscopy (SEM) of undigested trichomes embedded in frass pellets of (A and C) tobacco hornworm (*Manduca sexta*: Sphingidae) caterpillar fed on trichome rich plant material of horsenettle (*Solanum carolinense*; Solanaceae). Scanning of sample was carried out at 300X and 400X using traditional Cambridge S360 scanning electron microscope following conventional sample fixation with gluteraldehyde, tissue dehydration with ethanol washes, critical point drying of sample and sputter coating, and (B and D) cabbage looper (*Trichoplusia ni*: Noctuidae) after caterpillar fed on cucumber (*Cucumis sativa*; Cucurbitaceae) and bottle gourd (*Lagenaria Sicerraria*; Cucurbiitaceae) plant material and scanning of sample done at 450X and 150X using no sample preparation desktop scanning electron microscope.

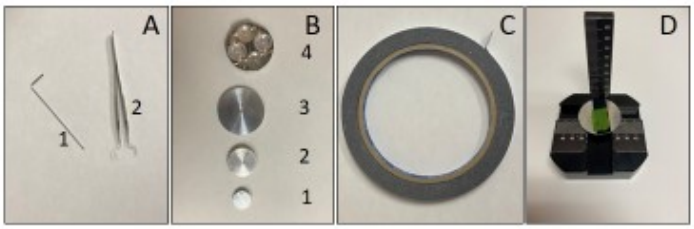

Figure 12. Frequently used tools for sample preparation and handling while operating Desktop Scanning Electron Microscope: (A) 1. Hex key to loosen or tighten the screws of stage while taking out or putting the sample stage (aluminum stub with sample mounted on it) in vacuum chamber 2. SEM mount forceps to handle the aluminum stubs without damaging the sample, (B) Aluminum stubs of diameter 1. 15 mm, 2. 25 mm, 3. 40 mm and 4. 40 mm stub to handle multiple (1-4) 15mm stubs at one time, (C) Double-sided carbon tape used to fix sample on the aluminum stubs, and (D) Machine Jig to measure the diameter and height of sample stage.

CHAPTER III

PICKING SIDES: FEEDING ON THE ABAXIAL LEAF SURFACE IS COSTLY FOR CATERPILLARS

Main Conclusion

The study provides us with the evidence that caterpillars tend to feed on the abaxial leaf surface despite the damage caused to them because of higher trichome density.

Abstract

To defend against herbivory, plants have evolved physical and chemical defense mechanisms, including trichomes (hair like appendages on leaves and stem) being one of them. Caterpillars, a major group of insect herbivores are generally found to occupy the abaxial (underside) leaf surface, considered as an avoidance mechanism from biotic and abiotic stresses. Since trichomes are a first line of defense, we examined the correlation between abaxial vs adaxial (above side) trichomes and caterpillar feeding, behavior, and growth. A combination of field, lab and microscopy experiments were performed using tobacco hornworm, *Manduca sexta* (Lepidoptera: Sphingidae), a Solanaceae specialist caterpillar, and multiple host species. We found that *M. sexta* caterpillars overwhelmingly preferred to stay and feed on the abaxial leaf

surface, but the abaxial leaf surface also had significantly more trichomes, and consequently, caterpillars took significantly longer to commence feeding. In addition, lab-based diet experiment containing shaved trichomes showed that feeding on the abaxial leaf surface with more trichomes also affected caterpillar growth. Taken together, our study shows that although caterpillars prefer to feed on the abaxial leaf surface, they accrue feeding delays and developmental constraints, indicating tradeoffs affecting performance, and exposure to predation and abiotic stressors.

Introduction

Most caterpillars are commonly found to sustain and feed on the abaxial (underside) of leaves (Heinrich 1979; Tagawa et al. 2008; Watanabe et al. 2018; Despland 2019). This is primarily considered as an avoidance mechanism against predators and parasitoids, and also to protect against abiotic factors such as sunlight and winds (Heinrich 1979). To counter herbivory (Reid and Cuthbert 1964; Savary et al. 2019; Saha et al. 2020), plants employ a suite of structural and chemical defenses (Coley and Barone 1996; Hare 2005; Mithöfer and Boland 2012; Horgan et al. 2009; Paudel et al. 2019). Among structural defenses, leaf trichomes are a major group that delay caterpillar feeding, cause toxicity through both pre and post-ingestive effects (Kariyat et al. 2017, 2018, 2019). For example, non-glandular trichomes delay and hinder *Manduca sexta* caterpillars from feeding on *Lycopersicum esculentum* and *Solanum carolinense* (Solanaceae) (Kariyat et al. 2017; Wilken et al. 1996). On the other hand, glandular trichomes produce toxins (Peiffer et al. 2009), and even sugars that can alter caterpillars' body odor to give away their location to predators and parasitoids (Weinhold and Baldwin 2011; Stork et al. 2011). Adaxial and abaxial leaf surfaces tend to differ in their characteristics including stomatal density, trichome morphology and their density (Hardin 1979; Maffei et al. 1989; Dahlin et al. 1992).

However, whether the variation in leaf surface trichome density, affects herbivore feeding and growth has been seldom tested.

Solanaceae is a diverse plant family with economically important food crops and weeds found in all habitats (Symon 1981; Childers et al. 1998; Knapp 2002; Vallejo-Marín and O'Brien 2007; Shah et al. 2013). Previous studies have reported that Solanaceae members possess a wide variety of trichomes, and can limit caterpillar feeding (Kariyat et al. 2018, 2019; Fürstenberg-Hägg et al. 2013). For this study, we exploited these features of Solanaceae to test the following hypotheses using tobacco hornworm (*M. sexta*), a Solanaceae specialist, and 11 species (wild and cultivated) as host plants. We hypothesized that *M. sexta* caterpillars would prefer to feed and develop on the abaxial side, however, will accrue negative consequences due to higher trichome density. To test these, we used (a) field observations to examine caterpillar preference on leaves, (b) electron microscopy to estimate trichome density and (c) manipulative lab experiments to examine the role of trichomes in caterpillar growth.

Materials and Methods

Plants and Insects: We used 11 Solanaceae species in the study (Fig 1 (a); Online Resource 1). Our objective was to get a collection of species with different types of growth habits and variation in trichome morphology and density. Eggs of *M. sexta* were obtained from our laboratory reared colony and a commercial vendor (Great Lake Hornworm Ltd. Romeo, Michigan, USA), and were reared as previously described (Kariyat et al. 2017). For details, see Online Resource 1.

Assays

1. Field observations of M. sexta on Solanum elaeagnifolium: During the past 3 years, we routinely observed native populations of *S. elaeagnifolium* in McAllen- Edinburg area of south Texas for *M. sexta* caterpillars. Around ~5000 plants were sampled for *M. sexta* caterpillar presence during the light phase and every caterpillar observed was recorded for its position.

2. *Trichome density assessment*: To determine the trichome density (n= 6/species/side except n=3/side for *S. lycopersicum*, n= 4/side for *S. dulcamara* and *S. aethiopicum*, and n= 5/side for *Capsicum annum*), a desktop Scanning Electron Microscope (SNE- 4500 Plus Tabletop; Nanoimages LLC, Pleasanton, California, USA) was employed. For details, see Online Resource 1.

3. *Time to initiate feeding*: To examine whether *M. sexta* takes longer to initiate feeding on the abaxial surface, starved first instar caterpillars (n=3/plant/side; 5 plants/species except n=4 for *S. dulcamara*) were used for all the species. The time taken by each caterpillar to have its first bite from leaf tissue was recorded (Kariyat et al. 2017, 2018). For details, see Online Resource 1.

4. *Trichome shaving assay*: To test and quantify the effect of trichome density on caterpillar growth, first instar *M. sexta* caterpillars (n= 15 per treatment) were fed on three diets: artificial diet containing adaxial trichomes, or abaxial trichomes of *S. pyracanthos* and no trichomes. Mass and mass gain by caterpillars were recorded at 48h and 96h after start of the experiment (Tayal et al., 2020). For details, see Online Resource 1.

5. *Mass gain on taped leaves:* To further examine whether caterpillars tend to stay or leave the surface on which they were originally placed, 1st instars were forced to feed on either surface of leaves (n=15/species/side) of *Solanum anguivi*, *Solanum lanceifolium* and *Capsicum annum*. Caterpillar mass gain (only if caterpillar was found feeding on the same surface on which it was

placed) and percentage of total caterpillars found stuck on the tape around the leaf was recorded after 24h of start of the experiment. For details, see Online Resource 1.

6. *Feeding site assessment of M. sexta:* To examine the feeding site of *M. sexta* caterpillars, two second instars were placed on adaxial surface of one young and one older leaf on the same plant (n=15) of *S. melanocerasum*, *S. lycopersicum* and *S. pyracanthos* during the day. Data on caterpillar feeding position (adaxial vs abaxial), for those found actively feeding, after 24h and 72h of start of the experiment was collected.

Statistical Analysis

Field observations of *M. sexta* on *Solanum elaeagnifolium* was expressed in percentage of caterpillars found on abaxial, adaxial or on stem. Since our interest was to identify differences in position, we pooled all the species data and pairwise comparison of trichome density on adaxial and abaxial surface was done using Mann-Whitney test. Mann-Whitney test was also used to analyze pooled data of time taken by caterpillars to initiate feeding. For trichome shaving assay, mass and mass gain data at 48h and 96h were analyzed using one-way ANOVA and pairwise comparisons with Tukey's test. For the taped leaves experiment, data of mass gain on adaxial and abaxial leaf surface was analyzed using Mann-Whitney test. For *M. sexta* feeding site assessment, pairwise comparison of caterpillar position was done using two-tailed Fischer's Exact test. All analyses were carried out using JMP (SAS institute, Cary, NC, USA) and GraphPad prism (La Jolla, CA, USA).

Results

1. *M. sexta caterpillars from Solanum elaeagnifolium in field*: Over the past 3 years, we observed a total of 107 *M. sexta* caterpillars on *S. elaeagnifolium*. Of these, 89.72% were found on the abaxial leaf surface when compared to 6.5% on adaxial, and 3.7% on the stem.

2. *Trichome density assessment*: The results from our trichome density data showed that in general, Solanaceae species had significantly higher abaxial than adaxial trichome density (Mann Whitney test; two tailed; p= <0.0001; Figure 13(a-d) and Figure 18). Besides, three trichome types viz. stellate non-glandular, uniseriate non-glandular and globular headed glandular trichomes were the most common trichome types in the species included in the study. Among these types, stellate non-glandular was the most prevalent type.

3. *Time to initiate feeding*: Consistent with higher trichome density on the abaxial leaf surface, time to initiate feeding by *M. sexta* caterpillars was significantly higher (longer) on abaxial than adaxial surface for pooled data on all the species (Mann-Whitney test; two tailed; p= 0.0171) (Figure 14).

4. *Trichome shaving assay*: Mass of caterpillars at 48h (One-way ANOVA; df= 40; F= 14.77; p= < 0.0001) and 96h (one-way ANOVA; df= 39; F= 34.86; p= < 0.0001) was significantly different for three treatments (Figure 15). Pairwise comparison for different diets revealed significantly lower mass of caterpillars on abaxial diet than adaxial and control diet at 48h (Tukey's test; p= < 0.0001 and p= 0.0010) and 96h (Tukey's test; p= < 0.0001 and p= < 0.0001) but the difference was non-significant between adaxial and control diet at 48 h (Tukey's test; p=0.3731) and 96h (Tukey's test; p= 0.1635) (Figure 15). Mass gain at 48h (one-way ANOVA; df= 41; F= 10.79; p= 0.0002), 96h (one-way ANOVA; df= 41; F= 4.41; p= 0.0187) and total mass gain (one-way ANOVA; df= 39; F= 25.54; p= < 0.0001) by caterpillars was

significantly different among three treatments (Figure 16). Pairwise comparisons revealed significantly lower mass gain on abaxial diet than adaxial at 48h (Tukey's test; p= 0.0002), 96h (Tukey' test; p= 0.0161) and total mass gain (Tukey's test; p= < 0.0001). Significantly lower mass gain on abaxial than control diet was obtained at 48h (Tukey's test; p= 0.0047) and for total mass gain (Tukey's test; p= < 0.0001), but the difference was non-significant at 96h (Tukey's test; p= 0.1483) (Figure 16). The difference in mass gain between adaxial and control diet was non-significant at all the times (Tukey's test: 48h; p= 0.5305, 96h; p= 0.5721 and total mass gain; p= 0.3055) (Figure 16).

5. *Mass gain on taped leaves*: Significantly higher mass gain (Mann-Whitney test; p= 0.0341) was observed for caterpillars placed on adaxial than abaxial leaf surface (Figure 17). Moreover, the 13.33% of caterpillars were found stuck on tape with the abaxial side exposed and 40% were found stuck with adaxial side exposed.

6. *Feeding site assessment of M. sexta*: Significantly higher number caterpillars were found on abaxial than adaxial leaf surface on all three species at 24h (Fisher's Exact test: *S. melanocerasum*; p= < 0.0001, *S. lycopersicum*; p= 0.0002 and *S. pyracanthos*; p= < 0.0001) and 72h (Fisher's Exact test: *S. melanocerasum*; p= < 0.0001, *S. lycopersicum*; p= 0.0005 and *S. pyracanthos*; p= 0.0003) of starting the experiment (Figure 19).

Discussion

Our study clearly shows that in general, trichome density is higher on abaxial than adaxial surface in Solanaceae. In tandem with higher abaxial trichome density, caterpillars took longer to initiate feeding on the abaxial surface. We also found consistent results for the taped leaves experiment, and shaved trichomes experiment, where caterpillars gained more mass on adaxial than abaxial surface. Moreover, the majority of *M. sexta* caterpillars placed onto the

adaxial leaf surface moved to the underside of leaves for feeding, which support the findings from our field observations where they were consistently observed on the abaxial leaf surface. Collectively, we show that while hiding on the abaxial leaf surface has possible benefits, this can also lead to potential fitness consequences, where their growth is affected, leading to possible cascading effects (Portman et al. 2015).

Many studies have demonstrated that caterpillars tend to stay on the abaxial surface to feed (Heinrich 1979; Tagawa et al. 2008; Watanabe et al. 2018; Despland 2019), consistent with our observations that regardless of the trichome density, the caterpillars tend to stay and feed on the abaxial side. However, it has been documented that *Chlosyne lacinia* (Lepidoptera: Nymphalidae) caterpillars feed exclusively on the adaxial leaf surface having lower trichome density than the abaxial surface of *Tithonia diversifolia* (Asteraceae) (Ambrósio et al. 2008). Notably, we found that when the caterpillars were forced to feed on one side or the other, ~40% of caterpillars originally placed on adaxial surface escaped the surface and got stuck (attempting to reach the abaxial surface) on tape in contrast to only 13.33% of caterpillars stuck on tape originally placed on the abaxial surface. Therefore, *M. sexta* appear to have an innate preference for remaining on the abaxial leaf surface regardless of higher trichome density and negative consequences associated with it. Future studies should also consider whether *M. sexta* females oviposit more on the abaxial side, in line with mother knows best hypothesis.

A possible explanation for having higher trichome density on abaxial than adaxial leaf surface might be because caterpillars prefer abaxial over adaxial side and thus, higher trichome density can discourage/harm herbivores, by affecting their growth and development, since feeding on trichomes can cause damage, than just deterring feeding (Kariyat et al. 2017, 2019; Malakar and Tingey 2000; Hurley and Dussourd 2014). We show that trichome mediated

defenses are even more complicated than understood before and can differentially affect caterpillar growth based on their preferred feeding site.

M. sexta caterpillars fed on diet containing *S. pyracanthos* abaxial non-glandular trichomes (~ 44 trichomes/ 5.32 mm^2/ trichome number in 60X magnified SEM image of leaf) gained lower mass than those fed on diet containing adaxial (~ 29 trichomes/ 5.32 mm^2) trichomes or no trichomes. The results for abaxial trichomes added to the diet were in line with our previous work (Kariyat et al. 2017), but the mass gain by caterpillars fed on diet containing adaxial trichomes was not significantly different than control diet, probably because of caterpillars possessing a threshold for damage imposed by high trichome density, but needs further investigation. Taken together, the study concludes that the trichome density is higher on abaxial leaf surface and has a negative correlation with caterpillars' growth. Despite negative effects of the abaxial trichomes on caterpillars, they still tend to settle and feed on the abaxial surface possibly, to protect themselves from abiotic and biotic stresses. In context of host plants, Solanaceae plants most likely evolved higher trichome density on the abaxial surface to discourage chewing herbivores as an evolutionary adaption but warrants further investigation.

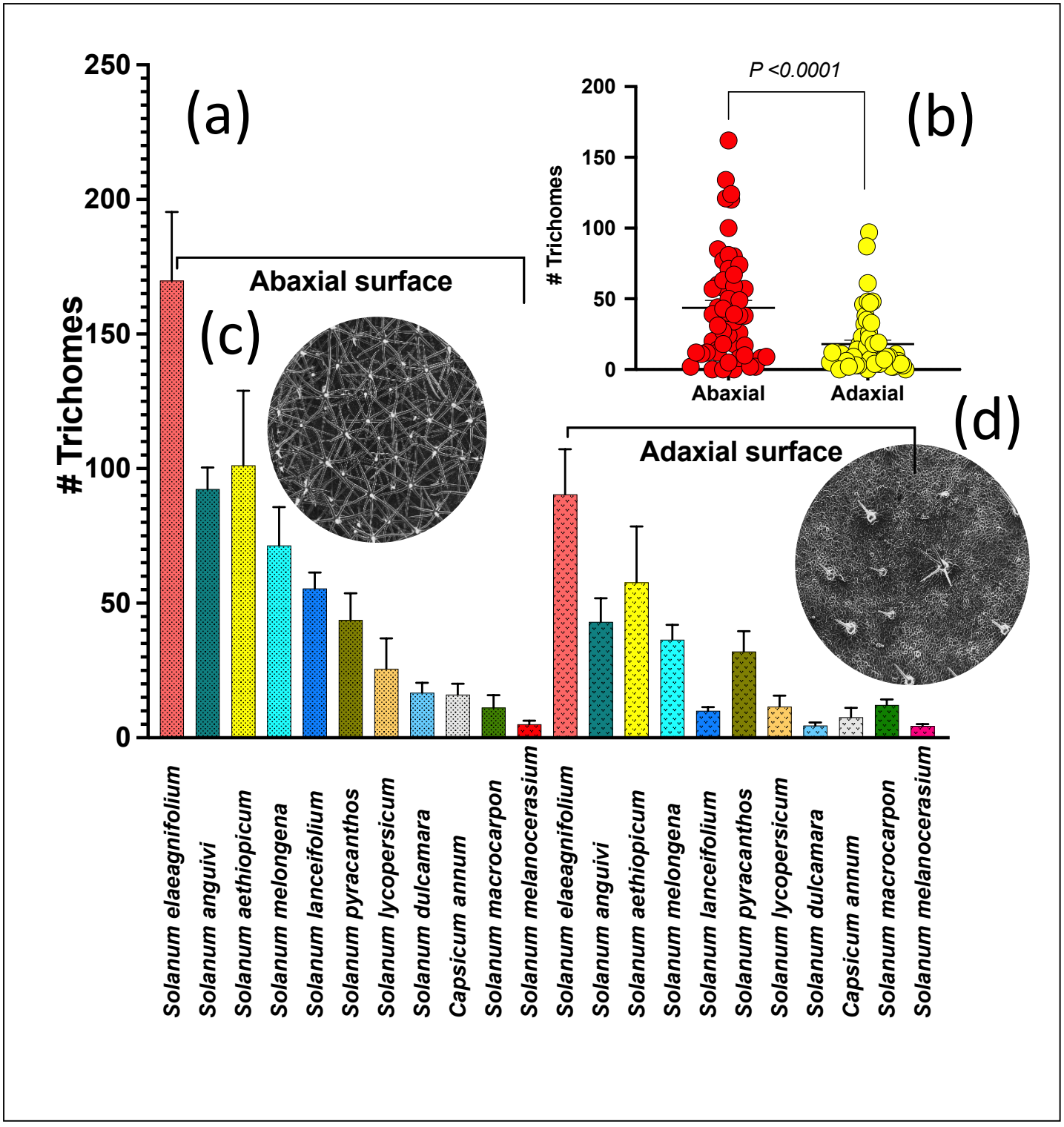

Figure 13 (a). Variation in adaxial and abaxial leaf trichome density in different Solanaceae species

(b) Result of pooled trichome density on adaxial and abaxial leaf surface of 11 Solanaceae species (Mann Whitney test; two tailed; $p = <0.0001$). Image of (c) abaxial and (d) adaxial leaf surface of *Solanum aethiopicum* at 60X magnification showing higher abaxial than adaxial trichome density.

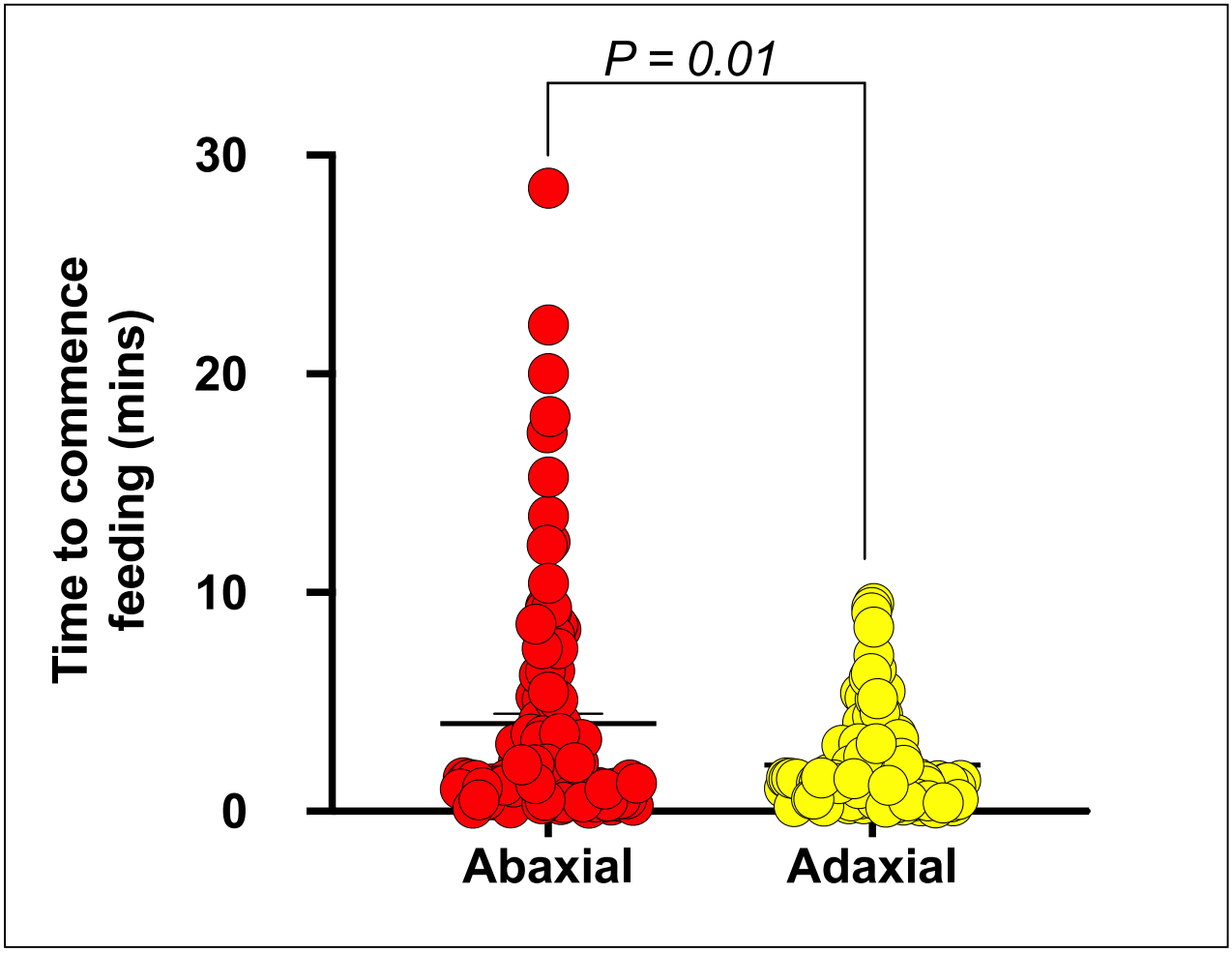

Figure 14. Results of first bite experiment time (in minutes) by *M. sexta* caterpillars to commence feeding from on 10 Solanaceae species (Mann-Whitney test; two tailed; p= 0.0171).

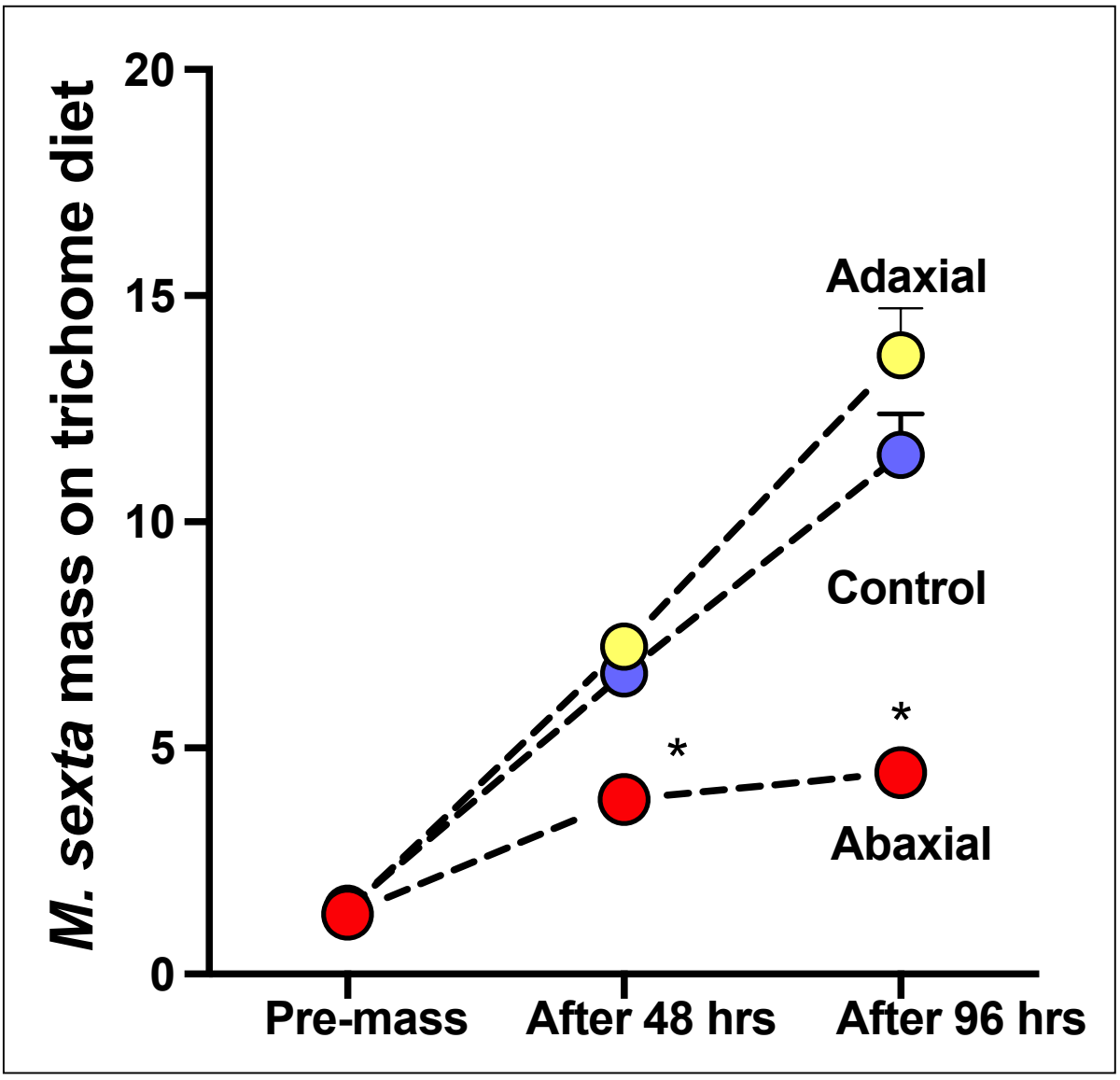

Figure 15. Results of mass of *M. sexta* on artificial diet containing shaved trichomes from abaxial and adaxial leaf surface of *Solanum pyracanthos* at 0h (pre-mass), 48h and 96h.

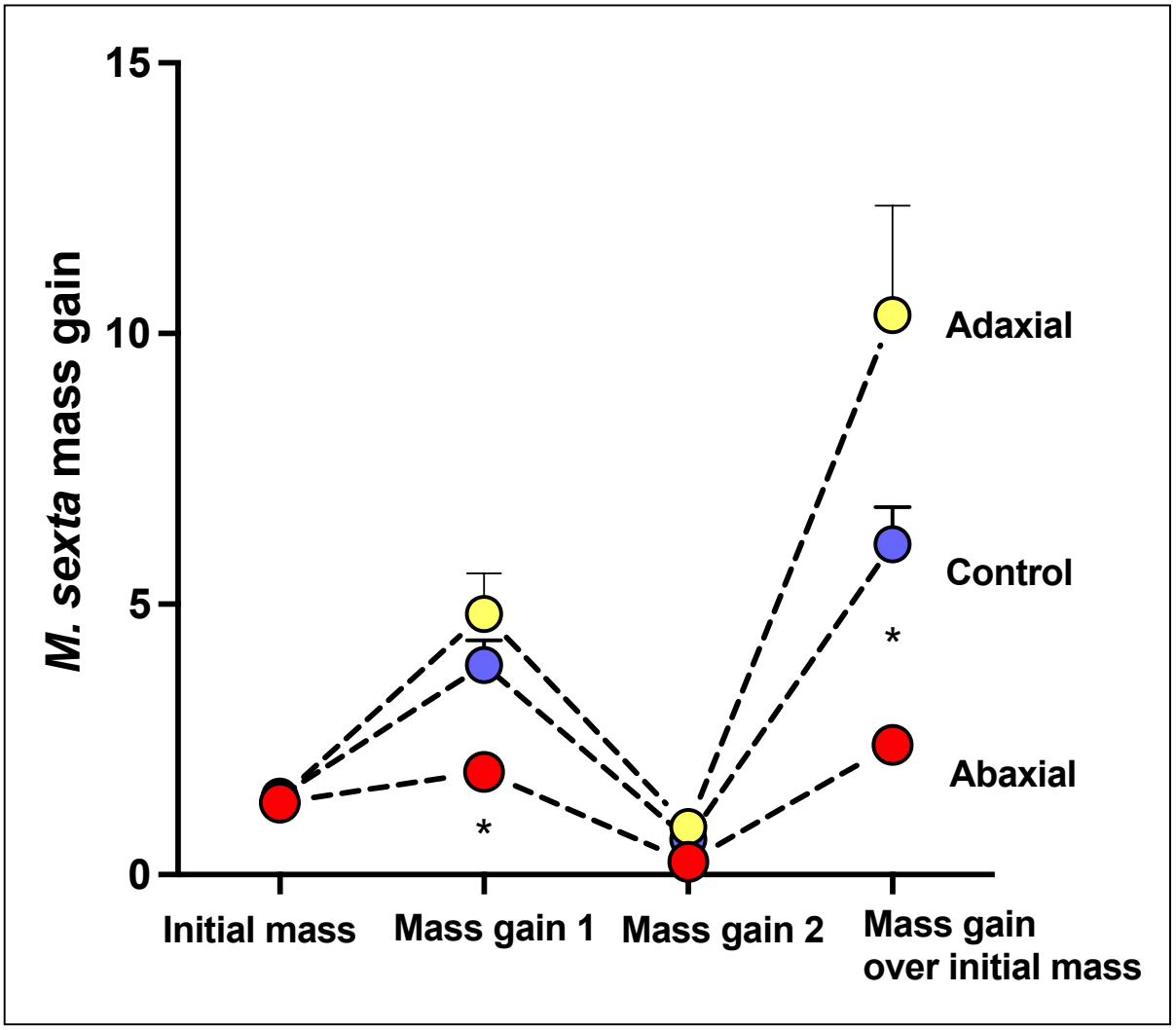

Figure 16. Results of mass gain of *M. sexta* on artificial diet containing shaved trichomes from abaxial and adaxial leaf surface of *Solanum pyracanthos* at 0h (initial mass), 48h (mass gain 1) and 96h (mass gain 2).

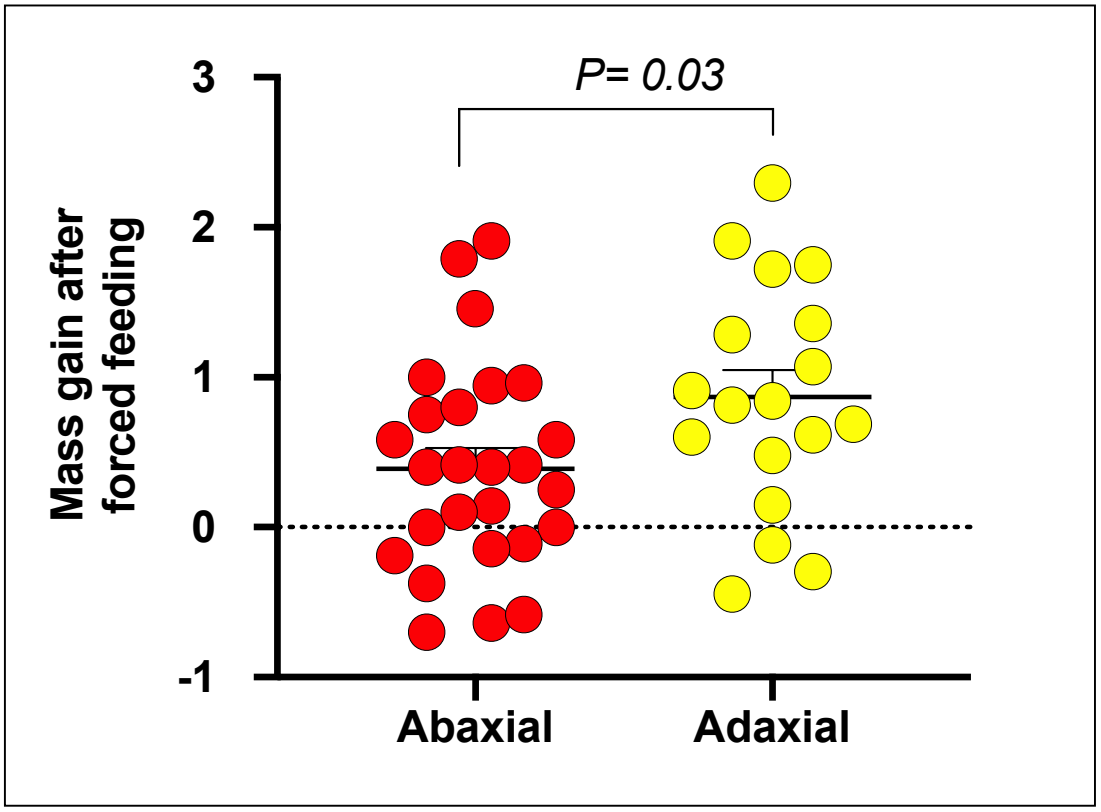

Figure 17. Results of forced feeding experiment with higher mass gain by 1st instar *M. sexta* caterpillars on adaxial than abaxial leaf surface of 3 Solanaceae species (pooled data; Mann-Whitney test; p= 0.0341).

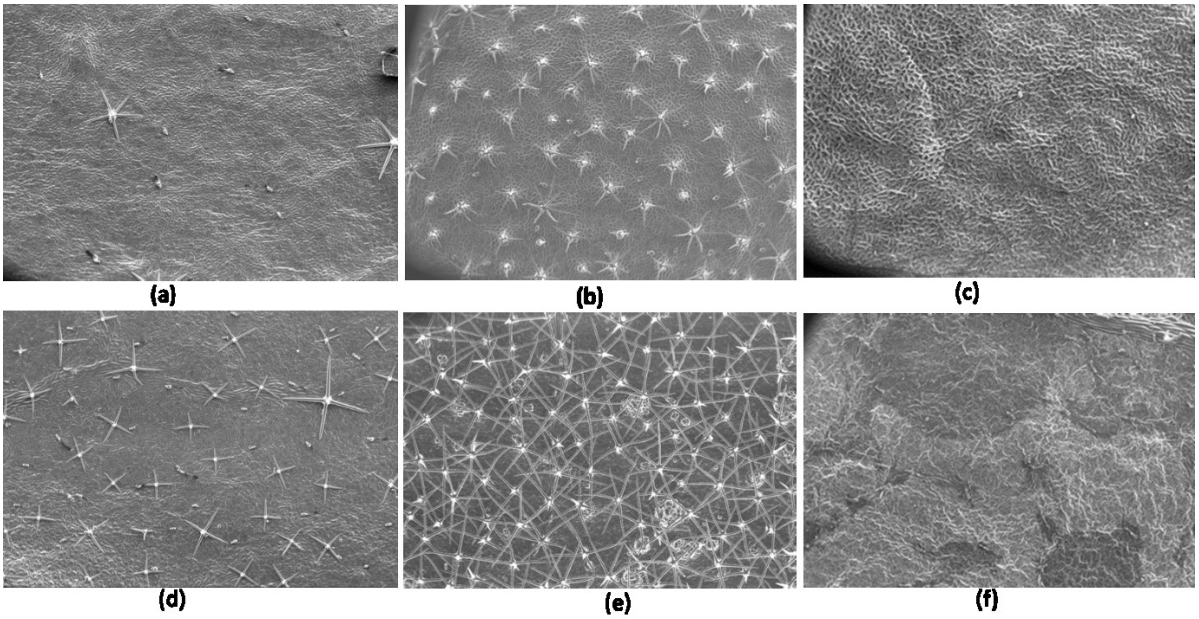

Figure 18. Electron microscopic images of (a, b, c) adaxial and abaxial (d, e, f) leaf surface of (a, d) *Solanum lanceifolium*, (b, e) *Solanum anguivi* and (c, f) *Capsicum annum* at 60X magnification.

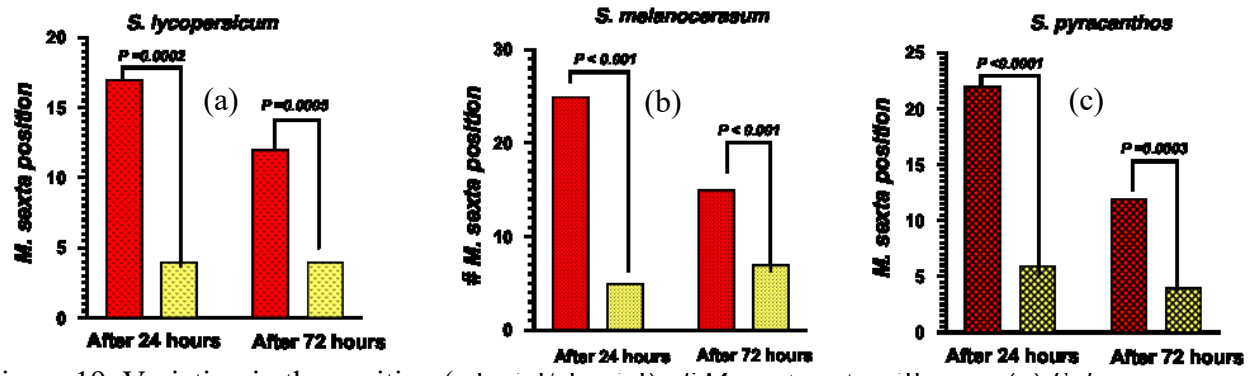

Figure 19. Variation in the position (adaxial/abaxial) of *M. sexta* caterpillars on (a) *Solanum melanocerasum*, (b) *Solanum lycopersicum* and (c) *Solanum pyracanthos* analyzed using Fisher's Exact test with significantly higher number of caterpillar found on abaxial (red bars) than adaxial (yellow bars) leaf surface after 24h and 72h of originally placing them on adaxial leaf surface.

CHAPTER IV

ARE EPICUTICULAR WAXES A BETTER SURFACE BARRIER THAN TRICHOMES IN PLANT DEFENSE? A TEST USING TWO *SOLANUM* SPECIES AND A SPECIALIST HERBIVORE.

Abstract

Although plants possess a suite of structural defenses including trichomes, waxes and spines to name a few, more studies have focused on trichomes. Trichomes, can have both pre and post ingestive effects and have been consistently found to reduce herbivory in a density dependent manner. Along with trichomes, few studies have also focused on epicuticular waxes (hydrophobic layer in outermost leaf surface) being an important abiotic and biotic defense, however manipulated pairwise comparisons examining herbivore growth and development is quite limited. In this study, using two *Solanum* species (*Solanum glaucescens* and *Solanum macrocarpon*) that show natural variation in both defenses, we tested our hypothesis that the herbivore feeding will be differentially affected by the variation in defenses primarily restricting feeding commencement. We tested this using a series of experiments including electron microscopy, plant-based and diet-based manipulative experiments using tobacco hornworm (*Manduca sexta*; Lepidoptera: Sphingidae; chewing type herbivore) as the model herbivore. We

found that *Solanum glaucescens* had significantly lower trichomes and significantly higher wax content when compared to *Solanum macrocarpon*. We also found that *S. glaucescens* waxes acted as a stronger physical barrier resulting into low mass gain and very high mortality of caterpillars compared to *S. macrocarpon*. And, diet manipulation experiments also suggest possible toxicity of waxes, leaf tissue added diet experiments had no differential effects on caterpillar growth. Collectively, we show that epicuticular waxes can play a significant role as a strong surface barrier and should be examined further independent and in combination with trichomes.

Introduction

It is a well-established fact that plants use both physical and chemical defenses to protect against arthropod herbivores (Coley and Barone 1996; Hare 2005; Mithöfer and Boland 2012; Horgan et al. 2009; Paudel et al. 2019; Singh and Kariyat, 2020; Tayal et al., 2020a; 2020b; Singh et al., 2021). Physical defenses mainly include waxes, trichomes and spines and chemical defenses include numerous secondary metabolites that can directly or/and indirectly defend plants (Howe and Jander, 2008). Among physical defenses, trichomes are one of the most important, and possibly the most studied defenses (Levin, 1973; Kariyat et al., 2013; 2017; 2018; 2019; Karabourniotis et al., 2019; Kaur and Kariyat, 2020a; 2020b; Watts et al., 2021; Watts and Kariyat, 2021a; 2021b). They are epidermal hairs present on various plant parts including leaves, stems and flowers (Kaur and Kariyat, 2020a).

Although trichomes are primarily classified as glandular and non-glandular types based on the presence or absence of a glandular head, deeper inspection revealed much more complicated morphological variation, both inter and intra specifically (Watts and Kariyat 2021a) including variation in size, shape, density and dimensions, that also varies between abaxial and

adaxial leaf surfaces (Watts and Kariyat 2021a; 2021b). In addition to trichomes, plant epicuticular waxes also play a major role in herbivore defense (Jetter et al., 2008). Waxes are basically a hydrophobic layer (made up of lipids and hydrocarbons) within an outer layer of cells (cutin) and have been found to layer most aerial parts of plants (Konno et al., 2006; Kaur et al., 2021 In Press). Waxes discourage the movement and feeding of herbivores by making leaf surface slippery and lowering crevices on leaf surfaces (Whitney and Federle, 2013). If ingested, herbivores have also been found to spend additional time cleaning their mouthparts when covered with waxes (Shelomi et al., 2010). In this regard, waxes too have both pre and post ingestive effects on insect herbivores, quite like trichomes. Trichomes deter herbivore movement and feeding pre-ingestion but can also cause post-ingestive effects by damaging caterpillar inner gut lining (peritrophic matrix) and determine multitrophic interactions by providing cues to herbivore's natural enemies (Kariyat et al., 2017; Weinhold and Baldwin, 2011). Moreover, higher trichome density is usually associated with reduced herbivory (Watts and Kariyat, 2021b). Understanding physical defenses in plants and their role in deterring herbivores had been a well-researched area, with both morphological variations, and molecular bases. And, for herbivores, estimating fitness impacts at various life stages, behavioral modifications to avoid them, and the mechanisms underlying multi-trophic interactions mediated by physical defenses have also been of interest for empirical work in this field. However, studies that examine trichomes and waxes together and independently have been limited. To understand the role of waxes and trichomes in tandem, also warrants plant species that are phylogenetically close, and exhibit variation for defenses, that are easy to manipulate for experiments. Over the past decade, we had been using Solanaceae family to understand the effects of inter and intraspecific variation in physical defenses, and their impact on mediating plant-herbivore interactions. More recently, we found

that among the sampled leaves of 14 species in *Solanum* genus, *Solanum macrocarpon* (Gboma) has both glandular and non-glandular trichomes (Watts and Kariyat, 2021a), but almost no waxes on leaf surface. On the other hand, another species used in the study, *Solanum glaucescens* (Cuatomate) has a thick wax layer on its leaf surface with almost no trichomes (Kaur et al., 2021a; in press). This natural variation for trichome-wax presence-absence provided us with an opportunity to test the impact of these defenses both in situ and in vitro. We used a combination of microscopy, herbivore behavior and growth assays to test our hypothesis that the trichomes and waxes would differentially affect herbivore feeding, with consequences for their growth and development.

Materials

a. *Plants:* We bought the seeds of two Solanaceae species viz. *Solanum glaucescens* (Product code: Y5SSSOGL) and *Solanum macrocarpon* (Product code: Y5SSSOLG) from rarepalmseeds.com. For details of how the plants were grown, see Watts and Kariyat (2021a).

b. *Insects:* Tobacco hornworm (*Manduca sexta*; Lepidoptera: Sphingidae) was used for laboratory-based assays. *M. sexta* is a Solanaceae specialist chewing type herbivore that feeds voraciously on a variety of Solanaceae species (Watts and Kariyat, 2021b). For details of rearing of insect colony, see Tayal et al. (2020a) and Watts and Kariyat (2020b).

c. *Desktop Scanning Electron Microscopy (DSEM):* To capture images of leaves for trichome morphology, dimension and density analysis (n= 3-11 plants/side/species), a desktop Scanning Electron Microscope (SNE- 4500 Plus Tabletop; Nanoimages LLC, Pleasanton, California, USA; Watts et al., 2021) was employed. For details on operational procedures and methodology of DSEM, see Watts and Kariyat (2021a) and Watts et al. (2021).

Assays

a. *Trichome morphology*: Fresh leaf samples (n= 3-11 plants/side/species) as described above were used and magnified ranging from 45X to 1000X depending on trichome type and size, to achieve maximum resolution to extract finer details of trichomes. For fine details of procedure, see Watts et al. (2021) and Watts and Kariyat (2020a).

2. *Trichome density estimation*: To determine the trichome density on both the species (n= 3-11 plants/side/species), sample preparation was done as described above. The images for trichome count were consistently captured at 60X magnification which contains approximately 5.32 mm^2 leaf area measured using 'Nanoeye' software linked to DSEM. We calculated the total trichome number, total glandular trichomes and total non-glandular trichomes as follows (Chavana et al., 2021; Watts and Kariyat, 2021b).

Trichome count (5.32 mm^2 of leaf area) = Number of trichomes counted manually in the image at 60X magnification

3. *Wax quantification*: The epicuticular waxes from the leaves of both the species were quantified. 50 circular leaf discs (0.63 cm in diameter) were punctured uniformly allover each plant (n=20: *S. glaucescens*; n= 13: *S. macrocarpon*) using hole puncher. The leaf discs from each plant were placed in a pre-weighed Eppendorf (2 ml) tube containing anhydrous chloroform. Following this, Eppendorf tubes were vortexed (VWR; ~1500rpm) for a minute. The leaf discs were removed from Eppendorf tubes post-vortexing and the tubes containing chloroform+wax solution were left under fume hood for 24h to let chloroform evaporate leaving the wax behind. The tubes were weighed again and the difference in post and pre weight of tubes was recorded as the wax amount for each sample (Kariyat et al., 2019).

4. *Time to first bite*: To examine whether caterpillar takes longer time to initiate feeding on one species over the other, first instar caterpillars (n= 15 per species) were used. Twenty minutes was decided as a limit to stop each observation if the caterpillar does not start feeding since a starved caterpillar should not take so long to start feeding. For details, see Watts and Kariyat (2020b).

5. *Mass gain and mortality by caterpillars*: This experiment was used to estimate the amount of plant tissue/artificial diet fed, and mortality by 1st (n= 15; control diet: n=30) instar *M. sexta* caterpillars on *S. glaucescens* and artificial diet. Pre-weighed 1st instars were placed on plants and allowed to feed. Each pre-weighed caterpillar was placed on a diet pellet in a separate petri-plate as control. The caterpillars were placed for 24h on plants and control diet, and then collected to weigh. After recording their mass, the caterpillars were placed back on their respective treatments from where they were collected and were weighed again after 24h (48h in total). While recording mass gain at 24h and 48h, mortality by caterpillars was also recorded on treatment and control. Data of mass gain by caterpillars was recorded as following:

Mass gain= (Final Mass-Initial Mass)/ Initial Mass

6. *Mass gain and mortality by caterpillars on diet pellets coated with waxes:* Waxes extracted from the wax quantification experiment was used for this experiment. Five Eppendorf tubes containing extracted waxes of each species were selected randomly. 200µl of chloroform was added to each tube as solvent and the Eppendorf tubes were vortexed (VWR; ~1500rpm) for one minute to dissolve waxes in chloroform. The dissolved waxes were coated thrice on artificial diet pellets using a paint brush. There were two treatments: Diet pellets coated with waxes extracted from *S. glaucescens*; diet pellets coated with waxes extracted from *S. macrocarpon*, one positive control: diet pellet coated with chloroform only, and one control: artificial diet pellet

with no waxes or chloroform. Pre-weighed 1st instar caterpillars (n=15 per treatment) were allowed to feed for 24 and were weighed at 24h. After weighing caterpillars at 24h, they were put back on diet pellets and weighed again after another 24h (48h in total). After 48h, all four batches of caterpillars were moved to control artificial diet separately and were allowed to feed for another 24h (72h in total), and then weighed again. Mass gain by caterpillars at 24h, 48h and 72h was recorded as mentioned above. Mortality of caterpillars was also recorded during all three times.

7. *Mass gain and mortality by caterpillars in diet containing leaf tissue*: 50g of leaf tissue of each species (from 8 different plants) was subjected to cryo-drying, followed by grinding (Mitton et al., 1979) and adding it into 0.5 l of artificial diet. 0.5 l of control artificial diet was prepared in the similar manner, but without leaf tissue. Pre-weighed caterpillars (n=30) were then allowed to feed on diet pellets on all three treatments. Mass and mortality of caterpillars was recorded after 24h and 48h of starting the experiment. Mass gain of caterpillars was recorded as mentioned above (Kariyat et al., 2019).

Analysis

Following Watts and Kariyat (2021a), we identified and named trichomes in *S. glaucescens* and S. *macrocarpon*. The trichome number (response variable) was analyzed using Wilcoxon 2 sample test by considering species as explanatory variable for all trichome types (total, total glandular trichomes and total non-glandular trichomes). Further, wax quantity (in mg) in both species was analyzed using Wilcoxon 2 sample test. Time to first bite by 1st instars was analyzed using Wilcoxon 2 sample test by considering species as explanatory variable. Mass gain by caterpillars at 24h and 48h on plant species and artificial diet was analyzed using one-way ANOVA. Mortality of caterpillars in mass gain experiment at both 24h and 48h was

analyzed using Generalized regression with binomial distribution (alive/dead). Mass gain of caterpillars on pellets coated with waxes at 24h was analyzed using One-way ANOVA and pairwise comparison was done using Tukey's test. For 48h and 72h, because of data not being normally distributed, Kruskal-Wallis test was used and pairwise comparison was done using Wilcoxon test. Mortality of caterpillars on pellets coated with waxes was analyzed using Generalized regression with binomial distribution (alive/dead) for all the times. Mass gain by caterpillars in diet containing leaf tissue (both 24h and 48h) were analyzed using Kruskal-Wallis test followed by pairwise comparison using Wilcoxon test. All the analyses were carried out using JMP (SAS institute, Cary, NC, USA), and the plots were built using GraphPad Prism (La Jolla, CA, USA).

Results

1. *Trichome morphology*: While scanning leaves of both species, we observed *S. glaucescens* possessed two glandular trichomes: *glandular* hair with globular head; acuminate *glandular* hair with multicellular stalk and small glandular tip. *S. macrocarpon* had *glandular* hair with globular head and single stalk cell on; attenuate basilatus *glandular* hair with small glandular tip, and subulate *non-glandular* hair with pulvinate base and pedestal (Figure 20).

2. *Trichome density assessment*: In case of *S. macrocarpon*, we observed more trichomes than *S. glaucescens* in Scanning electron microscopic (SEM) images. As expected, we found significantly higher total trichome number (Wilcoxon 2 sample test; p= 0.0049), total glandular trichome number (Wilcoxon 2 sample test; p= 0.0073), and total non-glandular trichome number (Wilcoxon 2 sample test; p= 0.0084) in *S. macrocarpon* than *S. glaucescens* (Figure 21).

3. *Wax quantification*: In SEM images of leaves, we observed a thick mat of epicuticular waxes on leaf surface of *S. glaucescens* and no wax mat on *S. macrocarpon*. With quantification,

we found significantly higher amount of waxes on leaves of *S. glaucescens* (Wilcoxon test; $p<0.0001$) than *S. macrocarpon* (Figure 22).

4. *Time to first bite*: After quantification of physical defenses in both species, we found that 1st instar caterpillars took significantly longer time to initiate feeding on *S. glaucescens* than *S. macrocarpon* (Wicoxon 2 sample test; $p<0.0001$) (Figure 23).

5. *Mass gain and mortality by caterpillars*: Mass gain by caterpillars on *S. glaucescens* was significantly lower than control artificial diet at both 24h (One-way ANOVA; $p<0.0001$) and 48h (One-way ANOVA; $p=0.0015$). Consistent with mass gain results, mortality of caterpillars on *S. glaucescens* was significantly higher than control diet (Generalized regression; $p<0.0001$) at both 24h and 48h (Generalized regression; $p<0.0001$) (Figure 24 and 25).

6. *Mass gain by caterpillars on diet pellets coated with waxes:* When diet pellets were smeared with waxes, mass gain by 1st instar caterpillars was significantly different among four treatments at 24h (One-way ANOVA; $p<0.0001$). Post-hoc tests showed that caterpillars placed on pellets coated with *S. glaucescens* waxes had significantly lower mass gain than caterpillars placed on control diet (Tukey's test; $p=0.0062$). Other interactions were non-significant (Tukey's test; $p>0.05$). At 48h of the experiment, there was no significant difference among all four treatments (Kruskal-Wallis test; $p=0.1217$). But for post hoc tests, caterpillars placed on pellets coated with *S. glaucescens* waxes had significantly lower mass gain than caterpillars placed on control diet (Wilcoxon test; $p=0.0278$). At 72h of experiment, there was significant difference among all treatments (Kruskal-Wallis test; $p=0.0306$). And caterpillars initially placed on pellets coated with *S. glaucescens* waxes (Wilcoxon test; $p=0.0320$) and *S. macrocarpon* (Wilcoxon test; $p=0.0141$) had significantly lower mass gain than caterpillars placed on control artificial diet throughout the experiment (Figure 26). But there was no significant difference in mortality of

caterpillars among all treatments at 24h, 48h and 72h (Generalized regression; $p>0.05$) (Figure 27).

7. *Mass gain by caterpillars on diet containing leaf tissue*: When plant tissue was added into artificial diet, there was no significant difference in the mass gain by caterpillar among diets treatments during both 24h (Kruskal-Wallis; $p=0.7698$) and 48h (Kruskal-Wallis; $p=0.6952$) (Figure 28). There was no significant difference between treatments at both timings (Wilcoxon test; $p>0.05$), and no mortality was recorded in any of the treatments at both timings.

Discussion

Our results collectively show that although different trichome types are present in both *S. glaucescens* and *S. macrocarpon*, trichome density is greater on *S. macrocarpon* leaves. Behavioral assays show that *M. sexta* caterpillars tend not to initiate feeding, and have decreased mass and high mortality on leaf surface with greater wax amount viz. *S. glaucescens*. Caterpillars also gained lower mass after ingestion of *S. glaucescens* waxes smeared on artificial diet pellets, but when leaf tissue was added into artificial diet of both species, it did not have any differential effects on herbivore growth, in case of manipulative diet-based experiments.

Both *Solanum* species have both glandular and non-glandular trichomes. But non-glandular trichomes are present in considerably greater number in *S. macrocarpon* than *S. glaucescens*. Previously, non-glandular trichomes have been found to have deterrent effects on caterpillar feeding (Kariyat et al., 2017) especially in earlier instars (Kariyat et al., 2018). And trichome density of all trichome types (total, glandular and non-glandular) is higher in *S. macrocarpon*, thus creating comparatively stronger physical barrier against various stresses. Higher trichome density is usually associated with decreased herbivory (Fordyce and Agrawal, 2002; Eaton and Karba, 2014; Pastório et al., 2019; Watts and Kariyat, 2021b) and increased

abiotic stress tolerance (Liakoura et al., 1997; Li et al., 2018). Thus, we expected *S. macrocarpon* to be more resistant to herbivore feeding than *S. glaucescens*, but *S. glaucescens* has a thick epicuticular wax layer and higher wax content than *S. macrocarpon*. Waxes are also considered as a strong physical defense against herbivores (Daoust et al., 2010; Whitney and Federle, 2013; Kaur et al., 2021 in press) and here we show that these waxes can also be a significant physical barrier for herbivores to cross and commence feeding.

Herbivore feeding behavior assays showed that starved 1st instar caterpillars took much longer to initiate feeding on species with more waxes (Varela and Bernays, 1988; Shelomi et al., 2010). And as a matter of fact, the caterpillars did not even start feeding on leaves of *S. glaucescens* in 20 minutes (some feeding was observed afterwards). Additionally, caterpillars did not gain any mass, and even lost mass, possibly due to desiccation, after caterpillars placed on *S. glaucescens*. Mortality of caterpillars was also very high (more than 90%) on *S. glaucescens* plants, with almost zero mortality on artificial diet (Wójcicka, et al., 2016). These results when combined with the fact that *S. glaucescens* has more epicuticular waxes and low trichome numbers suggest that *S. glaucescens* acts as a stronger physical barrier for caterpillars, independent of trichomes. Although a combination of different defense strategies are usually employed by plants to mount "an efficient defense phenotype" based on their ancestry and evolution (Agrawal and Fishbein, 2006), in this case, epicuticular waxes have an upper hand than trichomes because the combination of high trichome density and thin wax layer present on *S. macrocarpon* leaf surface failed to hinder caterpillar feeding when compared to *S. glaucescens*.

When artificial diet pellets were coated with waxes from both plant species, mass gain by caterpillars placed on diet pellets smeared with waxes of *S. glaucescens* was lower than caterpillars placed on control diet at 24h and 48h. Although the mass gain was lower, mortality

on all treatments was similar which indicates that the wax layer primarily acted as a barrier, but not as severe as on the actual leaf. However, these results also show that wax composition also matters since possible toxins in wax (Belete, 2018) of *S. glaucescens* did not allow caterpillars to gain mass and grow to its full potential. Later when all caterpillars from four treatments were moved (separately) to artificial diet, mass gain by caterpillars initially placed on pellets smeared with waxes of *S. glaucescens* and *S. macrocarpon* was lower than mass gain by caterpillars placed on artificial diet with no coating throughout the experiment. This result also indicates the significance of chemical composition (Eigenbrode and Espelie, 1995) of waxes playing an important role in caterpillars' mass gain and growth (Johnson, 2021). For instance, Negin et al. (2021) found that fatty alcohols in the epicuticular waxes of *Nicotiana glauca* (Solanaceae) tend to reduce the various caterpillars' growth. Moreover, mass gain was decreased in case of *S. glaucescens* caterpillars at 24h, but it was lower at 72h on *S. macrocarpon* wax smeared pellets, which again points that waxes on *S. glaucescens* act as stronger barrier, most likely due to higher wax amount. And, although the caterpillars were moved away from waxes (after 48h), reduction in growth was recorded which emphasize the impact of waxes acting against caterpillars even after the caterpillars were saved. Thus, the chemical composition of waxes in both plant species, and more specifically *S. glaucescens* should be explored to identify and extract anti herbivore compounds, an area we are currently exploring.

We also tested whether composition of leaf tissue (chemistry rather than physical barrier) acts as a factor (Matsuki and Maclean, 1994; Lill and Marquis, 2001) (without surface defenses) in herbivore growth, leaf tissues from both species were added into artificial diet separately and caterpillars were allowed to feed on diet pellets (Kariyat et al., 2017; Watts and Kariyat, 2021b). The caterpillars gained equal mass on both treatment and control diet pellets. The results suggest

that composition of leaf tissue has no negative/positive effects on caterpillars' mass gain and thus, mass gain of caterpillars on plants is most likely solely affected by surface defenses. However, we acknowledge that these effects should be further studied over a longer period, growth stages, or even generations (Tayal et al., 2020b; Portman et al., 2020). For example., Lill and Marquis (2001) which found that low quality oak leaves (*Quercus alba*; Fagaceae) lead to reduced survivorship of first generation of leaf tying caterpillars (*Psilocorsis quercicella*; Lepidoptera: Despressariidae), but the second generation feeding on the same leaves were unaffected.

Taken together, in this study, waxes proved to be stronger and possibly a better surface defense, although more surface defense studies are focused on trichomes, and demands more attention (Kaur et al., 2021; in press). Additional work should also focus on understanding wax-trichome interplay and how other contributing factors could influence the efficiency of these surface defenses both under favorable and harsh environmental conditions (Lewandowska et al., 2020), and with different herbivores (White and Eigenbrode, 2000) and their natural enemies of herbivores (Yao et al., 2021).

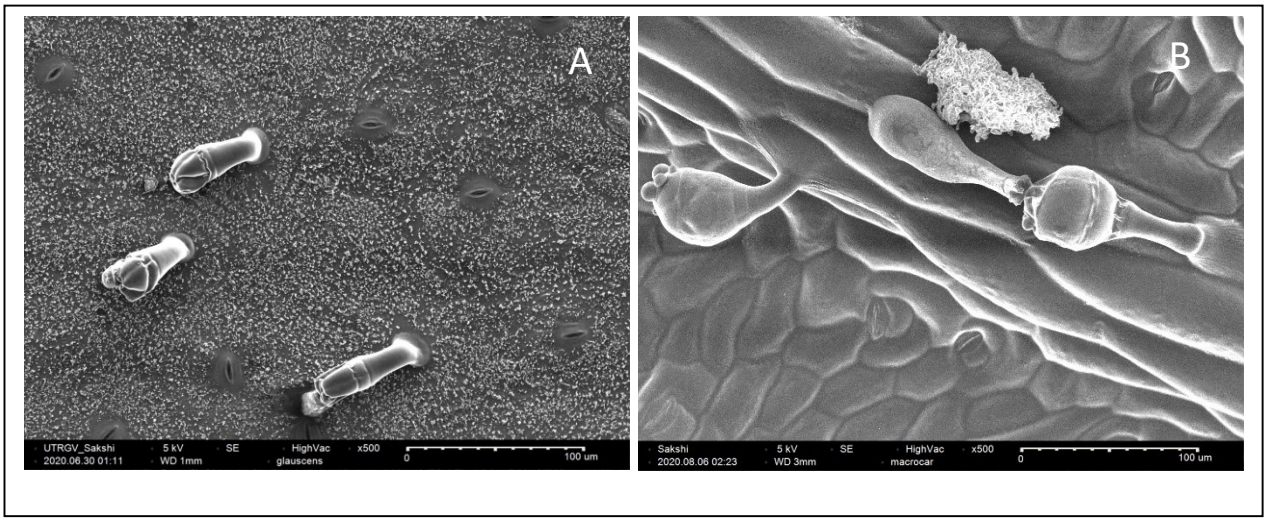

Figure 20. Scanning electron microscopic images of adaxial leaf surfaces of (A) *Solanum glaucescens* (Solanaceae), and (B) *Solanum macrocarpon* (Solanaceae) at 500X. A thick wax layer and glandular trichomes with globular head can be observed in *Solanum glaucescens*, and no visible wax layer, and glandular hair with globular head and single stalk cell, and attenuate basilatus glandular hair with small glandular tip on adaxial leaf surface can be observed in *S. macrocarpon*.

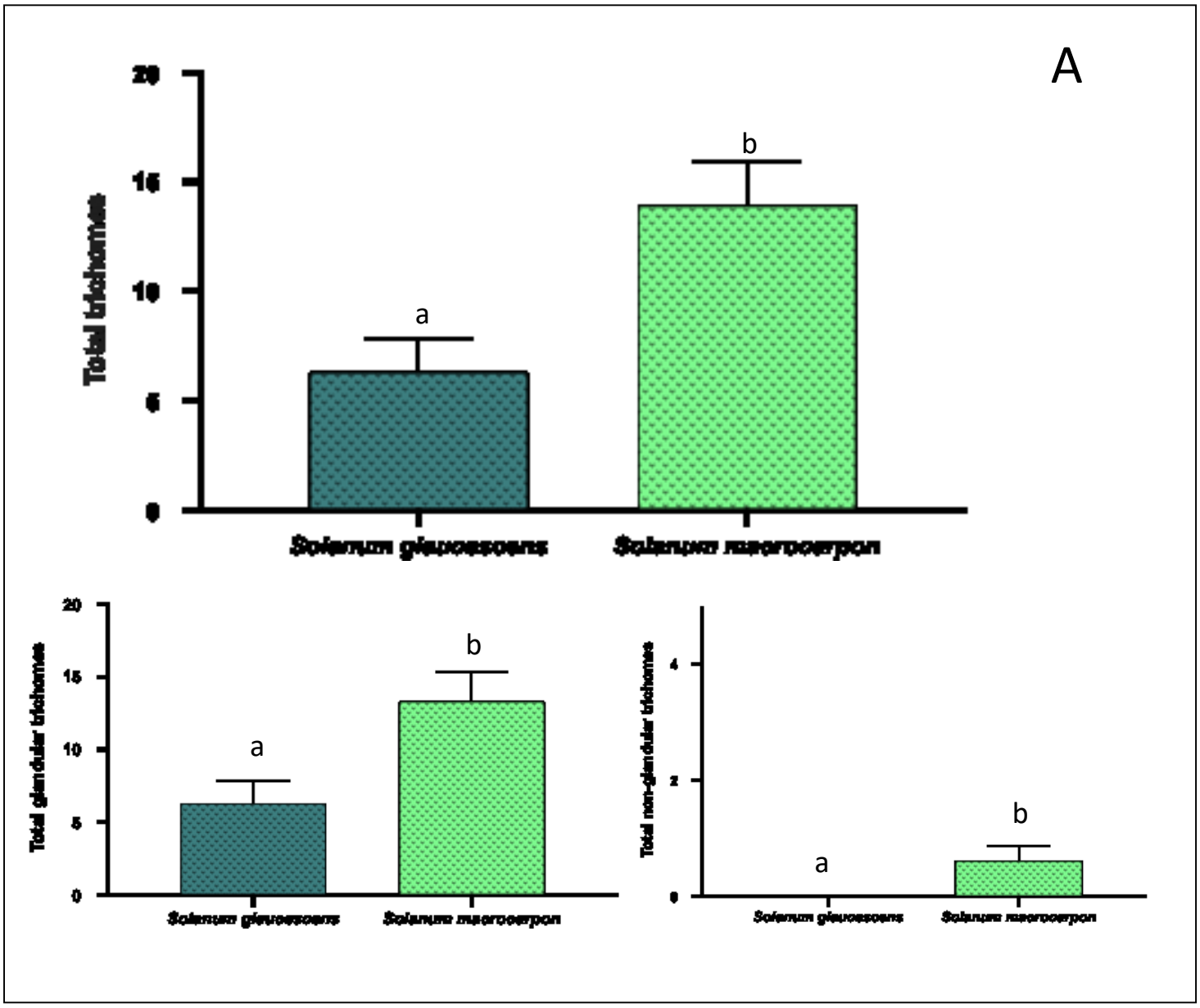

Figure 21. Trichome number (n; in Scanning electron microscopic images at 60X magnification; 5.32 mm^2 of leaf area) was found significantly higher in *S. macrocarpon* than *S. glaucescens* for

(A) total trichomes (Wilcoxon test; p= 0.0049), (B), total glandular trichomes (Wilcoxon test; p= 0.0073), and (C) total glandular trichomes (Wilcoxon test; p= 0.0084). Different letters (a, b) on bars of both species for comparison of each trichome type (total; glandular; non-glandular) represent significant difference.

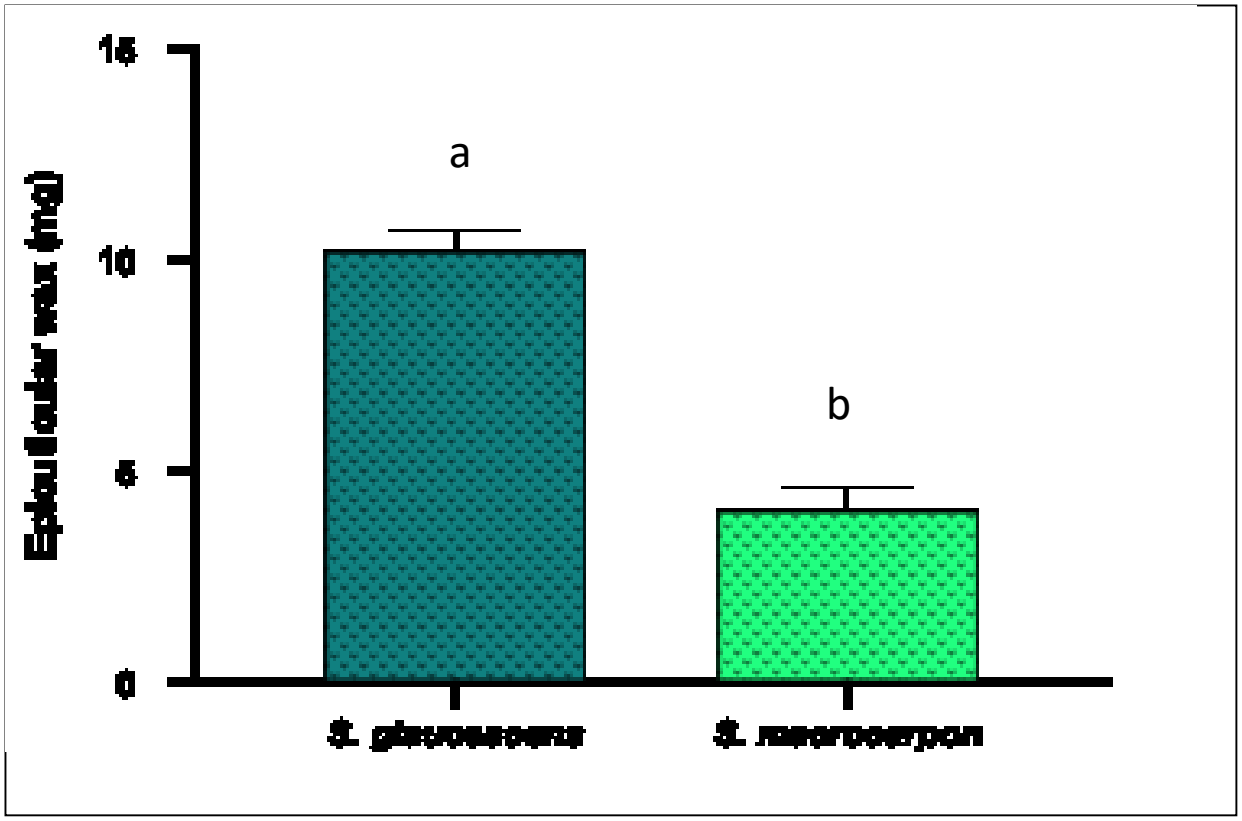

Figure 22. Epicuticular waxes were present in significantly higher amount on *S. glaucescens* leaves than *S .macrocarpon* leaves (Wilcoxon test; $p<0.0001$). Different letters on the bars represent significant difference. Different letters on the bars represent significant difference.

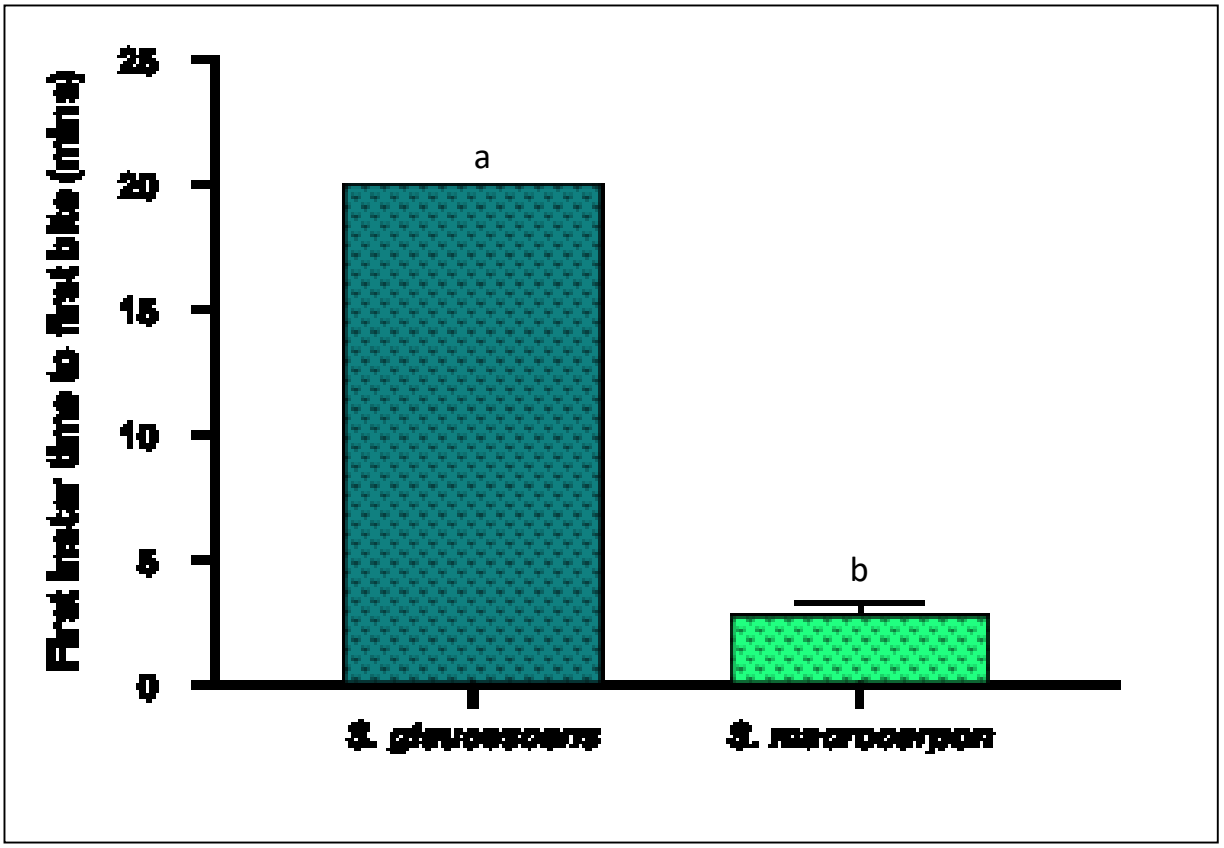

Figure 23. Time taken by starved 1st instar Manduca sexta (Lepidoptera: Sphingidae) caterpillars (in minutes) to initiate feeding on leaf surface was higher on S. glaucescens than S. macrocarpon (Wicoxon 2 sample test; $p<0.0001$). Different letters on the bars represent significant difference.

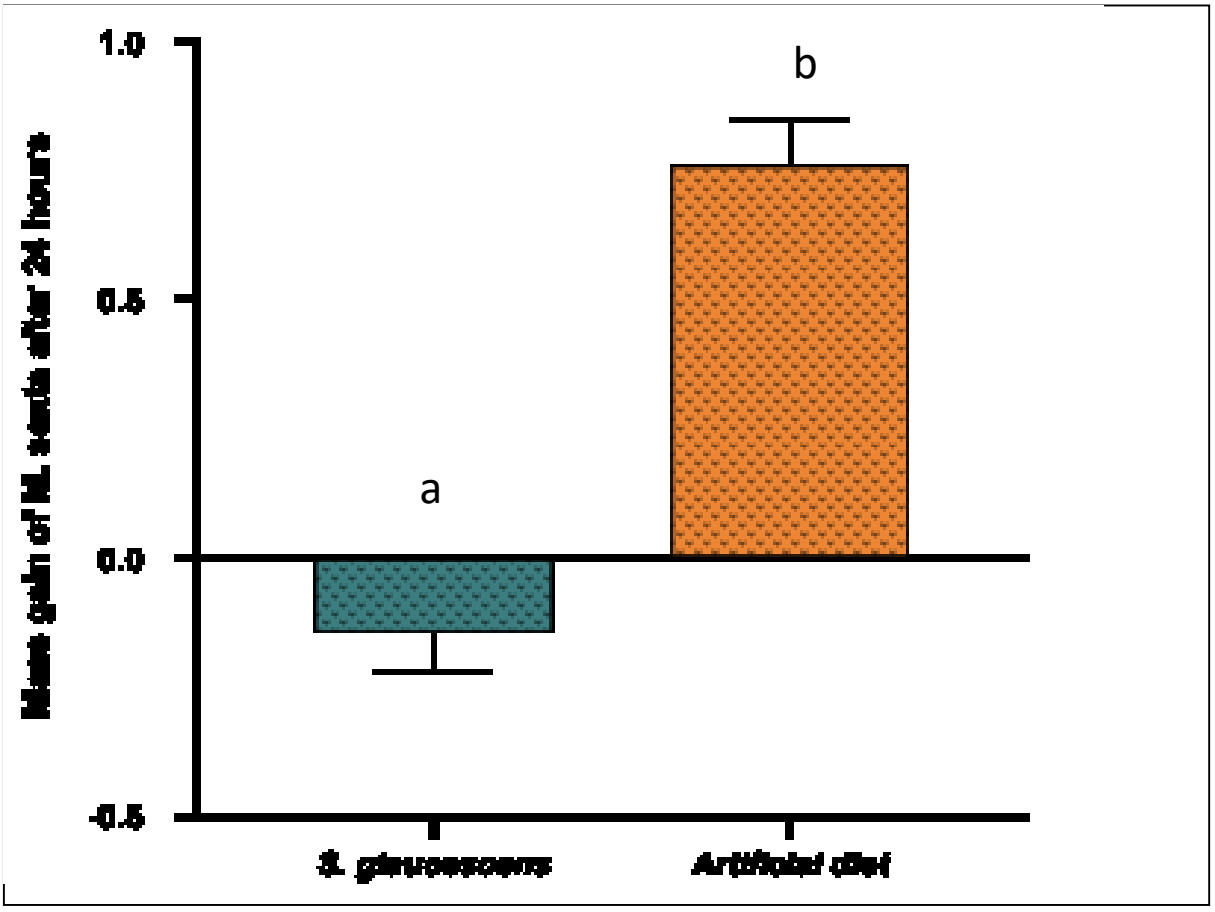

Figure 24. *M. sexta* 1st instars gained significantly higher mass (in mg) on artificial diet than *S. glaucescens* plants (One-way ANOVA; $p<0.0001$) after 24h of start of experiment. Different letters on the bars represent significant difference.

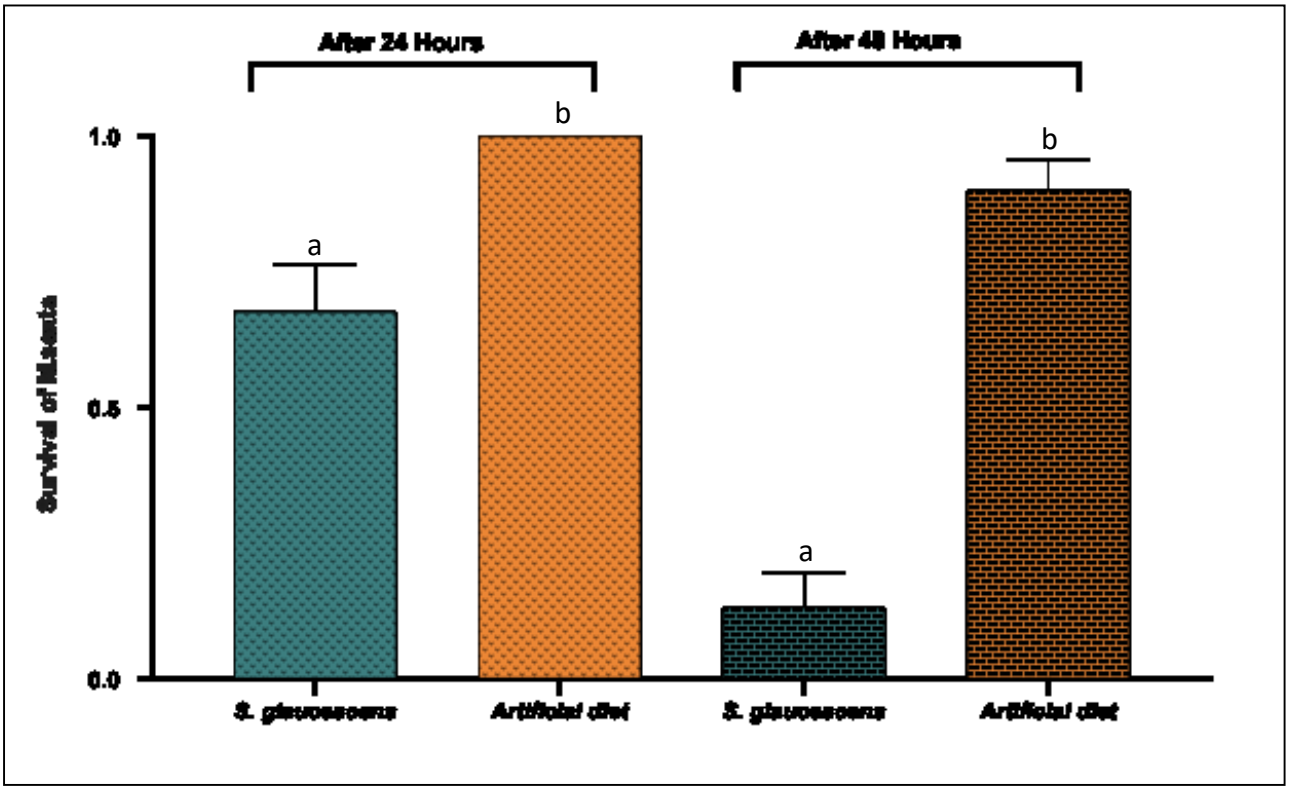

Figure 25. Survival (1-mortality; 0- dead and 1-alive) of *M. sexta* caterpillars was significantly higher on control artificial diet than *S. glaucescens* plants at both 24 h (Generalized regression; $p<0.0001$) and 48h (Generalized regression; $p<0.0001$) during mass gain experiment. Different letters (a, b) on the bars during each timing (24h and 48h; independent) represent significant difference.

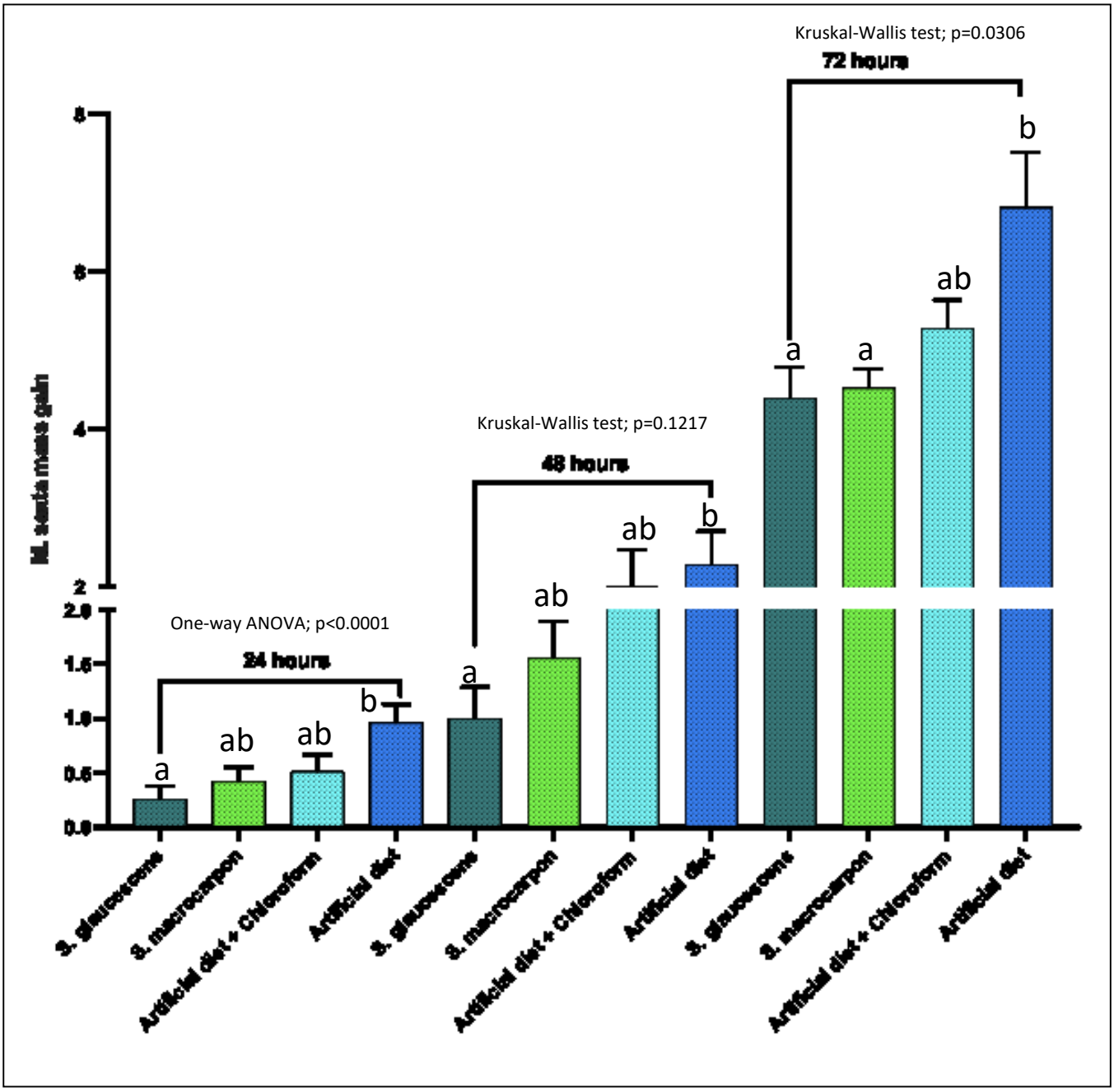

Figure 26. Caterpillars had significant difference in mass gain among four treatments (diet pellets coated with waxes extracted from *S. glaucescens*; diet pellets coated with waxes extracted from *S. macrocarpon*, diet pellet coated with chloroform, and artificial diet pellet with no waxes or chloroform) at 24h (One-way ANOVA; $p<0.0001$) and 72h (Kruskal-Wallis test; $p=0.0306$), but the difference was non-significant at 48h (Kruskal-Wallis test; $p=0.1217$). Post-hoc analysis

reveals significantly lower mass gain by caterpillars placed on pellets with *S. glaucescens* waxes than caterpillars placed on control diet at 24h (Tukey's test; p=0.0062) and 48h (Wilcoxon test; p=0.0278). At 72h, caterpillars placed on *S. glaucescens* (Wilcoxon test; p=0.0320) and *S. macrocarpon* (Wilcoxon test; p=0.0141) wax pellets initially had significantly lower mass gain than caterpillars on control diet throughout the experiment. Different letters (a, b) on the bars during each timing (24h, 48h and 72h; independent) represent significant difference.

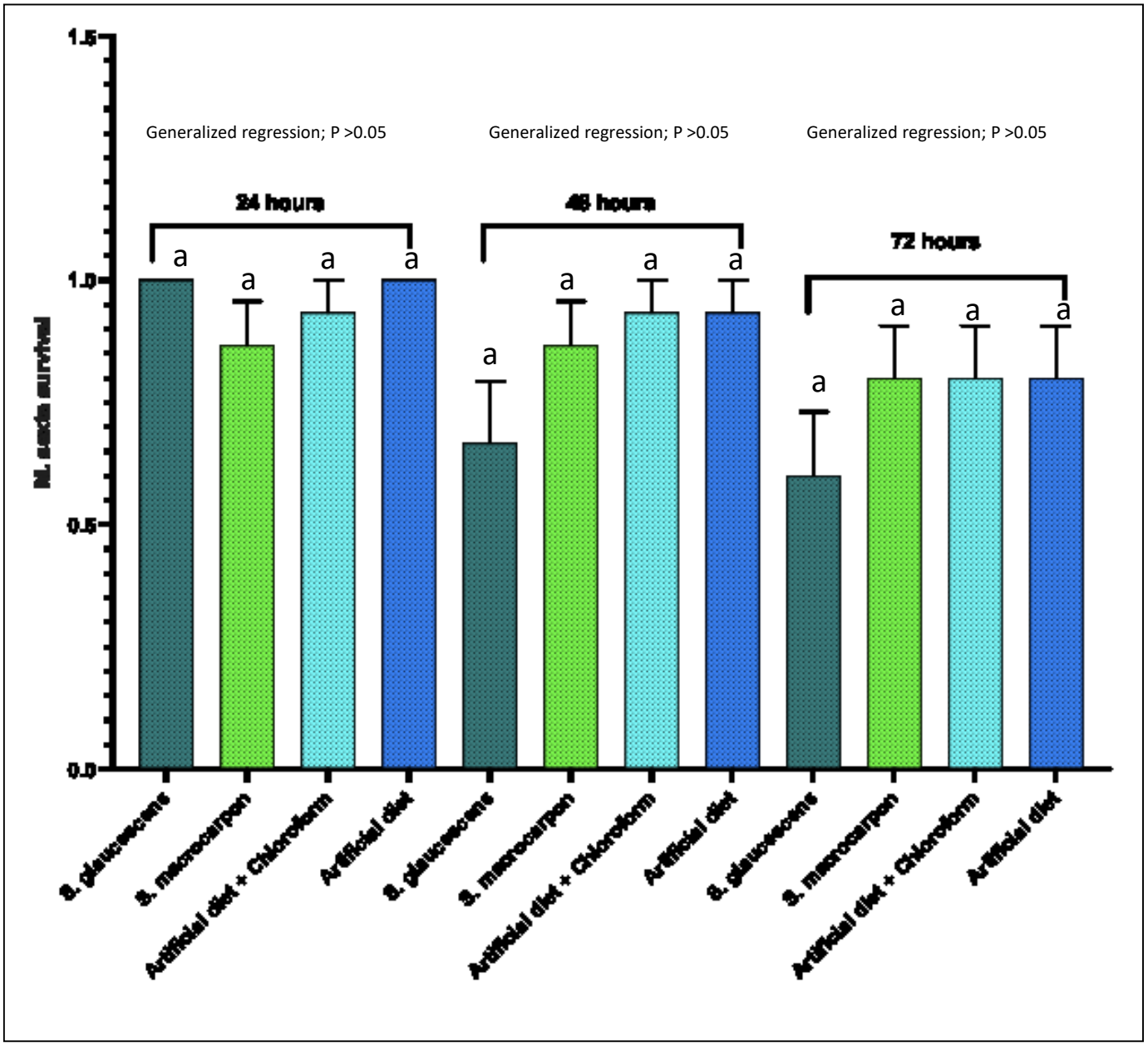

Figure 27. No significant difference in the survival (1-mortality; 0- dead and 1-alive) of *M. sexta* caterpillars placed on four treatments (diet pellets coated with waxes extracted from *S. glaucescens*; diet pellets coated with waxes extracted from *S. macrocarpon*, diet pellet coated with chloroform, and artificial diet pellet with no waxes or chloroform) at 24h, 48h and 72h was observed (Generalized regression; P >0.05). Similar letters on the top of bars during each time represent non-significant differences among treatments.

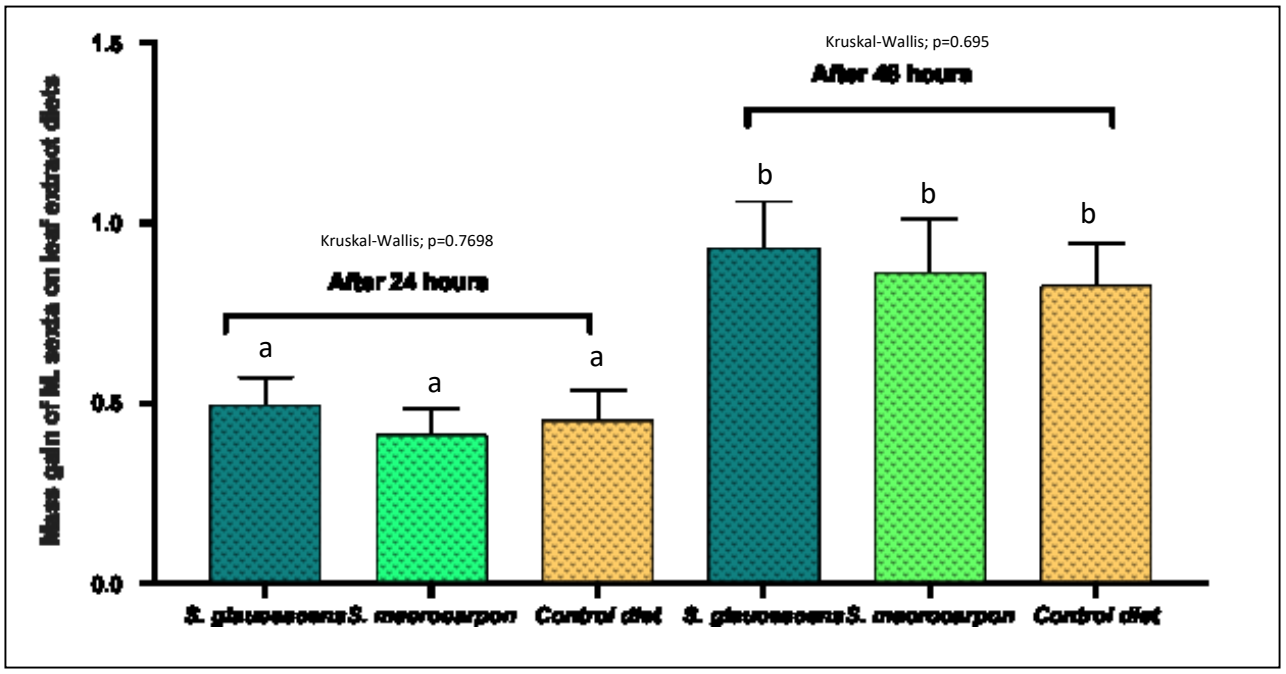

Figure 28. Caterpillars when fed on diets containing leaf tissue of *S. glaucescens* and *S. macrocarpon*, and control artificial diet had non-significant mass gain among (24h; Kruskal-Wallis; p=0.7698 and 48 h; Kruskal-Wallis; p=0.6952) and between treatments (Wilcoxon test; p>0.05) during both 24h and 48h of experiment. Same letters (a or b) on the bars in each timing (24h and 48h; independent) represent non-significant difference.

CHAPTER V

CONCLUSIONS AND FUTURE DIRECTIONS

Through a series of lab, field, and microscopy experiments, we conclude that there is tremendous trichome diversity in *Solanum* genus, and this variation has functional consequences for plant defense against insect herbivores. Trichomes vary a lot both inter and intraspecifically, and among a mixture of wild and domesticated, annual, and perennial, food crops and weed species. Overall, exploring trichome diversity by considering fourteen species from various groups (for example, *S. macrocarpon* and *S. lycopersicum* are cultivated species, while *S. anguivi* and *S. pyracanthos* are wild species) of *Solanum* genus provided us with an updated data source of trichome characteristics with such details that never has been done before.

Additionally, we documented a detailed procedure as a possible alternative to traditional electron microscopy that removes the major bottlenecks such precise expertise in use of machinery, and longer preparation time, while sustaining comparable image quality. We demonstrated that using Desktop Scanning Electron Microscope (DSEM), which is fast, easy to operate, and inexpensive, can produce quality images like other SEM, with significantly lower costs of equipment, maintenance, and methodology. Next, we showed that caterpillars tend to feed on the abaxial leaf surface despite the damage caused to them because of higher trichome

density on leaf surface. Additionally, epicuticular waxes are quite strong physical barrier against caterpillars which can lead to lowering their mass gain and high mortality.

Future directions in trichome studies should be focused on understanding variability and organ development while studying targeted (e.g., glandular trichomes) gene expression simultaneously using trichomes as a model. Moreover, trichomes are also known to play role in multi-trophic interactions in various natural and agroecosystems (Weinhold and Baldwin, 2011; Kariyat et al., 2013) and thus, each trichome type can be explored for its potential in strengthening plants' defenses, either directly or indirectly, and whether host plant genetic variation plays a role in modifying these interactions (Kariyat et al., 2013; Nihranz et al., 2019). In addition to this, using a more efficient method for capturing scanning electron microscope images by placing the sample on the stage can produce similar results as produced by using more complicated and traditional SEM. This tool can especially be used more oftenly for plant-insect interactions studies where routine imaging of plant and insect parts could be fast tracked using DSEM. With finding that while hiding on the abaxial leaf surface has possible benefits, this can also lead to potential fitness consequences, where their growth is affected, leading to possible cascading effects, which can be explored. Although waxes proved to be a strong physical barrier, chemistry of waxes needs to be explored to understand if there are any specific chemical leading to reduced mass gain of caterpillars' post-ingestion of plant materials.

Taken together, trichomes, possibly the most common structural defense in flowering plants can be of immense research potential for ecologists, entomologists, and plant biologists. And since most plant species in nature must deal with biotic and abiotic stressors, trichomes which are thought to be evolved as an abiotic stress response may help us in understanding both the external manifestation of "plant defense phe1notype" and their mechanistic underpinnings, as

an additional index in estimating plant-herbivore interactions (Kariyat and Portman, 2016). And Solanaceae may possibly be one of the best plant families to ask these questions.

REFERENCES

Adedeji, O., Ajuwon, O., & Babawale, O. (2007). Foliar epidermal studies, organographic distribution and taxonomic importance of trichomes in the family Solanaceae. *International Journal of Botany, 3*(3), 276-282. doi:10.3923/ijb.2007.276.282

Agrawal, A. A., & Fishbein, M. (2006). Plant defense syndromes. *Ecology, 87*(Sp7). doi:10.1890/0012-9658(2006)87[132:pds]2.0.co;2

Ambrósio, S. R., Oki, Y., Heleno, V. C., Chaves, J. S., Nascimento, P. G., Lichston, J. E., . . . Costa, F. B. (2008). Constituents of glandular trichomes of *Tithonia diversifolia*: relationships to herbivory and antifeedant activity. *Phytochemistry, 69*(10), 2052-2060. doi:10.1016/j.phytochem.2008.03.019

Andama, J. B., Mujiono, K., Hojo, Y., Shinya, T., & Galis, I. (2020). Non-glandular silicified trichomes are essential for rice defense against chewing herbivores. *Plant, Cell & Environment, 43*(9), 2019-2032. doi:10.1111/pce.13775

Avé, D. A., Gregory, P., & Tingey, W. M. (1987). Aphid repellent sesquiterpenes in glandular trichomes of *Solanum berthaultii* and *S. tuberosum*. *Entomologia Experimentalis Et Applicata, 44*(2), 131-138. doi:10.1111/j.1570-7458.1987.tb01057.x

Belete, T. (2018). Defense mechanisms of plants to insect pests: from morphological to biochemical approach. *Trends in Technical & Scientific Research, 2*(2). doi:10.19080/ttsr.2018.02.555584

Blamey, F. P., Joyce, D. C., Edwards, D. G., & Asher, C. J. (1986). Role of trichomes in sunflower tolerance to manganese toxicity. *Plant and Soil, 91*(2), 171-180. doi:10.1007/bf02181785

Blamey, P., Hernandez-Soriano, M., Cheng, M., Tang, C., Paterson, D., Lombi, E., . . . Kopittke, P. M. (2015). Synchrotron-based techniques shed light on mechanisms of plant sensitivity and tolerance to high manganese in the root environment. *Plant Physiology*. doi:10.1104/pp.15.00726

Burrows, G. E., White, R. G., Harper, J. D., Heady, R. D., Stanton, R. A., Zhu, X., . . . Lemerle, D. (2013). Intrusive trichome bases in the leaves of silverleaf nightshade (*Solanum*

elaeagnifolium; solanaceae) do not facilitate fluorescent tracer uptake. *American Journal of Botany, 100*(12), 2307-2317. doi:10.3732/ajb.1300034

Cantino, Philip. (1990). The Phylogenetic Significance of Stomata and Trichomes in the Labiatae and Verbenaceae. Journal of the Arnold Arboretum. Arnold Arboretum. 71. 323-370. 10.5962/p.184532

Caldwell, D., & Iyer-Pascuzzi, A. S. (2019). A scanning electron microscopy technique for viewing plant− microbe interactions at tissue and cell-type resolution. *Phytopathology*, *109*(7), 1302-1311.

Channarayappa, C., Shivashankar, G., Muniyappa, V., & Frist, R. H. (1992). Resistance of Lycopersicon species to *Bemisia tabaci*, a tomato leaf curl virus vector. *Canadian Journal of Botany, 70*(11), 2184-2192. doi:10.1139/b92-270

Chavana, J., Singh, S., Vazquez, A., Christoffersen, B., Racelis, A., & Kariyat, R. R. (2021). Local adaptation to continuous mowing makes the noxious weed *Solanum elaeagnifolium* a superweed candidate by improving fitness and defense traits. *Scientific Reports, 11*(1), 1-15. doi:10.1038/s41598-021-85789-z

Childers, N. F., & Margoles, M. S. (1998). Relation of Nightshades (Solanaceae) to Arthritis. *HortScience, 33*(3), 505c-505. doi:10.21273/hortsci.33.3.505c

Cho, K., Kwon, M., Cho, J., Im, J., Park, Y., Hong, S., . . . Kang, J. (2017). Characterization of trichome morphology and aphid resistance in cultivated and wild species of potato. *Horticulture, Environment, and Biotechnology, 58*(5), 450-457. doi:10.1007/s13580-017-0078-4

Coley, P. D., & Barone, J. A. (1996). Herbivory and plant defenses in tropical forests. *Annual Review of Ecology and Systematics, 27*(1), 305-335. doi:10.1146/annurev.ecolsys.27.1.305

Corsi, G., & Bottega, S. (1999). Glandular hairs of *Salvia officinalis*: new data on morphology, localization and histochemistry in relation to function. *Annals of Botany, 84*(5), 657-664. doi:10.1006/anbo.1999.0961

Dahlin, R. M., Brick, M. A., & Ogg, J. B. (1992). Characterization and density of trichomes on three common bean cultivars. *Economic Botany, 46*(3), 299-304. doi:10.1007/bf02866628

Dalin, P., Ågren, J., Björkman, C., Huttunen, P., & Kärkkäinen, K. (2008). Leaf trichome formation and plant resistance to herbivory. *Induced Plant Resistance to Herbivory,* 89-105. doi:10.1007/978-1-4020-8182-8_4

Daoust, S. P., Mader, B. J., Bauce, E., Despland, E., Dussutour, A., & Albert, P. (2010). Influence of epicuticular-wax composition on the feeding pattern of a phytophagous insect: Implications for host resistance. *The Canadian Entomologist, 142*(3), 261-270. doi:10.4039/n09-064

Deore, C. R. (2020). Morphological variation of trichomes in some common species of angiosperm and their systimatic enumieration useful for taxonomic significance.

Despland, E. (2019). Caterpillars cooperate to overcome plant glandular trichome defenses. *Frontiers in Ecology and Evolution, 7*. doi:10.3389/fevo.2019.00232

Eaton, K. M., & Karban, R. (2014). Effects of trichomes on the behavior and distribution of *Platyprepia Virginalis* caterpillars. *Entomologia Experimentalis Et Applicata, 151*(2), 144-151. doi:10.1111/eea.12178

Ehleringer, J. (1982). The influence of water stress and temperature on leaf pubescence development in *Encelia farinosa*. *American Journal of Botany, 69*(5), 670. doi:10.2307/2442956

Eigenbrode, S. D., & Espelie, K. E. (1995). Effects of plant epicuticular lipids on insect herbivores. *Annual Review of Entomology, 40*(1), 171-194. doi:10.1146/annurev.en.40.010195.001131

Elle, E., Van Dam, N. M., & Hare, J. D. (1999). Cost of glandular trichomes, a "resistance" character in *Datura wrightii* regel (Solanaceae). *Evolution, 53*(1), 22. doi:10.2307/2640917

Ensikat, H., Wessely, H., Engeser, M., & Weigend, M. (2021). Distribution, ecology, chemistry and toxicology of Plant Stinging Hairs. *Toxins, 13*(2), 141. doi:10.3390/toxins13020141

Eyvazadeh Khosroshahi, E., & Salmaki, Y. (2019). Evolution of trichome types and its systematic significance in the Genus *Phlomoides* (lamioideae–lamiaceae). *Nordic Journal of Botany, 37*(5). doi:10.1111/njb.02132

Fordyce, J. A., & Agrawal, A. A. (2001). The role of plant trichomes and caterpillar group size on growth and defence of the pipevine swallowtail *Battus philenor*. *Journal of Animal Ecology, 70*(6), 997-1005. doi:10.1046/j.0021-8790.2001.00568.x

Fürstenberg-Hägg, J., Zagrobelny, M., & Bak, S. (2013). Plant defense against insect herbivores. *International Journal of Molecular Sciences, 14*(5), 10242-10297. doi:10.3390/ijms140510242

Gallon, M. E., Silva-Junior, E. A., Amaral, J. G., Lopes, N. P., & Gobbo-Neto, L. (2019). Natural products diversity in plant-insect interaction between *Tithonia diversifolia* (Asteraceae) and *Chlosyne lacinia* (Nymphalidae). *Molecules, 24*(17), 3118. doi:10.3390/molecules24173118

Hardin, J. W. (1979). Patterns of variation in foliar trichomes of Eastern North American *Quercus*. *American Journal of Botany, 66*(5), 576-585. doi:10.1002/j.1537-2197.1979.tb06260.x

Hare, J. D. (2005). Biological activity of acyl glucose esters from *Datura wrightii* glandular trichomes against three native insect herbivores. *Journal of Chemical Ecology, 31*(7), 1475-1491. doi:10.1007/s10886-005-5792-1

Heinrich, B. (1979). Foraging strategies of caterpillars. *Oecologia, 42*(3), 325-337. doi:10.1007/bf00346597

Horgan, F. G., Quiring, D. T., Lagnaoui, A., & Pelletier, Y. (2009). Effects of altitude of origin on trichome-mediated anti-herbivore resistance in wild Andean potatoes. *Flora - Morphology, Distribution, Functional Ecology of Plants, 204*(1), 49-62. doi:10.1016/j.flora.2008.01.008

Howe, G. A., & Jander, G. (2008). Plant immunity to insect herbivores. *Annual Review of Plant Biology, 59*(1), 41-66. doi:10.1146/annurev.arplant.59.032607.092825

Hülskamp, M. (2004). Plant trichomes: A model for cell differentiation. *Nature Reviews Molecular Cell Biology, 5*(6), 471-480. doi:10.1038/nrm1404

Hurley, K. W., & Dussourd, D. E. (2014). Toxic geranium trichomes trigger vein cutting by soybean loopers, *Chrysodeixis includens* (Lepidoptera: Noctuidae). *Arthropod-Plant Interactions, 9*(1), 33-43. doi:10.1007/s11829-014-9348-6

Inkson, B.J.. (2016). Scanning Electron Microscopy (SEM) and Transmission Electron Microscopy (TEM) for Materials Characterization. 10.1016/B978-0-08-100040-3.00002-X.

Jetter, R., Kunst, L., & Samuels, A. L. (2008). Composition of plant cuticular waxes. *Biology of the Plant Cuticle,* 145-181. doi:10.1002/9780470988718.ch4

Johnson, Z. (2021). Physical and Chemical Defense Mechanisms in *Aloe Barbadensis* against insect herbivores (Unpublished master's thesis). The University of Texas Rio Grande Valley.

Kang, J., Liu, G., Shi, F., Jones, A. D., Beaudry, R. M., & Howe, G. A. (2010). The tomato Odorless-2 mutant is defective in trichome-based production of diverse specialized metabolites and broad-spectrum resistance to insect herbivores. *Plant Physiology, 154*(1), 262-272. doi:10.1104/pp.110.160192

Kanno, K., Nakamura, M., Tateishi, K., Naoya, W., Tamura, Y., Hirayama, C., . . . Kohno, K. (2006). Various ingredients in plant latex: their crucial roles in plant defense against herbivorous insects. *Plant Cell Pysiol*.

Karabourniotis, G., Liakopoulos, G., Nikolopoulos, D., & Bresta, P. (2019). Protective and defensive roles of non-glandular trichomes against multiple stresses: structure–function coordination. *Journal of Forestry Research, 31*(1), 1-12. doi:10.1007/s11676-019-01034-4

Kariyat, R. R., Balogh, C. M., Moraski, R. P., De Moraes, C. M., Mescher, M. C., & Stephenson, A. G. (2013). Constitutive and herbivore-induced structural defenses are compromised by inbreeding in *Solanum carolinense* (solanaceae). *American Journal of Botany, 100*(6), 1014-1021. doi:10.3732/ajb.1200612

Kariyat, R. R., Hardison, S. B., Ryan, A. B., Stephenson, A. G., De Moraes, C. M., & Mescher, M. C. (2018). Leaf trichomes affect caterpillar feeding in an instar-specific manner. *Communicative & Integrative Biology, 11*(3), 1-6. doi:10.1080/19420889.2018.1486653

Kariyat, R. R., Portman SL. Plant–herbivore interactions: Thinking beyond larval. American Journal of Botany. 2012; 103:1–3.

Kariyat, R. R., Raya, C. E., Chavana, J., Cantu, J., Guzman, G., & Sasidharan, L. (2019). Feeding on glandular and non-glandular leaf trichomes negatively affect growth and development in tobacco hornworm (*Manduca sexta*) caterpillars. *Arthropod-Plant Interactions, 13*(2), 321-333. doi:10.1007/s11829-019-09678-z

Kariyat, R. R., Sinclair JP, Golenberg EM. Following Darwins trail. Interactions affecting the evolution of plant mating systems. Am J Bot. 2013;100:999–1001. https://doi.org/10.3732/ajb.1300157.

Kariyat, R. R., Smith, J. D., Stephenson, A. G., De Moraes, C. M., & Mescher, M. C. (2017). Non-glandular trichomes of *Solanum carolinense* deter feeding by *Manduca sexta* caterpillars and cause damage to the gut peritrophic matrix. *Proceedings of the Royal Society B: Biological Sciences, 284*(1849), 20162323. doi:10.1098/rspb.2016.2323

Kaur, I., & Kariyat, R. R. (2020). Eating barbed wire: Direct and indirect defensive roles of non-glandular trichomes. *Plant, Cell & Environment, 43*(9), 2015-2018. doi:10.1111/pce.13828

Kaur, I., Watts, S., Raya, C., Raya, J., & Kariyat, R. (2021; under press) Surface Warfare: plant structural defenses challenge caterpillar feeding. ln: R. J. Marquis, S. Koptur (eds) *Caterpilars in the Middle*. Springer, Switzerland.

Kaur, J., & Kariyat, R. (2020). Role of trichomes in plant stress biology. ln: Núñez-Farfán J., Valverde P. (eds) *Evolutionary Ecology of Plant-Herbivore Interaction*. Springer, Cham. https://doi.org/10.1007/978-3-030-46012-9_2

Kaur, J., Chavana, J., Soti, P., Racelis, A., & Kariyat, R. (2020). Arbuscular mycorrhizal fungi (AMF) influences growth and insect community dynamics in Sorghum-sudangrass (Sorghum x drummondii). *Arthropod-Plant Interactions, 14*(3), 301-315. doi:10.1007/s11829-020-09747-8

Kelly, J. K., Rasch, A., & Kalisz, S. (2002). A method to estimate pollen viability from pollen size variation. *American Journal of Botany, 89*(6), 1021-1023. doi:10.3732/ajb.89.6.1021

Kennedy, G. G. (2003). Tomato, pests, parasitoids, and predators: tritrophic interactions involving the genus *Lycopersicon*. *Annual Review of Entomology, 48*(1), 51-72. doi:10.1146/annurev.ento.48.091801.112733

Knapp, S. (2002). Tobacco to tomatoes: a phylogenetic perspective on fruit diversity in the Solanaceae. *Journal of Experimental Botany*

Kotula, P. G., Keenan, M. R., & Michael, J. R. (2003). Automated analysis of SEM X-ray spectral images: A powerful new microanalysis tool. *Microscopy and Microanalysis*, *9*(1), 1-17.

Krenn H.W. (2019) Form and Function of Insect Mouthparts. In: Krenn H. (eds) Insect Mouthparts. Zoological Monographs, vol 5. Springer, Cham. https://doi.org/10.1007/978-3-030-29654-4_2 *y, 53*(377), 2001-2022. doi:10.1093/jxb/erf068

Levin, D. A. (1973). The role of trichomes in plant defense. *The Quarterly Review of Biology, 48*(1, Part 1), 3-15. doi:10.1086/407484

Lewandowska, M., Keyl, A., & Feussner, I. (2020). Wax biosynthesis in response to danger: Its regulation upon abiotic and biotic stress. *New Phytologist, 227*(3), 698-713. doi:10.1111/nph.16571

Li, C., Wu, J., Blamey, F. P., Wang, L., Zhou, L., Paterson, D. J., . . . Kopittke, P. M. (2021). Non-glandular trichomes of sunflower are important in the absorption and translocation of foliar-applied Zn. *Journal of Experimental Botany, 72*(13), 5079-5092. doi:10.1093/jxb/erab180

Li, S., Tosens, T., Harley, P. C., Jiang, Y., Kanagendran, A., Grosberg, M., . . . Niinemets, Ü. (2018). Glandular trichomes as a barrier against atmospheric oxidative stress: relationships with ozone uptake, leaf damage, and emission of lox products across a diverse set of species. *Plant, Cell & Environment, 41*(6), 1263-1277. doi:10.1111/pce.13128

Li, Y., Lei, L., Luo, R., Li, C., & Luo, C. (2020). Morphological structures of bamboo (*Bambusa emeiensis*) shoot shells and trichomes and functions in response to herbivory. *Journal of Plant Growth Regulation*. doi:10.1007/s00344-020-10195-0

Liakoura, V., Stefanou, M., Manetas, Y., Cholevas, C., & Karabourniotis, G. (1997). Trichome density and its UV-B protective potential are affected by shading and leaf position on the canopy. *Environmental and Experimental Botany, 38*(3), 223-229. doi:10.1016/s0098-8472(97)00005-1

Lill, J. T., & Marquis, R. J. (2001). The effects of leaf quality on herbivore performance and attack from natural enemies. *Oecologia, 126*(3), 418-428. doi:10.1007/s004420000557

Lin, S. Y., Trumble, J. T., & Kumamoto, J. (1987). Activity of volatile compounds in glandular trichomes of *Lycopersicon* species against two insect herbivores. *Journal of Chemical Ecology, 13*(4), 837-850. doi:10.1007/bf01020164

Løe, G., Toräng, P., Gaudeul, M., & Ågren, J. (2007). Trichome production and spatiotemporal variation in herbivory in the perennial herb A*rabidopsis lyrata*. *Oikos, 116*(1), 134-142. doi:10.1111/j.2006.0030-1299.15022.x

LoPresti, E. F., Pearse, I. S., & Charles, G. K. (2015). The siren song of a sticky plant: columbines provision mutualist arthropods by attracting and killing passer by insects. *Ecology, 96*(11), 2862-2869. doi:10.1890/15-0342.1

Luckwill, L. C. (1943). The genus *Lycopersicon*: a historical, biological, and taxonomic survery of the wild and cultivated tomatoes. Aberdeen, Scotland: Aberdeen University Press.

Maffei, M., Chialva, F., & Sacco, T. (1989). Glandular trichomes and essential oils in developing peppermint leaves. I. Variation of peltate trichome number and terpene distribution within leaves. *New Phytologist, 111*(4), 707-716. doi:10.1111/j.1469-8137.1989.tb02366.x

Malakar, R., & Tingey, W. M. (2000). Glandular trichomes of *Solanum berthaultii* and its hybrids with potato deter oviposition and impair growth of potato tuber moth. *Entomologia Experimentalis Et Applicata, 94*(3), 249-257. doi:10.1046/j.1570-7458.2000.00627.x

Mannethody, S., & Purayidathkandy, S. (2018). Trichome micromorphology and its systematic significance in Asian Leucas (Lamiaceae). *Flora, 242*, 70-78. doi:10.1016/j.flora.2018.03.007

Matsuki, M., & MacLean, S. F. (1994). Effects of different leaf traits on growth rates of insect herbivores on Willows. *Oecologia, 100-100*(1-2), 141-152. doi:10.1007/bf00317141

McCully, M. E, Canny, M. J, & Huang, C. X. (2009). Invited Review: Cryo-scanning electron microscopy (CSEM) in the advancement of functional plant biology. Morphological and anatomical applications. *Functional plant biology, 36*, 97-124. doi: 10.1071/FP08304

Medeiros, L., & Moreira, G. R. (2005). Larval feeding behavior of *Gratiana spadicea* (klug) (Coleoptera: Chrysomelidae: Cassidinae) on its host plant, *Solanum sisymbriifolium* Lamarck (Solanaceae): interaction with trichomes. *The Coleopterists Bulletin, 59*(3), 339-350. doi:10.1649/778.1

Mehdi Talebi, S., Ghorbani Nohooji, M., Yarmohammadi, M., Azizi, N., & Matsyura, A. (2018). Trichomes morphology and density analysis in some "Nepeta" species of Iran. *Mediterranean Botany, 39*(1), 51-62. doi:10.5209/mbot.59574

Mithöfer, A., & Boland, W. (2012). Plant defense against herbivores: chemical aspects. *Annual Review of Plant Biology, 63*(1), 431-450. doi:10.1146/annurev-arplant-042110-103854

Mitton, J. B., Linhart, Y. B., Sturgeon, K. B., & Hamrick, J. L. (1979). Allozyme polymorphisms detected in mature needle tissue of ponderosa pine. *Journal of Heredity, 70*(2), 86-89. doi:10.1093/oxfordjournals.jhered.a109220

Munien, P., Naidoo, Y., & Naidoo, G. (2015). Micromorphology, histochemistry and ultrastructure of the foliar trichomes of *Withania somnifera* (L.) Dunal (Solanaceae). *Planta, 242*(5), 1107-1122. doi:10.1007/s00425-015-2341-1

Muravnik, L. E., Kostina, O. V., & Mosina, A. A. (2019). Glandular trichomes of the leaves in three *Doronicum* species (Senecioneae, Asteraceae): morphology, histochemistry, and ultrastructure. *Protoplasma, 256*(3), 789-803. doi:10.1007/s00709-018-01342-2

Murungi, L. K., Kirwa, H., Salifu, D., & Torto, B. (2016). Opposing roles of foliar and glandular trichome volatile components in cultivated nightshade interaction with a specialist herbivore. *PLOS ONE, 11*(8). doi:10.1371/journal.pone.0160383

Mustafa, A., Ensikat, H., & Weigend, M. (2018). Stinging hair morphology and wall biomineralization across five plant families: conserved morphology versus divergent cell wall composition. *American Journal of Botany, 105*(7), 1109-1122. doi:10.1002/ajb2.1136

Nakamura, R., Matsumoto, A., & Ishimaru, M. (2021). Explosive crystallization of sputter-deposited amorphous germanium films by irradiation with an electron beam of SEM-level energies. *Journal of Applied Physics*, *129*(21), 215301.

Navarro, T., & El Oualidi, J. (1999).Trichome morphology in *Teucrium* L. (Labiatae). A taxonomic review. *Anales Del Jardín Botánico De Madrid, 57*(2) PP. 277-297. doi:10.3989/ajbm.1999.v57.i2.203

Neal, J. J., Tingey, W. M., & Steffens, J. C. (1990). Sucrose esters of carboxylic acids in glandular trichomes of *solanum berthaultii* deter settling and probing by green peach aphid. *Journal of Chemical Ecology, 16*(2), 487-497. doi:10.1007/bf01021780

Negin, B., Shachar, L., Meir, S., Ramirez, C. C., Horowitz, A. R., Jander, G., & Aharoni, A. (2021). Fatty alcohols, a minor component of the tree tobacco surface wax, reduce insect herbivory. doi:10.1101/2021.07.15.452450

Newbury DE, Ritchie NW. Performing elemental microanalysis with high accuracy and high precision by scanning electron microscopy/silicon drift detector energy-dispersive X-ray spectrometry (SEM/SDD-EDS). J Mater Sci. 2015;50(2):493-518. doi: 10.1007/s10853-014-8685-2. Epub 2014 Nov 12. PMID: 26346887; PMCID: PMC4555346.

Nihranz, C. T., Kolstrom, R. L., Kariyat, R. R., Mescher, M. C., De Moraes, C. M., & Stephenson, A. G. (2019). Herbivory and inbreeding affect growth, reproduction, and resistance in the rhizomatous offshoots of Solanum carolinense (Solanaceae). *Evolutionary Ecology*, *33*(4), 499-520.

Nurit-Silva, K., & De Fátima Agra, M. (2011). Leaf epidermal characters of *Solanum* Sect. Polytrichum (Solanaceae) as taxonomic evidence. *Microscopy Research and Technique, 74*(12), 1186-1191. doi:10.1002/jemt.21013

Oksanen, E. (2018). Trichomes form an important first line of defence against adverse environment-new evidence for ozone stress mitigation. *Plant, Cell & Environment, 41*(7), 1497-1499. doi:10.1111/pce.13187

Palaiologou, E., Goggin, P., Chatelet, D. S., Ribeiro de Souza, R., Chiu, W., Ashley, B., . . . Lewis, R. M. (2020). Serial block-face scanning electron microscopy reveals novel intercellular connections in human term placental microvasculature. *Journal of Anatomy, 237*(2), 241-249. doi:10.1111/joa.13191

Pan, Z., Guo, W., Zhang, Y., Schreel, J. D., Gao, J., Li, Y., & Yang, S. (2021). Leaf trichomes of dendrobium species (epiphytic orchids) in relation to foliar water uptake, leaf surface wettability, and water balance. *Environmental and Experimental Botany, 190*, 104568. doi:10.1016/j.envexpbot.2021.104568

Pastório, M. A., Hoshino, A. T., Oliveira, L. M., Lima, W. F., Fernandes, T. A., Menezes Júnior, A. D., & Androcioli, H. G. (2019). Cassava varieties trichome density influence the infestation of *Vatiga illudens* (Hemiptera: Tingidae). *Journal of Agricultural Science, 11*(17), 319. doi:10.5539/jas.v11n17p319

Pathan, A. K., Bond, J., & Gaskin, R. E. (2008). Sample preparation for scanning electron microscopy of plant surfaces—horses for courses. *Micron*, *39*(8), 1049-1061.

Paudel, S., Lin, P., Foolad, M. R., Ali, J. G., Rajotte, E. G., & Felton, G. W. (2019). Induced plant defenses against herbivory in cultivated and wild tomato. *Journal of Chemical Ecology, 45*(8), 693-707. doi:10.1007/s10886-019-01090-4

Payne, W. W. (1978). A glossary of plant hair terminology. *Brittonia, 30*(2), 239. doi:10.2307/2806659

Peiffer, M., Tooker, J. F., Luthe, D. S., & Felton, G. W. (2009). Plants on early alert: Glandular trichomes as sensors for insect herbivores. *New Phytologist, 184*(3), 644-656. doi:10.1111/j.1469-8137.2009.03002.x

Portman, S. L., Felton, G. W., Kariyat, R. R., & Marden, J. H. (2020). Host plant defense produces species specific alterations to flight muscle protein structure and flight-related fitness traits of two armyworms. *Journal of Experimental Biology*. doi:10.1242/jeb.224907

Portman, S. L., Kariyat, R. R., Johnston, M. A., Stephenson, A. G., & Marden, J. H. (2015). Inbreeding compromises host plant defense gene expression and improves herbivore survival. *Plant Signaling & Behavior, 10*(5). doi:10.1080/15592324.2014.998548

Rebora, M., Salerno, G., Piersanti, S., Gorb, E., & Gorb, S. (2020). Entrapment of *Bradysia paupera* (Diptera: Sciaridae) by *Phaseolus vulgaris* (Fabaceae) plant leaf. *Arthropod-Plant Interactions, 14*(4), 499-509. doi:10.1007/s11829-020-09760-x

Reid, W. J., & Cuthbert, F. P. (1964). Control of caterpillars on commercial cabbage and other cole crops in the South /. doi:10.5962/bhl.title.95521

Roe, K. E. (1971). Terminology of hairs in the genus *Solanum*. *TAXON, 20*(4), 501-508. doi:10.2307/1218251

Sack, L., & Buckley, T. N. (2020). Trait multi-functionality in plant stress response. *Integrative and Comparative Biology, 60*(1), 98-112. doi:10.1093/icb/icz152

Saha, T., Chandran, N., & Anu, B. C. (2020). Major Insect Pests of Vegetable Crops in Bihar and Their Management. *Sustainable Agriculture,* 395-429. doi:10.1201/9780429325830-23

Savary, S., Willocquet, L., Pethybridge, S. J., Esker, P., Mcroberts, N., & Nelson, A. (2019). The global burden of pathogens and pests on major food crops. *Nature Ecology & Evolution, 3*(3), 430-439. doi:10.1038/s41559-018-0793-y

Seithe, A., & Sullivan, J. R. (1990). Hair morphology and systematics of *Physalis* (Solanaceae). *Plant Systematics and Evolution, 170*(3-4), 193-204. doi:10.1007/bf00937703

Shah, V. V., Shah, D. N., & Patrekar, V. P. (2013). Medicinal plants from Solanaceae Family. *Research Journal of Pharmacy and Technology*.

Shelomi, M., Perkins, L. E., Cribb, B. W., & Zalucki, M. P. (2010). Effects of leaf surfaces on first-instar *Helicoverpa armigera* (hübner) (Lepidoptera: Noctuidae) behaviour. *Australian Journal of Entomology, 49*(4), 289-295. doi:10.1111/j.1440-6055.2010.00766.x

Silva, E.O., Feio, A.C., Cardoso-Gustavson, P. *et al.* Extrafloral nectaries and plant–insect interactions in *Passiflora* L. (Passifloraceae). *Braz. J. Bot* 40, 331–340 (2017). https://doi.org/10.1007/s40415-016-0329-0

Singh, S., & Kariyat, R. R. (2020). Exposure to polyphenol-rich purple corn pericarp extract restricts fall armyworm (*Spodoptera frugiperda*) growth. *Plant Signaling & Behavior, 15*(9), 1784545. doi:10.1080/15592324.2020.1784545

Singh, S., Kaur, I., & Kariyat, R. (2021). The multifunctional roles of polyphenols in plant-herbivore interactions. *International Journal of Molecular Sciences, 22*(3), 1442. doi:10.3390/ijms22031442

Singh, S., & Kumari, B. (2020). Roving survey of major insect pests of rice crop (Oryza sativa L.) in different blocks of Patna district of Bihar state, India.

Sletvold, N., Huttunen, P., Handley, R., Kärkkäinen, K., & Ågren, J. (2010). Cost of trichome production and resistance to a specialist insect herbivore in *Arabidopsis lyrata*. *Evolutionary Ecology, 24*(6), 1307-1319. doi:10.1007/s10682-010-9381-6

Stokes, Debbie. (2004). Recent advances in electron imaging, image interpretation and applications: Environmental scanning electron microscopy. Philosophical transactions. Series A, Mathematical, physical, and engineering sciences. 361. 2771-87. 10.1098/rsta.2003.1279.

Stork, W. F., Weinhold, A., & Baldwin, I. T. (2011). Trichomes as dangerous lollipops: do lizards also use caterpillar body and frass odor to optimize their foraging? *Plant Signaling & Behavior, 6*(12), 1893-1896. doi:10.4161/psb.6.12.18028

Sujata, K., Jennings, H.M. Advances in Scanning Electron Microscopy. *MRS Bulletin* 16, 41–45 (1991). https://doi.org/10.1557/S0883769400057390 Symon, D. E. (1981). A revision of the genus *Solanum* in Australia. *Journal of Adelaide Botanic Gardens*.

Tagawa, J., Matsushita, A., & Watanabe, T. (2008). Leaf surface preference in the cabbage worm, Pieris rapae crucivora, and parasitism by the gregarious parasitoid *Cotesia glomerata*. *Entomologia Experimentalis Et Applicata, 129*(1), 37-43. doi:10.1111/j.1570-7458.2008.00750.x

Tang, T., Li, C., Li, D., Jing, S., Hua, J., Luo, S., . . . Li, S. (2020). Peltate glandular trichomes of *Colquhounia vestita* harbor diterpenoid acids that contribute to plant adaptation to UV radiation and cold stresses. *Phytochemistry, 172*, 112285. doi:10.1016/j.phytochem.2020.112285

Tayal, M., Somavat, P., Rodriguez, I., Martinez, L., & Kariyat, R. (2020). Cascading effects of polyphenol-rich purple corn pericarp extract on pupal, adult, and offspring of tobacco hornworm (*Manduca sexta* L.). *Communicative & Integrative Biology, 13*(1), 43-53. doi:10.1080/19420889.2020.1735223

Tayal, M., Somavat, P., Rodriguez, I., Thomas, T., Christoffersen, B., & Kariyat, R. (2020). Polyphenol-rich purple corn pericarp extract adversely impacts herbivore growth and development. *Insects, 11*(2), 98. doi:10.3390/insects11020098

Thitz, P., Possen, B., Oksanen, E., Mehtätalo, L., Virjamo, V., & Vapaavuori, E. (2017). Production of glandular trichomes responds to water stress and temperature in silver Birch (BETULA pendula) leaves. *Canadian Journal of Forest Research, 47*(8), 1075-1081. doi:10.1139/cjfr-2017-0036

Tian, D., Tooker, J., Peiffer, M., Chung, S. H., & Felton, G. W. (2012). Role of trichomes in defense against herbivores: Comparison of herbivore response to woolly and hairless trichome mutants in tomato (*Solanum lycopersicum*). *Planta, 236*(4), 1053-1066. doi:10.1007/s00425-012-1651-9

Tingey, W. M., & Laubengayer, J. E. (1981). Defense against the green peach aphid and potato leafhopper by glandular trichomes of *Solanum berthaultii*123. *Journal of Economic Entomology, 74*(6), 721-725. doi:10.1093/jee/74.6.721

Tissier, A. (2012). *Trichome Specific Expression: Promoters and Their Applications*. INTECH Open Access Publisher.

Tsujii, Y., Onoda, Y., Izuno, A., Isagi, Y., & Kitayama, K. (2016). A quantitative analysis of phenotypic variations of *Metrosideros polymorpha* within and across populations along environmental gradients on Mauna Loa, Hawaii. *Oecologia, 180*(4), 1049-1059. doi:10.1007/s00442-015-3416-1

Uphof, J. C. (1962). *Plant Hairs*. Berlin: Gebr. Borntraeger.

Vallejo-Marín, M., & O'Brien, H. E. (2007). Correlated evolution of self-incompatibility and clonal reproduction in *Solanum* (Solanaceae). *New Phytologist, 173*(2), 415-421. doi:10.1111/j.1469-8137.2006.01924.x

Van Dam, N. M. (1999). Inheritance and distribution of trichome phenotypes in *Datura wrightii*. *Journal of Heredity, 90*(1), 220-227. doi:10.1093/jhered/90.1.220

Van Dam, N. M., Hare, J. D., & Elle, E. (1999). Inheritance and distribution of trichome phenotypes in *Datura wrightii*. *Journal of Heredity, 90*(1), 220-227. doi:10.1093/jhered/90.1.220

Varela, L. G., & Bernays, E. A. (1988). Behavior of newly hatched potato tuber moth larvae, *Phthorimaea operculella* Zell. (Lepidoptera: Gelechiidae), in relation to their host plants. *Journal of Insect Behavior, 1*(3), 261-275. doi:10.1007/bf01054525

Watanabe, T., Nakamura, K., & Tagawa, J. (2018). Host-plant leaf-surface preferences of young caterpillars of three species of *Pieris* (Lepidoptera: Pieridae) and its effect on parasitism by the gregarious parasitoid *Cotesia glomerata* (Hymenoptera: Braconidae). *European Journal of Entomology, 115*, 25-29. doi:10.14411/eje.2018.004

Watts, S., & Kariyat, R. (2021). Morphological characterization of trichomes show enormous variation in shape, density, and dimensions across the leaves of 14 *Solanum* species. *AoB PLANTS*. doi:10.1093/aobpla/plab071

Watts, S., & Kariyat, R. (2021). Picking sides: Feeding on the abaxial leaf surface is costly for caterpillars. *Planta, 253*(4) 1-6. doi:10.1007/s00425-021-03592-6

Watts, S., Kaur, I., Singh, S., Jimenez, B., Chavana, J., & Kariyat, R. (2021). Desktop scanning electron microscopy in plant-insect interactions research: A fast and effective way to capture electron micrographs with minimal sample preparation. *Biology Methods and Protocols*. doi:10.1093/biomethods/bpab020

Weigend, M., Mustafa, A., & Ensikat, H. (2018). Calcium phosphate in plant trichomes: The overlooked biomineral. *Planta, 247*(1), 277-285. doi:10.1007/s00425-017-2826-1

Weinhold, A., & Baldwin, I. T. (2011). Trichome-derived o-acyl sugars are a first meal for caterpillars that tags them for predation. *Proceedings of the National Academy of Sciences, 108*(19), 7855-7859. doi:10.1073/pnas.1101306108

Werker, E. (2000). Trichome diversity and development. *Advances in Botanical Research,* 1-35. doi:10.1016/s0065-2296(00)31005-9

White, C., & Eigenbrode, S. D. (2000). Effects of surface wax variation in *Pisum sativum* on herbivorous and entomophagous insects in the field. *Environmental Entomology, 29*(4), 773-780. doi:10.1603/0046-225x-29.4.773

Whitney, H. M., & Federle, W. (2013). Biomechanics of plant–insect interactions. *Current Opinion in Plant Biology, 16*(1), 105-111. doi:10.1016/j.pbi.2012.11.008

Wilkens, R. T., Shea, G. O., Halbreich, S., & Stamp, N. E. (1996). Resource availability and the trichome defenses of tomato plants. *Oecologia, 106*(2), 181-191. doi:10.1007/bf00328597

Wójcicka, A. (2016). Effect of epicuticular waxes from triticale on the feeding behaviour and mortality of the grain aphid, *Sitobion avenae* (Fabricius) (Hemiptera: Aphididae). *Journal of Plant Protection Research, 56*(1), 39-44. doi:10.1515/jppr-2016-0006

Wollman, A. J., Nudd, R., Hedlund, E. G., & Leake, M. C. (2015). From animaculum to single molecules: 300 years of the light microscope. *Open Biology, 5*(4), 150019. doi:10.1098/rsob.150019

Yao, F., Lin, S., Wang, L., Mei, W., Monticelli, L. S., Zheng, Y., . . . Weng, Q. (2020). Oviposition preference and adult performance of the whitefly predator *Serangium japonicum* (Coleoptera: Coccinellidae): Effect of leaf microstructure associated with Ladybeetle Attachment Ability. *Pest Management Science, 77*(1), 113-125. doi:10.1002/ps.6042

Yu, X., Liang, C., Fang, H., Qi, X., Li, W., & Shang, Q. (2018). Variation of trichome morphology and essential OIL composition of seven *Mentha s*pecies. *Biochemical Systematics and Ecology, 79*, 30-36. doi:10.1016/j.bse.2018.04.016

Zalucki, M. P., Clarke, A. R., & Malcolm, S. B. (2002). Ecology and behavior of first instar larval Lepidoptera. *Annual Review of Entomology, 47*(1), 361-393. doi:10.1146/annurev.ento.47.091201.145220

Zhang, W., Dong, Z., Zhu, L., Hou, Y., & Qiu, Y. (2020). Direct observation of the release of nanoplastics from commercially recycled plastics with correlative Raman imaging and scanning electron microscopy. *ACS nano*, *14*(7), 7920-7926.

Zhou, L. H., Liu, S. B., Wang, P. F., Lu, T. J., Xu, F., Genin, G. M., & Pickard, B. G. (2017). The Arabidopsis trichome is an active mechanosensory Switch. *Plant, Cell & Environment, 40*(5), 611-621. doi:10.1111/pce.12728

Zhu, Y., Inada, H., Nakamura, K., & Wall, J. (2009). Imaging single atoms using secondary electrons with an aberration-corrected electron microscope. *Nature materials*, *8*(10), 808-812.

BIOGRAPHICAL SKETCH

Sakshi Watts is a MS biology student who graduated from high school in Holy Heart Senior Secondary Day Boarding Public School, Fazilka, Punjab, India in 2015. Afterwards, she pursued her career in B.Sc. Agriculture (Hons.) 4-year program from Punjab Agricultural University, Punjab, India. With growing interest in Entomology, she admitted herself in M.S. Biology (Major-Entomology; thesis based) in The University of Texas Rio Grande Valley, USA. She worked in Dr. Rupesh Kariyat's lab for two years and gained experience and skills in entomology, plant biology and chemical ecology. She earned M.S. in Biology from The University of Texas Rio Grande Valley, TX, USA in Decemeber, 2021. Sakshi Watts will move to University of California Riverside Entomology Department to pursue PhD in Entomology in Winter 2022 session.

To contact Sakshi Watts, please email her at: sakshiwatts1998@gmail.com